Chapter 5
Integral Equations in the Kinetic Theory of Gases and Related Topics

Abstract Integral equations occur in many areas of chemistry, physics and engineering. We consider in this chapter the integral equations that arise in radiative transfer theory and in the study of transport processes in dilute gases modeled with the Boltzmann equation. The first use of a collocation was the Gauss-Legendre quadrature for the solution of the integro-differential isotropic radiative transfer equation. The integral equations that are used to calculate the heat conductivity and viscosity of a dilute monatomic gas are derived with the Chapman-Enskog method of solution of the Boltzmann equation. The integral equations are solved with spectral and pseudospectral methods. These numerical methods are also used to calculate the eigenfunctions and eigenvalues for the linearized collision operator for a one component gas as well as for the linear collision operator for a binary mixture. The solution of the Boltzmann equation for many applications can be expressed in terms of the eigenfunctions and eigenvalues of the collision operators that in general possess an infinite number of discrete eigenvalues and a continuum. The eigenvalue spectra of these operators are calculated and discussed. A pseudospectral method of solution of the Boltzmann integral equation is used for the calculation of the nonequilibrium reaction rate for a model reactive system. A pseudospectral method is also used to solve the Chapman-Enskog integral equation that gives the viscosity of a dilute gas. The relaxation to equilibrium of an initial anisotropic nonequilibrium distribution for a binary gas mixture versus the mass ratio of the two components is studied. Also presented are the spectral solutions of Boltzmann equation for the Milne problem of rarefied gas dynamics, the escape of light atoms from a planetary atmosphere and the calculation of ion mobilities. Pseudospectral methods with nonclassical weight functions are used in some of these applications. The chapter concludes with the study of the relaxation to equilibrium of a one component gas as described by the nonlinear isotropic Boltzmann equation.

5.1 Introduction

Integral equations in which the desired function appears as an integrand in an integral operator occur in diverse subjects in science and engineering, and include such fields as radiative transfer theory (Chandrasekhar 1960), neutron transport (Kourganoff

B. Shizgal, *Spectral Methods in Chemistry and Physics*, Scientific Computation,
DOI 10.1007/978-94-017-9454-1_5

1963; Case and Zweifel 1967; Garcia 1999; Ganapol 2008), kinetic theory (Chapman and Cowling 1970), electromagnetic theory (Volakis and Sertel 2012), geophysics (Eskola 2012), quantum mechanics and scattering theory (Canto and Hussein 2013) and many other applications. Many partial differential equations can be transformed to integral equations with the appropriate Green's functions that satisfy the boundary conditions. There are several textbooks devoted to the solution of integral equations (Tricomi 1985; Delves and Mohamed 1985; Jerri 1999; Kythe and Puri 2002).

In this chapter, spectral and pseudospectral methods are applied to the solution of several different integral equations that arise in radiative transport and in kinetic theory based on the Boltzmann equation. Quadratures are used to reduce a linear integral equation to a set of coupled linear equations for the solution at the quadrature points. The first use of a similar collocation based on Gauss-Legendre quadratures was by Wick (1943) and Chandrasekhar (1944) for the solution of the radiative transfer equation (Chandrasekhar 1960). The overlap of radiative transfer theory with neutron transport also based on the Boltzmann equation is described in the books by Case and Zweifel (1967) and by Ganapol (2008). Recent historical reviews of these research areas were presented by Peraiah (1996) and Shore (2002). An historical account of the development of nuclear reactor theory based on the fundamental advances in radiative transfer and neutron transport was presented by Williams (2000). Although kinetic theory (Chapman and Cowling 1970) and neutron transport theory (Ganapol 2008) are based on the Boltzmann equation, there is a considerable difference in the notation employed. The book by Ganapol (2008) has an extensive bibliography to research papers and monographs on neutron transport theory.

We illustrate the application of spectral and pseudospectral methods to the solution of the integral equations for the Boltzmann equation of kinetic theory. A summary of the Chapman-Enskog method (Hirschfelder et al. 1954; Huang 1967; Chapman and Cowling 1970; Ferziger and Kaper 1972) is presented. This method is a special solution of the Boltzmann equation for a monatomic gas in the collision dominated regime constructed specifically for the calculation of the transport coefficients for diffusion, heat conduction and viscosity in terms of the differential cross sections describing binary collisions between particles. This formalism yields integral equations whose solutions present interesting applications for spectral methods.

The Chapman-Enskog method of solution of the Boltzmann equation provides a derivation of the hydrodynamic equations of fluid mechanics. This is an alternative approach to the methods based on control volumes and conservation principles presented in books on fluid dynamics (Fletcher 1991; Kundu et al. 2012). In physical situations where the gas density is very low and the mean free path, the average distance travelled between particle collisions, is comparable to or greater than the local scale length, the hydrodynamic equations are no longer valid and a kinetic theory treatment is required. This is the subject of rarefied gas dynamics (Sone 2007; Struchtrup 2005) and pertains to shock waves, aerodynamics, microfluidics (Gad-el-Hak 1999) and the high altitude regions of planetary atmospheres from which energetic atoms and ions can escape (Fahr and Shizgal 1983; Shizgal and Arkos 1996; Pierrard 2003; Echim et al. 2011). The direct simulation Monte Carlo method (Bird 1994) is often used to study such rarefied gaseous systems.

In this chapter, spectral and pseudospectral methods are used to study the spectral properties of the linearized collision operator defined by Eq. (5.41) as well as the analogous linear operator for a binary gas, Eq. (5.104). A spectral method is used to calculate the nonequilibrium effects that occur in a simple reactive system (Shizgal and Karplus 1970). The pseudospectral solutions of the Boltzmann equation for the viscosity in a one component gas (Siewert 2002; Sharipov and Bertoldo 2009) and the equilibration of nonequilibrium distributions in a binary gas are also described (Shizgal and Blackmore 1983).

The departure of distribution functions from spherical symmetry are considered in the applications to the Milne problem (Lindenfeld and Shizgal 1983) and for the escape of light species from a planetary atmosphere (Shizgal and Blackmore 1986). We review the development of spectral methods used to solve the Boltzmann equation for the drift of ions in a background gas under the influence of a uniform electrostatic field (Viehland 1994). In the last section, the nonlinear isotropic Boltzmann equation is used to study the approach to equilibrium of a one component gas and the relationship with the spectral properties of the linearized operator is discussed. A finite difference method is used which requires a cubature for the evaluation of the integral collision operator. A review of alternative methods based on spectral methods with both polynomial basis functions (Weinert et al. 1980; Ender et al. 2011) as well as Fourier methods (Filbet and Mouhot 2011; Wu et al. 2013) is presented.

5.2 Classes of Integral Equations and the Use of Quadratures

Fredholm integral equations of the 1st and 2nd kind (Delves and Mohamed 1985; Jerri 1999; Slevinsky and Safouhi 2008) are defined by

$$\int_a^b K(x, y) f(y) dy = S(x), \tag{5.1}$$

and

$$\int_a^b K(x, y) f(y) dy - g(x) f(x) = S(x), \tag{5.2}$$

respectively, where the kernel, $K(x, y)$, and the functions $g(x)$ and $S(x)$ are known. These integral equations can also be expressed as eigenvalue problems

$$\int_a^b K(x, y) \phi_n(y) dy = \lambda_n \phi_n(x), \tag{5.3}$$

and

$$\int_a^b K(x, y)\phi_n(y)dy - g(x)f(x) = \lambda_n \phi_n(x), \tag{5.4}$$

respectively. Volterra integral equations, which we do not consider, are similar with the upper boundary $b = x$.

The method of solution chosen for a particular problem depends on the behavior of the kernel versus x and y. If the kernel is well behaved in both variables, the solution can be easily computed. If there is a discontinuous lower order derivative or a strong singularity, then the numerical method to be used should be adapted to the particular behavior of the kernel. The types of singularities include a logarithmic singularity for which $K(x, y) = k(x, y)\log|x - y|$ or an algebraic singularity for which $K(x, y) = k(x, y)/|x - y|$. This aspect has been discussed by Atkinson and Shampine (2008) and MATLAB codes for the numerical solution of a large class of integral equations are readily available (Driscoll 2010).

Many current solution methods of integral equations involve the reduction of the integral equation to a set of algebraic equations with a suitable quadrature procedure with grid points $\{x_i\}$ and associated weights $\{w_i\}$ based on polynomials orthogonal with respect to weight function $w(x)$ on the interval $[a, b]$. With the use of a quadrature to perform the integral over y in Eq. (5.2), the integral operator is reduced to the sum over quadrature weights and points, that is

$$\sum_{i=1}^{N} W_i K(x, x_i) f(x_i) - g(x)f(x) = S(x), \tag{5.5}$$

where $W_i = w_i/w(x_i)$. If we evaluate this equation at the same set of grid points, we have the system of linear algebraic equations,

$$\sum_{i=1}^{N} W_i K(x_j, x_i) f(x_i) - g(x_j)f(x_j) = S(x_j). \tag{5.6}$$

Inversion of this set of linear equations gives the desired solution at the grid points. This is the method often used to solve integral equations and referred to as the Nyström method (Delves and Mohamed 1985; Kythe and Puri 2002). Obviously we need to know further details of the behavior of the kernel in order to choose the appropriate quadrature, and study the convergence of the solution.

To illustrate the method, this technique is used to solve the integral equation,

$$\int_{-1}^{1} \sinh(x + y)\phi(y)dy - \phi(x) = -x^2, \tag{5.7}$$

which is Example 2.2.2 from Kythe and Puri (2002). This equation has the exact solution

$$\phi_{exact}(x) = \alpha \sinh(x) + \beta \cosh(x) + x^2, \tag{5.8}$$

where $\alpha = 16e^3(e^2-5)/(1-34e^4+e^8)$, $\beta = [1+\frac{1}{4}(\frac{1}{e^2}-e^2)]\alpha$ and $e = 2.718282\ldots$ Since the domain is $x \in [-1, 1]$, we choose a Gauss-Legendre quadrature, for which $W_i = w_i$ and reduce the integral equation to a coupled set of linear algebraic equations for the solution evaluated at the quadrature points analogous to the linear set of equations, Eq. (5.6). We have that

$$\sum_{i=1}^{N} w_i \sinh(x_j + x_i)\phi^{(N)}(x_i) - \phi^{(N)}(x_j) = -x_j^2, \tag{5.9}$$

and the solution is represented by $\phi^{(N)}(x_i)$ at the N quadrature points. We measure the error of the numerical solution in comparison with the exact solution as given by the L^2 error

$$E_2^{(N)} = \sqrt{\frac{1}{N}\sum_{n=1}^{N}\left[\phi^{(N)}(x_i) - \phi_{exact}(x_i)\right]^2}. \tag{5.10}$$

The numerical solution of Eq. (5.9) and the $E_2^{(N)}$ error are computed with a MATLAB code. The variation of $\log_{10}[E_2^{(N)}]$ versus N is shown in Fig. 5.1. The solution converges to machine accuracy very quickly owing to the smooth, well behaved kernel and inhomogeneous term. The variation of the exact solution given by Eq. (5.8) is well approximated by a low order polynomial for $x \in [-1, 1]$ which explains the rapid convergence. There are numerous examples of such integral equations in Kythe and Puri (2002).

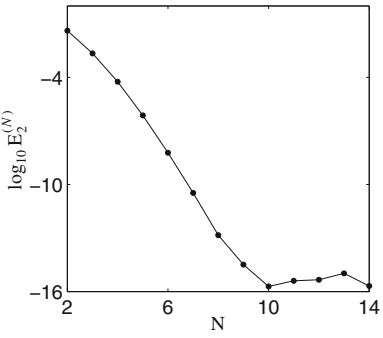

Fig. 5.1 Variation of the least squares error, $\log_{10} E_2^{(N)}$, for the integral equation, Eq. (5.7), versus the number of Gauss-Legendre quadrature points, N

5.3 Radiative Transfer and Neutron Transport Theory

The transfer of radiation in matter is an important aspect of atmospheric science and climate (Stamnes et al. 1988; Peraiah 1996; Liou 2002; Thomas and Stamnes 2002), astrophysics (Rybicki and Lightman 1979; Rybicki 1996), satellite remote sensing (Liang 2005), medical physics (Kan et al. 2013), neutron transport (Siewert 2000; Yilmazer and Kocar 2009) and other applications (Shore 2002). The propagation of radiation through a medium involves both absorption and reemission of the radiation. Radiative transfer theory is concerned with the variation of the radiative intensity with position in the medium, the direction of propagation as well as the frequency.

We consider the radiative transfer equation in recognition that almost every current publication in this field cites the original work by Chandrasekhar (1960). The numerical treatment introduced by Wick (1943) and developed further by Chandrasekhar (1960) is perhaps the first use of a quadrature, specifically the Gauss-Legendre quadrature, to reduce the radiative trnasfer equation, Eq. (5.14) to discrete form.

The system of interest is the plane-parallel atmosphere shown in Fig. 5.2. We define the radiative intensity, $I(z, \theta)$, with assumed azimuthal symmetry, as the energy contained in a pencil of radiation at position z moving in direction θ with respect to the polar direction. The intensity of radiation directed along z changes owing to the absorption of radiation by the medium, characterized by a mass attenuation coefficient, κ, and density $\rho(z)$. The change in incident intensity, I, directed at an angle θ with the vertical direction on traversing a slab of the medium of vertical thickness dz is

$$dI = -\kappa \rho I dz/\mu, \tag{5.11}$$

where $\mu = \cos\theta$. We now transform the vertical altitude, z, to optical depth, τ, defined by

$$d\tau = -\kappa \rho I dz, \tag{5.12}$$

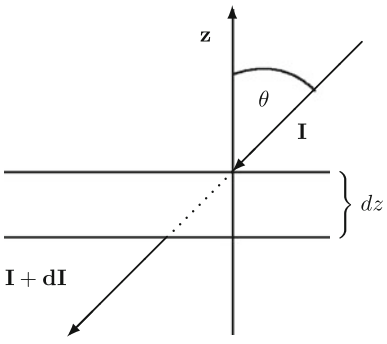

Fig. 5.2 Optical depth and radiative absorption

or in integral form

$$\tau(z) = \int_z^\infty \kappa\rho dz. \tag{5.13}$$

The integral of Eq. (5.11) in the absence of the emission of radiation from the medium gives the Beer-Lambert law,

$$I(\tau, \mu) = I(0)e^{-\tau(z)/\mu}.$$

In general, there is stimulated radiation emitted from the medium and the radiative intensity $I(\tau, \mu)$ is given by the radiative transfer equation,

$$\mu \frac{dI(\tau, \mu)}{d\tau} = I(\tau, \mu) - \frac{1}{2}\int_{-1}^{1} k(\mu, \mu')I(\tau, \mu')d\mu', \tag{5.14}$$

where the kernel, $k(\mu, \mu')$, accounts for the anisotropic absorption and reemission of radiation induced by the incident radiation.

With the assumption of isotropic scattering, that is $k(\mu, \mu') = 1$, we have the radiative transfer equation in the form

$$\mu \frac{dI(\tau, \mu)}{d\tau} = I(\tau, \mu) - \frac{1}{2}\int_{-1}^{1} I(\tau, \mu')d\mu'. \tag{5.15}$$

This is the simplest integro-differential equation of radiative transfer theory and is related to several other problems in rarefied gas dynamics. The radiative intensity, $I(\tau, \mu)$, varies with position, τ, and also with direction through μ. A collocation based on Gauss-Legendre quadratures is used to solve Eq. (5.15). The presentation follows the work in Chandrasekhar (1960) with a change in notation.

We use the quadrature on the interval $\mu \in [-1, 1]$ with $2N$ quadrature points μ_i, $i = \pm 1, \pm 2, \ldots, \pm N$ and corresponding weights w_i. We note that since the number of quadrature points is even, there is no point at $\mu = 0$. The discretized version of Eq. (5.14) is

$$\mu_i \frac{dI_i(\tau)}{d\tau} = I_i(\tau) - \frac{1}{2}\sum_{j=-N, j\neq 0}^{N} w_j I_j(\tau), \tag{5.16}$$

where $I_i(\tau) \equiv I(\tau, \mu_i)$. If the solution is assumed to be of the form, $I_i(\tau) = a_i e^{-\lambda\tau}$, then

$$a_i(1 + \mu_i\lambda) = \frac{1}{2}\sum_{j=-N, j\neq 0}^{N} w_j a_j = C, \tag{5.17}$$

with

$$a_i = \frac{C}{1 + \lambda\mu_i}, \tag{5.18}$$

which when substituted into Eq. (5.17) gives

$$1 = \frac{1}{2} \sum_{j=-N, j\neq 0}^{N} \frac{w_j}{1 + \lambda\mu_j} = \sum_{j=1}^{N} \frac{w_j}{1 - \lambda^2\mu_j^2}. \tag{5.19}$$

In the second equality we have used $w_{-j} = w_j$ and $\mu_{-j} = -\mu_j$. Because the sum of the weights is normalized to unity, $\sum_{j=1}^{N} w_j = 1$, $\lambda^2 = 0$ satisfies Eq. (5.19), which is the eigenvalue equation for the $2N - 2$ eigenvalues and two zero eigenvalues. The eigenvalues necessarily come in positive and negative pairs, $\pm\lambda_n, n = 1, 2, \ldots, N - 1$.

The roots of Eq. (5.19) each lie between the reciprocal of the quadrature points $[1/\mu_{i+1}, 1/\mu_i]$. A simple search combined with a bisection method gives the eigenvalues listed in Table 5.1. Alternatively, one can rewrite Eq. (5.19) as a polynomial of degree N and search for the roots of the polynomial (Kawabata et al. 1991). This can be numerically unstable for higher orders. The entries up to $N = 8$ agree with the limited results in Table VIII in Chandrasekhar (1960).

It is clear that the eigenvalues do not appear to converge to distinct values. The reason for this is that the discrete spectrum of the radiative transfer equation consists of only two zero eigenvalues. The remaining eigenvalues all lie in the continuum and hence there is no convergence. The mathematical properties of the continuum eigenfunctions have been the subject of considerable research (Case and Zweifel 1967; Liou 1973; McCormick and Kuščer 1973; Stamnes et al. 1988; Kuščer and McCormick 1991; Ven Den Eynde et al. 2007) (and references therein). In Sects. 5.5 and 5.6, we compare this behaviour with the spectral properties of the Boltzmann collision operators for a dilute monatomic gas that are characterized by an infinite number of discrete eigenvalues and a continuum.

Table 5.1 Eigenvalues of the radiative transfer equation, Eq. (5.14)

N	λ_1	λ_2	λ_3	λ_4	λ_5	λ_6	q
2	1.97203						0.6940
6	1.225211	3.202945					0.7039
8	1.103188	1.591779	4.458086				0.7069
10	1.059426	1.297814	1.987330	5.721175			0.7082
12	1.038632	1.183180	1.519150	2.394194	6.987899		0.7089
14	1.027106	1.125058	1.330224	1.752305	2.806740	8.256597	0.7094
						Exact[a]	0.710446

[a] Loyalka and Naz (2008)

We note that

$$I_i = b(\tau + s_i), \tag{5.20}$$

is also a solution to the radiative transfer equation, Eq. (5.14), which leads to the result

$$\mu_i = s_i - \frac{1}{2}\sum_{j=1}^{N} w_j s_j, \tag{5.21}$$

and satisfied by

$$s_i = q + \mu_i. \tag{5.22}$$

To ensure that the solution remains finite for large τ, the terms with positive λ_i must be eliminated from the solution. Thus the general solution is

$$I_i = b\left[\sum_{n=1}^{N-1} \frac{c_n e^{-\lambda_n \tau}}{1 + \mu_i \lambda_n} + \tau + \mu_i + q\right]. \tag{5.23}$$

The constants c_n $(n = 1, 2, \ldots, N-1)$ and q are determined with the boundary condition that there is no incident radiation at $\tau = 0$, that is,

$$I(0, \mu) = 0, \quad -1 \le \mu \le 0. \tag{5.24}$$

With this boundary condition, $c_{-n} = 0$ at $\tau = 0$ and

$$\sum_{n=1}^{N-1} \frac{c_n}{1 - \lambda_n \mu_i} - \mu_i + q = 0 \quad (i = 1, 2, \ldots, N), \tag{5.25}$$

which are N equations for the $N-1$ constants, c_n, and the extrapolation length, q. The physical significance of the extrapolation length is discussed later.

The results for q in Table 5.1 show that the convergence of the Gauss-Legendre quadrature is slow. This arises because the numerical method cannot provide a good fit to the boundary condition that requires that the radiative intensity vanishes on the half space $\mu \in [-1, 0]$. There have been many discussions and improvements and in particular the use of half-range Legendre polynomials referred to as the "double Gauss" method (Sykes 1951; Liou 1973; Stamnes et al. 1988; Ven Den Eynde et al. 2007).

Radiative transfer theory has its origins in astrophysics (Rybicki and Lightman 1979) and the interest to determine the intensity of the emergent radiation from a star and the observation that it decreases from the centre of the disc to the limb, a phenomenon known as limb darkening (Milne 1921). Thus, the radiative transfer

problem is often referred to as a Milne problem which has many different variants. We provide a very brief overview of the analysis and refer readers to the original reference (Chandrasekhar 1960) for further details. It is useful to define two moments of the radiative intensity, namely

$$F = 2\sum_{i=1}^{N-1} w_i \mu_i I_i,$$
$$K = \frac{1}{2}\sum_{i=1}^{N-1} w_i \mu_i^2 I_i, \tag{5.26}$$

and one can show that $F = 4b/3$, where b is the multiplicative constant in Eq. (5.23). We can also show that $K = F(\tau + q)/4$. The emergent intensity is then

$$I(0, \mu) = \frac{3}{4} F \sum_{k=1}^{N-1} \frac{c_k}{1 + \lambda_k \mu} + \mu + q, \tag{5.27}$$

which is one of the important results sought.

The emergent radiation can be related to the Chandrasekhar $H(\mu)$ function. This requires several new definitions and considerable but straightforward algebra (Chandrasekhar 1960). The result is the relation

$$I(0, \mu) = \frac{\sqrt{3}}{4} F H(\mu), \tag{5.28}$$

where the Chandrasekhar H function is the solution of the nonlinear integral equation

$$H(\mu) = 1 + \frac{1}{2} a H(\mu) \int_0^1 \frac{H(\mu')}{\mu + \mu'} d\mu'. \tag{5.29}$$

Although the detailed derivations have not been provided, this nonlinear integral equation is of considerable interest as the object of several different numerical solution methods. It has been solved with a Simpson's rule (Hiroi 1994), rational Chebyshev functions (Boyd 2005), analytic approximations (Davidović et al. 2008), polynomial approximations (Kawabata and Limaye 2011), integral representations (Jablonski 2013) and other approaches cited in these references. It is remarkable that there is continued interest almost 70 years after the original publication by Chandrasekhar and Breen (1947).

In Sect. 5.7.2, we consider the Milne problem of rarefied gas dynamics (see Fig. 5.16) for a binary hard sphere gas with a test particle of mass m dilutely dispersed in a background gas of mass M. The Milne problem reduces to the radiative transfer equation for the Lorentz limit, that is $M/m \to \infty$. We use a spectral method to solve the Milne problem based on the concepts developed in this section. A similar

Milne problem was studied with a Fokker-Planck equation for Coulomb collisions (Barrett et al. 1992) as well as in the modeling of the sheath problem in plasma physics (Vasenkov and Shizgal 2000). The Milne problem is the basis for a model of the escape of light atoms from a planetary atmosphere presented in Sect. 5.7.3 (Fahr and Shizgal 1983; Shizgal and Blackmore 1986).

Neutron transport theory is the study of the time and spatial dependence of the neutron velocity distribution function in different materials or moderators given a steady or pulsed source of neutrons. The theory is based on the Boltzmann equation for neutrons analogous to dilute gases. It remains a very active area of research for physicists, applied mathematicians and numerical analysts. Neutron transport has developed alongside work in radiative transfer theory (Kourganoff 1963). The distinction between the two fields is that in radiative transfer the photons move at the speed of light and for neutrons there is a speed distribution to determine. Often the radiative transfer problem noted in Eq. (5.14) is referred to as the "one speed" problem. This implies that the neutrons all move at the same speed as do photons. There are several standard references for both subjects (Davison 1957; Kourganoff 1963; Williams 1966; Case and Zweifel 1967; Thomas and Stamnes 2002). An historical account of the development of the subject was provided by Shore (2002).

5.4 The Boltzmann Equation and Transport Theory

The central quantity of interest in the kinetic theory of gases is the distribution function for a large collection or ensemble of particles without internal degrees of freedom representing some species such as electrons, ions, neutrons, photons, atoms, etc. At sufficiently low densities, the single particle distribution function, f($\mathbf{v}$, $\mathbf{r}$,t), is sufficient to describe the state of the system. The distribution function that depends on the three dimensional velocity, $\mathbf{v}$, the three dimensional position $\mathbf{r}$, and the time, t, is defined such that

$$f(\mathbf{v}, \mathbf{r}, t)\mathrm{d}\mathbf{v}\mathrm{d}\mathbf{r} = \text{ number of particles with velocity in } [\mathbf{v}, \mathbf{v} + \mathrm{d}\mathbf{v}] \text{ and position in } [\mathbf{r}, \mathbf{r} + \mathrm{d}\mathbf{r}] \text{ at time t.}$$

The Boltzmann equation is a seven dimensional nonlinear integro-differential equation for the one particle distribution function, $f(\mathbf{v}, \mathbf{r}, t)$, given by

$$\frac{\partial f}{\partial t} + \mathbf{v} \cdot \nabla f + \frac{\mathcal{F}}{m} \cdot \nabla_{\mathbf{v}} f = \int \int [f' f_1' - f f_1] g \sigma(g, \Omega) d\Omega d\mathbf{v_1}, \tag{5.30}$$

where the gradient operators are ∇ in $\mathbf{r}$ and $\nabla_{\mathbf{v}}$ in $\mathbf{v}$.

The three terms on the left hand side of this equation are collectively referred to as the drift term where $\mathcal{F}$ is an external force. The term on the right hand side is the nonlinear collision term parameterized by the elastic collision cross section, $\sigma(g, \Omega)$, where the relative velocity of a pair of particles is $\mathbf{g} = \mathbf{v}_1 - \mathbf{v}$ and Ω is the scattering

solid angle. The prime, $f' \equiv f(\mathbf{v}')$, denotes the post-collisional velocity, $\mathbf{v}'$, and is expressed in terms of the pre-collisional velocity, $\mathbf{v}$, as given by Eqs. (5.47)–(5.49). The kinetic theory of gases is an integral part of theoretical chemistry and physics (Hirschfelder et al. 1954; Liboff 2003; Kremer 2010).

A Boltzmann equation is used to model a large number of systems in astrophysics (Spitzer and Härm 1958; Lightman and Shapiro 1978; Buhmann 2004; Binney and Tremaine 2008), space science (Fahr and Shizgal 1983; Pierrard and Lazar 2010; Khazanov 2011), semiconductor physics (Jüngel 2009), nuclear reactor technologies (Hebert 2009), radiative transfer (Chandrasekhar 1960), radiotherapy (Kan et al. 2013) plasma physics (Boyd and Sanderson 2003), fusion machines (Atenzi and Meyer-Ter-Vehn 2004) and many more. The different systems and processes that can be studied with the Boltzmann equation or Boltzmann-like equations is truly remarkable.

The main objective of this section is to apply spectral and pseudospectral methods to the integral equations that arise in the application of the Boltzmann equation to several physical problems. A brief overview of the derivation of these integral equations in kinetic theory is provided in the sections that follow.

5.4.1 The Chapman-Enskog Method of Solution of the Boltzmann Equation for Transport Coefficients

The Chapman-Enskog method of solution of the Boltzmann equation was developed independently by Sydney Chapman[1] and David Enskog[2] for a particular purpose, namely the calculation of transport coefficients for a dilute monatomic gas. The transport coefficients are the diffusion coefficient, the viscosity and the heat conductivity. They serve to relate fluxes of particles, momentum and energy with the corresponding gradients. These relations between the fluxes and gradients such as Fourier's law for heat conduction (de Groot and Mazur 1984) are referred to as linear phenomenological laws. The Chapman-Enskog method provides a separate integral equation for each transport process. The transport coefficients, such as the viscosity discussed in Sect. 5.4.5, are expressed as integrals of the solution of a particular integral equation. The details of the Chapman-Enskog method are described in standard texts (Huang 1967; Chapman and Cowling 1970; Ferziger and Kaper 1972; Kremer 2010). A concise overview of the methodology follows.

A small departure from a Maxwellian is assumed to occur owing to small macroscopic drift velocity and/or temperature gradients. The distribution function is

[1] Sydney Chapman (1888–1970) was a British mathematician and geophysicist who developed the Chapman-Enksog method of solution of the Boltzmann equation and contributed to the theory of stochastic processes. He also made several fundamental contributions to geophysics.

[2] David Enskog (1884–1947) was a Swedish mathematical physicist who contributed to the kinetic theory of gases with the method of solution of the Boltzmann equation developed with Chapman.

written as a small perturbation of the "local" Maxwellian, $F[\mathbf{v}, n(\mathbf{r}, t), T(\mathbf{r}, t), W(\mathbf{r}, t)]$, parameterized by the particle density $n(\mathbf{r}, t)$, the temperature, $T(\mathbf{r}, t)$ and the flow velocity of the gas, $W(\mathbf{r}, t)$; see Eq. (5.32). With the assumption that the distribution is slightly perturbed from the local Maxwellian, F, we set

$$f(\mathbf{v}, \mathbf{r}, t) = F(\mathbf{v}, n, T, \mathbf{W})\Big[1 + \epsilon\phi(\mathbf{v})\Big], \tag{5.31}$$

where the parameter ϵ is taken to be very small and $\phi(\mathbf{v})$ is sought. Equation (5.31) is often extended as a power series in ϵ as discussed later.

The Chapman-Enskog method proceeds as follows. With the substitution of Eq. (5.31) in (5.30), the term zeroth order in ϵ is

$$\int\int [F'F_1' - FF_1] g\sigma(g, \Omega) d\Omega d\mathbf{v_1} = 0,$$

and defines the local Maxwellian,

$$F(v, n, \mathbf{W}, T) = n(\mathbf{r}, t)\left[\frac{m}{2\pi k_B T(\mathbf{r}, t)}\right]^{3/2} \exp\left[\frac{-m(\mathbf{v} - \mathbf{W}(\mathbf{r}, t))^2}{2k_B T(\mathbf{r}, t)}\right], \tag{5.32}$$

where k_B is the Boltzmann constant, m is the particle mass, and the number density, $n(\mathbf{r}, t)$, is defined by,

$$n(\mathbf{r}, t) = \int F_{LM}(\mathbf{v}, \mathbf{r}, t) d\mathbf{v}. \tag{5.33}$$

The local Maxwellian, Eq. (5.32), supports a flux and the drift or flow velocity, $\mathbf{W}(\mathbf{r}, t)$, is

$$\mathbf{W}(\mathbf{r}, t) = \frac{1}{n(\mathbf{r}, t)} \int F_{LM}(\mathbf{v}, \mathbf{r}, t) \mathbf{v} d\mathbf{v}. \tag{5.34}$$

The temperature, $T(\mathbf{r}, t)$, is a measure of the average thermal energy of the gas and is related to the diagonal element of the pressure tensor

$$\mathbf{P} = m \int f(\mathbf{v}, \mathbf{r}, t)(\mathbf{v} - \mathbf{W})(\mathbf{v} - \mathbf{W}) d\mathbf{v}, \tag{5.35}$$

and $\mathbf{P}^{(LM)} = p\mathbf{I}$ where $\mathbf{I}$ is the unit matrix and $p = nk_B T$ is the ideal gas law.

For nonequilibrium systems, there is a departure from the equilibrium Maxwell-Boltzmann distribution and the pressure tensor is of the form

$$\mathbf{P} = p\mathbf{I} + \mathbf{\Pi}. \tag{5.36}$$

where $\mathbf{\Pi}$ depends on the velocity gradients. If there is a temperature gradient present, then there is a heat flux defined as

$$\mathbf{q} = \frac{m}{2}\int f(\mathbf{v},\mathbf{r},t)(\mathbf{v}-\mathbf{W})(\mathbf{v}-\mathbf{W})^2 d\mathbf{v}. \tag{5.37}$$

The Boltzmann equation is rewritten with the collision term multiplied by the factor $1/\epsilon$ so as to explicitly take into account the assumption that the collision operator is dominant relative to the drift term, that is

$$\frac{\partial f}{\partial t} + \mathbf{v}\cdot\nabla f + \frac{\mathcal{F}}{m}\cdot\nabla_{\mathbf{v}} f = \frac{1}{\epsilon}\int\int [f' f_1' - f f_1] g\sigma(g,\Omega) d\Omega d\mathbf{v_1}. \tag{5.38}$$

The parameter ϵ is often identified as the Knudsen[3] number, the ratio of the mean-free-path, L_{mfp}, to some macroscopic length scale, H, that is $Kn = L_{mfp}/H$. In the collision dominated situation, $Kn \ll 1$.

The equation of order ϵ is obtained with the drift term evaluated with $f \to F$ and the collision operator linear in $\phi(v)$. To this order in ϵ, the derivatives in the drift term on the left hand side of the Boltzmann equation are evaluated implicitly through the $\mathbf{r}$ and t variation of $n(\mathbf{r},t)$, $T(\mathbf{r},t)$, $W(\mathbf{r},t)$ in the local Maxwellian, and $\phi(\mathbf{v})$ does not contribute.

In order to evaluate the left hand side of Eq. (5.30) in this way, we need the $(\mathbf{r},t)$ variation of n, $\mathbf{W}$ and T. These relations can be obtained by noting that the particle number, momentum and energy are conserved in a binary elastic collision. Thus, we multiply successively the Boltzmann equation by m, $m\mathbf{v}$ and $mv^2/2$, known as the "summational invariants", and integrate over $\mathbf{v}$. The integral over the collision operator multiplied by these quantities gives zero owing to their conservation. The details are provided in other texts (Hirschfelder et al. 1954; Chapman and Cowling 1970; Ferziger and Kaper 1972). The result of this calculation, after some algebra, of the so-called "equations of change", are the set of hydrodynamic, non-dissipative fluid dynamic equations, referred to as the Euler equations, given by

$$\begin{aligned} \frac{\partial\rho}{\partial t} + \nabla\cdot(\rho\mathbf{W}) &= 0, \\ \rho\frac{D\mathbf{W}}{Dt} + \nabla p &= \rho\mathcal{F}, \\ nk\frac{DT}{Dt} + \frac{3T}{2}(\nabla\cdot\mathbf{W}) &= 0, \end{aligned} \tag{5.39}$$

where $\rho(\mathbf{r},t) = mn(\mathbf{r},t)$ and

$$\frac{D}{Dt} = \frac{\partial}{\partial t} + \mathbf{W}\cdot\nabla.$$

[3] Martin Knudsen (1871–1949) was a Danish physicist known for his work on the kinetic theory of gases and the Knudsen number which measures the degree of rarefaction of dilute gases.

The term linear in ϵ which gives the integral equation for $\phi(\mathbf{v})$ involves the evaluation of the drift term with f replaced with F and the evaluation of the drift term operator on F implicitly using the Euler fluid equations. The result, after considerable tensorial algebra using the chain rule for the derivatives, is the integral equation

$$J(\phi) = F\left[(x^2 - 5/2)\mathbf{v} \cdot \nabla \ln T + 2(\mathbf{vv} - \frac{1}{3}v^2\mathbf{I}) : \nabla \mathbf{W}\right], \tag{5.40}$$

where $x = v\sqrt{m/2k_BT}$ is the reduced speed and the linearized collision operator is given by

$$J(\phi) = \int\int F_1 F\left[\phi_1' + \phi' - \phi_1 + \phi\right]\sigma(g,\theta)d\Omega d\mathbf{v}_1. \tag{5.41}$$

It can be shown that J is a negative definite self-adjoint rotationally invariant operator. The matrix representation of J in Legendre polynomials is diagonal as previously noted in the discussion of the quadrature evaluation of the eigenvalues for the Maxwell-molecule model in Chap. 3.

We now write the solution of Eq. (5.40) in the form

$$\phi = -\mathbf{A} \cdot \nabla \ln T - \mathbf{B} : \nabla \mathbf{W}, \tag{5.42}$$

where the vector $\mathbf{A}$ and tensor $\mathbf{B}$ are written as

$$\begin{aligned} \mathbf{A} &= A(v)\mathbf{v}, \\ \mathbf{B} &= B(v)\mathbf{v}^o\mathbf{v}, \end{aligned} \tag{5.43}$$

and $\mathbf{v}^o\mathbf{v} = \mathbf{vv} - \frac{1}{3}v^2\mathbf{I}$ is a traceless tensor. The functions $A(v)$ and $B(v)$ satisfy the integral equations,

$$J[A(v)\mathbf{v}] = (x^2 - 5/2)\mathbf{v}F, \tag{5.44}$$

and

$$J[B(v)\mathbf{v}^o\mathbf{v}] = 2\mathbf{v}^o\mathbf{v}F. \tag{5.45}$$

where $x = v\sqrt{m/2k_BT_b}$ is the reduced speed. The details of this calculation, which involve considerable tensorial algebra, are straightforward and can be found in standard references (Huang 1967; Chapman and Cowling 1970; Ferziger and Kaper 1972). An important aspect of the Chapman-Enskog method is that the solutions of the homogeneous equations corresponding to Eqs. (5.44) and (5.45), namely the "summational invariants", are orthogonal to the inhomogeneous functions in these integral equations. This ensures the existence of solutions. We will discuss this again in Sect. 5.4.4 for a simpler physical problem.

The solutions $A(v)$ and $B(v)$ are used to determine the temperature dependence of the heat conductivity and viscosity for a dilute gas given the differential cross section, $\sigma(g, \Omega)$, for binary particle collisions. The Sonine-Laguerre polynomials, $S_\alpha^{(n)}(x^2)$, are the basis functions almost always used to solve these integral equations with $\alpha = 3/2$ for Eq. (5.44) and $\alpha = 5/2$ for Eq. (5.45). This formalism forms the basis for the determination of interatomic potentials from measurements of transport coefficients (Hirschfelder et al. 1954; Pascal and Brun 1993; Oh 2013).

A different integral equation is solved for each transport process and the transport processes of different tensorial order do not couple, consistent with the Curie principle of irreversible thermodynamics (de Groot and Mazur 1984); see also (Andersen 1969) and Appendix A of Shizgal and Karplus (1970) where chemical reactions are included. Mixtures of gases can also be considered and the algebra becomes more involved. We note that theoretical descriptions of transport phenomena in polyatomic gases are available (Wang-Chang and Uhlenbeck 1951; Snider 1960; McCourt et al. 1991; Singh et al. 1996; Brun 2009). Our primary interest is the spectral and pseudospectral methods for the solution of the integral equations.

The Chapman-Enskog method provides to order ϵ the Navier-Stokes equations of fluid mechanics by including the dissipative transport terms in the "equations of change". The method is usually presented as a power series expansion in ϵ with terms of order ϵ^2 and ϵ^3 in addition to the term in ϵ in Eq. (5.31). This expansion is believed to be a type of asymptotic expansion where perhaps only the first few terms have physical meaning. At each level, the resulting hydrodynamic equations are modified, that is the Euler equations for zero order in ϵ, the Navier-Stokes equations of order ϵ and for higher orders in ϵ there are the Burnett and the Super-Burnett hydrodynamic equations (Grad 1949; Cercignani 1988). A very good overview of the effort to extend the description of gaseous flows to the larger Knudsen number regime was provided by Agarwal et al. (2001). This overlaps the approach developed by Grad (1949) and referred to as the Grad 13-moment method (Struchtrup 2005).

The breakdown of hydrostatic equilibrium and the Chapman-Enskog approach occurs in particular at high altitudes of the terrestrial atmopshere where collisions are infrequent (Fahr and Shizgal 1983). This also applies to the solar atmosphere for which there is a supersonic expansion of the stellar plasma, referred to as the solar wind. There are both fluid models (Parker 1965) and kinetic theory models (Lemaire and Scherer 1973) to describe the expansion of the solar atmosphere. This is another example of the need for a kinetic theory in the $Kn \approx 1$ regime (Lemaire 2010; Echim et al. 2011). The loss of ions from the terrestrial atmosphere at high latitudes along open magnetic field lines, referred to as the polar wind (Lemaire and Scherer 1970; Lie-Svendsen and Rees 1996; Pierrard and Lemaire 1998) is another example. There is an ongoing discussion as to the relationship of both fluid and kinetic models for the solar wind expansion (Parker 2010; Lemaire 2010) These discussions are important to note but are beyond the scope of this book. However, there is some overlap with the Milne problem in Sect. 5.7.2 and the escape of light atoms or ions from planetary atmospheres in Sect. 5.7.3.

5.4.2 The Linearized Collision Operator, J, in the Boltzmann Equation

A fundamental problem in the kinetic theory of gases is the relaxation of an initial nonequilibrium distribution to the equilibrium Maxwellian distribution. We consider a one component spatially uniform gaseous system for which the linearized Boltzmann equation in the absence of external fields is the initial value problem of the form

$$\frac{\partial f(\mathbf{v},t)}{\partial t} = J[f(\mathbf{v},t)]. \tag{5.46}$$

The kinematics of an elastic collision that relate the post-collisional ($\mathbf{v}'$) and pre-collisional ($\mathbf{v}$) velocity variables in Eq. (5.41) are required to define the collision operator, J, (Chapman and Cowling 1970; Cercignani 1988; Ferziger and Kaper 1972; Liboff 2003; Kremer 2010). In an elastic collision, depicted in Fig. 5.3, the relative velocity vector, $\mathbf{g}$, is rotated to the new orientation, $\mathbf{g}'$, while the magnitudes remain the same, that is $|\mathbf{g}'| = |\mathbf{g}|$ owing to energy conservation. The vector $\mathbf{k}$, referred to as the "apse-line vector", is the external bisector so that $\theta = \pi - 2\chi$. Thus, we have the relation

$$\mathbf{g}' = \mathbf{g} - 2(\mathbf{k}\cdot\mathbf{g})\mathbf{k}. \tag{5.47}$$

In terms of the centre of mass velocity

$$\mathbf{G} = \frac{m_1\mathbf{v}_1 + m_2\mathbf{v}_2}{m_1 + m_2}, \tag{5.48}$$

we have that

$$\begin{aligned} \mathbf{v}_1' &= \mathbf{g}' + \frac{m_1 + m_2}{m_1}\mathbf{G}, \\ \mathbf{v}_2' &= \mathbf{g}' - \frac{m_1 + m_2}{m_2}\mathbf{G}. \end{aligned} \tag{5.49}$$

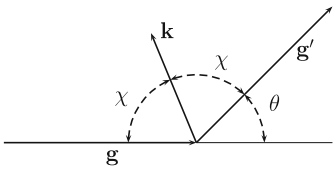

Fig. 5.3 Kinematics of an elastic collision; $\mathbf{g}$ and $\mathbf{g}'$ are the relative velocities before and after a collision, θ is the scattering angle, $\mathbf{k}$ is the external bisector of the angle between $\mathbf{g}$ and $\mathbf{g}'$ defined by χ

The centre-of-mass velocity is conserved, so that, $\mathbf{G}' = \mathbf{G}$. For the one component gas considered here, $m_1 = m_2$. The variables $(\mathbf{v}_1', \mathbf{v}_2')$ are related to the pair $(\mathbf{v}_1, \mathbf{v_2})$ with the substitution of $\mathbf{g}'$ from Eq. (5.47) into (5.49).

The linearized integral collision operator in Eq. (5.41) can be written in terms of a kernel so that we can recast Eq. (5.46) in the form,

$$\frac{\partial f(\mathbf{v}, t)}{\partial t} = \int K_J(\mathbf{v}, \mathbf{u}) f(\mathbf{u}) d\mathbf{u} - Z(v) f(\mathbf{v}, t), \tag{5.50}$$

where the collision frequency is

$$Z(v) = f(v) \int \int f_1(\mathbf{v}_1) \sigma_t(g) d\mathbf{v}_1. \tag{5.51}$$

The kernel for the hard sphere cross section, $\sigma(g, \Omega) = d^2/4$, expressed in reduced velocity variables, $\mathbf{x} = \mathbf{v}\sqrt{m/2k_BT}$ and $\mathbf{y} = \mathbf{u}\sqrt{m/2k_BT}$, is

$$K_J(x, y, \overline{\mu}) = \frac{Z(0)}{\pi\sqrt{\pi}} e^{-x^2} \left[\frac{2}{\sqrt{x^2 + y^2 - 2xy\overline{\mu}}} \exp\left[\frac{x^2 y^2 (1 - \overline{\mu}^2)}{x^2 + y^2 - 2xy\overline{\mu}} \right] - \sqrt{x^2 + y^2 - 2xy\overline{\mu}} \right], \tag{5.52}$$

where $\overline{\mu} = \cos\theta'$ and θ' is the angle between $\mathbf{x}$ and $\mathbf{y}$ and $Z(0) = n_b \pi d^2 \sqrt{2k_BT/m}$. The derivation of this kernel is lengthy but straightforward and is provided elsewhere (Nielsen and Bak 1964; Monchick and Mason 1967; Chapman and Cowling 1970; Ferziger and Kaper 1972; Williams 1976). For most of the applications presented here, the hard sphere cross section is used, although the kernel in Eq. (5.50) can be written for arbitrary differential scattering cross section (Kapral and Ross 1970; Sospedra-Alfonso and Shizgal 2013).

As the kernel depends only on the angle between $\mathbf{x}$ and $\mathbf{y}$, the operator J is rotationally invariant and diagonal in the Legendre polynomial basis set. It is customary in kinetic theory and radiative transfer theory to expand the kernel in Legendre polynomials in $\overline{\mu}$, that is,

$$K_J(x, y, \overline{\mu}) = \sum_{\ell=0}^{\infty} k_J^{(\ell)}(x, y) P_\ell(\overline{\mu}), \tag{5.53}$$

where the scalar kernels are

$$k_J^{(\ell)}(x, y) = \frac{2\ell + 1}{2} \int_{-1}^{1} K_J(x, y, \overline{\mu}) P_\ell(\overline{\mu}) d\overline{\mu}. \tag{5.54}$$

In radiative transfer theory this is often referred to as a P_N method with the kernel replaced with an analogous photon scattering phase function (Liou 2002; Thomas and Stamnes 2002; Ganapol 2008).

For the hard sphere cross section, the kernels, $k_J^{(\ell)}(x, y)$, are known analytically versus x and y for the lower order ℓ values as provided in Sect. 4.2.1 in the book by Williams (1971) and also by other researchers (Pekeris 1955; Pekeris and Alterman 1957; Desai and Nelkin 1966; Siewert 2002). The kernels can be calculated numerically with a Gauss-Legendre quadrature in Eq. (5.54) (Shizgal 1981a). We use the quadrature algorithms developed in Chap. 2 and discussed further in Chap. 3 to solve the initial value problem, Eq. (5.46), (Hoare and Kaplinsky 1970; Shizgal and Blackmore 1983; Shizgal 1984).

5.4.3 Matrix Representation of the Spherical Component ($\ell = 0$) of J in Sonine-Laguerre Basis Functions

It has been traditional in kinetic theory to solve the integral equations for the transport coefficients with the expansions in the direct product basis set of the Sonine-Laguerre basis functions and the spherical harmonics or Legendre polynomials. The choice of basis function is dictated in part by the fact that the Sonine-Laguerre polynomials are the eigenfunctions of J for the Maxwell molecule collision model as discussed in Sect. 3.6.4, although this is a not a sufficient reason for this choice. However, it is useful to note that the inhomogeneous functions for the Chapman-Enskog integral equations for the transport coefficients, Eqs. (5.44) and (5.45), are low order polynomials in x^2. The resulting inhomogeneous vector of the linear algebraic equations that are inverted in the spectral solution for the viscosity has only one nonzero component (Loyalka et al. 2007).

We restrict the discussion of the initial value problem, Eq. (5.46), to initial isotropic distributions, so that the eigenvalues, λ_n, and eigenfunctions, $\psi_n(x)$, are for $\ell = 0$ unless otherwise noted. We consider only the $\ell = 0$ component of the collision operator and do not show this explicitly to simplify the notation, and write

$$\frac{\partial f(x,t)}{\partial t} = J[f(x,t)]. \tag{5.55}$$

We solve Eq. (5.55) with the expansion of the initial distribution function in the eigenfunctions of J, that is

$$f(x,0) = \sum_{n=0}^{N} c_n \psi_n(x^2), \tag{5.56}$$

where

$$J[\psi_n(x^2)] = -\lambda_n \psi_n(x^2). \tag{5.57}$$

The solution of Eq. (5.55) can be written formally in terms of an evolution operator similar to the time dependent Schrödinger equation, that is

$$\begin{aligned} f(x,t) &= e^{Jt} f(x,0), \\ &= \sum_{n=2}^{\infty} c_n \psi_n(x^2) e^{-\lambda_n t}, \end{aligned} \tag{5.58}$$

where we have used

$$e^{Jt}\psi_n(x^2) = e^{-\lambda_n t}\psi_n(x^2). \tag{5.59}$$

The evolution operator is defined in term of the expansion of the exponential, $e^{Jt} = 1 + Jt + J^2t^2/2 + \cdots$ analogous to the evolution operator in quantum mechanics (Balint-Kurti 2008) discussed in Sect. 4.6.6. In the sections that follow, we are interested in the eigenvalue problem, Eq. (5.57), expressed in terms of a variational theorem. This eigenvalue problem is a fundamental aspect of the kinetic theory of gases, analogous to spectral theory in quantum mechanics.

The matrix elements of the collision operator for isotropic problems are defined by

$$J_{nm}^{(0)} = \int\int\int F_1 F_2 S_1^{(n)} \left[S_1^{(m)'} + S_2^{(m)'} - S_1^{(m)} - S_2^{(m)} \right] \sigma g d\Omega d\mathbf{v}_1 d\mathbf{v}_2, \tag{5.60}$$

which can be shown to be symmetric, that is, $J_{nm}^{(0)} = J_{mn}^{(0)}$. We denote the Sonine-Laguerre polynomials for $\ell = 0$ as $S^{(n)}(x^2)$ given explicitly by

$$\begin{aligned} S^{(n)}(x^2) &= \sum_{k=0}^{n} (-1)^k \frac{\Gamma(n+3/2)}{\Gamma(k+3/2)(n-k)k!} x^{2k}, \\ &= \sum_{k=0}^{n} S_{nk} x^{2k}, \end{aligned} \tag{5.61}$$

and orthogonal in accordance with

$$\int_0^{\infty} e^{-x^2} S^{(n)}(x^2) S^{(m)}(x^2) x dx^2 = \frac{\Gamma(n+3/2)}{n!} \delta_{nm}. \tag{5.62}$$

We evaluate the matrix elements with the generating function for the Sonine-Laguerre polynomials

$$G(t,x^2) = \frac{\exp[tx^2/(t-1)]}{(1-t)^{3/2}} = \sum_{k=0}^{\infty} S^{(k)}(x^2) t^k, \quad |t| < 1. \tag{5.63}$$

The matrix elements $J_{nm}^{(0)}$ are evaluated with the one matrix element between two generating functions, that is the element $\langle G_t|J|G_s\rangle$. This technique was first introduced by Mott-Smith (1954) and used subsequently by other researchers (Ford 1968; Foch and Ford 1970; Shizgal and Karplus 1971; Shizgal and Fitzpatrick 1974; Gust and Reichl 2009; Shizgal and Dridi 2010). The desired matrix element, $J_{nm}^{(0)}$, is then the coefficient of $s^n t^m$ of the expression below.

$$\begin{aligned}\langle G_s|J|G_t\rangle &= \frac{2Z(0)}{\sqrt{\pi}} s^2 t^2 \left(\frac{\sqrt{1-\frac{1}{2}s-\frac{1}{2}t}}{(1-st)^2}\right), \\ &= \sum_{n=2}^{\infty}\sum_{m=2}^{\infty} J_{nm}^{(0)} s^n t^m, \end{aligned} \tag{5.64}$$

Owing to particle number and energy conservation, $J_{nm}^{(0)} = 0$ for $(n, m) = (0, 1)$ and consequently $\lambda_0 = 0$ and $\lambda_1 = 0$. The evaluation of the generating function matrix element, Eq. (5.64), involves the kinematics of binary particle collisions, Eqs. (5.47)–(5.49).

It has been shown (Ford 1968; Foch and Ford 1970; Lindenfeld and Shizgal 1979a; Gust and Reichl 2009) that the matrix elements are given by

$$J_{nm}^{(0)} = \frac{2Z(0)}{\sqrt{\pi}2^{n+m}} \sqrt{\frac{n!m!}{8\Gamma(n+\frac{3}{2})\Gamma(n+\frac{3}{2})}} \sum_{j=0}^{N_m} \frac{4^j B_j \Gamma(n+m-2j-\frac{1}{2})}{(n-j)!(m-j)!}, \tag{5.65}$$

where $B_j = j - 1 + \delta_{j0}$ and $N_m = \min(n, m)$. We use this representation of J in the next section to analyze nonequilibrium effects for a model reactive system and in Sect. 5.5.1 for variational estimates of the eigenvalues and eigenfunctions of the operator.

It is useful to note that the matrix elements given by Eq. (5.65) involve both the integral operator in Eq. (5.50) and the collision frequency, $Z(x)$. For cross sections determined with classical mechanics, the integral operator and the collision frequency are not defined owing to the divergence of the differential scattering cross section at small scattering angles. By contrast, quantum cross sections are finite and the two terms in the collision operator can be considered separately. The matrix elements of the Hamiltonian for a problem in quantum mechanics is the sum of the matrix elements of the kinetic energy operator and the matrix elements of the potential often computed separately. The quadrature evaluations of the matrix elements of the potential in a Schrödinger equation (Harris et al. 1965; Dickinson and Certain 1968) are often cited as the origin of pseudospectral methods in quantum chemistry (Light and Carrington Jr. 2000).

5.4.4 Spectral Solution of the Boltzmann Equation for the Departure from Maxwellian for an Elementary Reaction in a Spatially Uniform System

It is well known that chemical reactions proceed with a concommitant departure of the particle distribution functions from equilibrium. This subject has a long history both for systems with only translational energy (Prigogine and Xhrouet 1949; Shizgal and Karplus 1970; Shizgal and Fitzpatrick 1978; Ross and Mazur 1961; Alves et al. 2011; Kustova and Giordano 2011; Dziekan et al. 2012) as well as for molecular systems with internal vibrational and rotational states (Shizgal 1972; Shizgal and Lordet 1996; Pascal and Brun 1993; Brun 2009). The theoretical treatment of such systems is based on a Boltzmann equation for the velocity distribution and in some instances on a Master equation for the distribution of vibrational and rotational states (Kim and Boyd 2013).

In this section, we consider a one-component atomic system (without internal degrees of freedom) and a single reactive process. We add a single reactive loss term to the Boltzmann eqation, Eq. (5.55), to model the nonequilibrium effects that arise from the reaction. An estimate of the departure from the equilibrium rate of reaction is obtained with a Chapman-Enskog method similar to its application to the calculation of transport coefficients discussed in Sect. 5.4.1. However, for this uniform system the Chapman-Enskog method is more transparent. We also discuss a nonlinear variational approach that provides a different approximate solution of the Boltzmann equation (Present and Morris 1969).

We consider a one component system undergoing a reaction

$$A + A \rightarrow \text{products}, \tag{5.66}$$

with a total reactive cross section, $\sigma_r(g)$, dependent on the relative speed, g, of the reactants. The spatially homogeneous Boltzmann equation for the isotropic distribution function of A is

$$\frac{\partial f(v,t)}{\partial t} = J[f(v,t)] - \epsilon f(v,t) \int f(v_1,t) g \sigma_r(g) d\mathbf{v_1}, \tag{5.67}$$

where a reactive collision term corresponding to the loss of particles by reaction is added to the right hand side of Eq. (5.46). The integral reactive term is the reactive collision frequency, Eq. (3.35), of Sect. 3.6. The parameter ϵ, which is assumed small, multiplies the reactive term and thus the reaction is considered as a small perturbation of the elastic collision term, J. The parameter ϵ is defined in terms of the elastic and reactive cross sections; see after Eq. (5.77).

The particle number is not conserved and we have on integration of Eq. (5.67) that the rate of reaction is

$$\frac{dn}{dt} = -\epsilon \iint f f_1 g \sigma_r(g) d\mathbf{v_1} d\mathbf{v}. \tag{5.68}$$

The local temperature also changes owing to the loss of energetic particles as given by

$$\frac{dT}{dt} = -\epsilon \frac{2T}{3n} \int\int f f_1 \left[\frac{mv^2}{2k_B T} - \frac{3}{2} \right] g \sigma_r(g) d\mathbf{v_1} d\mathbf{v}. \tag{5.69}$$

We employ a Chapman-Enskog approach to determine the departure of the distribution from Maxwellian and the nonequilibrium reaction rate. Since the rate of reactive collisions is much smaller than the rate of elastic collisions and the ratio of these rates to be of the order of ϵ, we set

$$f(v,t) = F[v, n(t), T(t)] \Big[1 + \epsilon \phi(v) \Big], \tag{5.70}$$

where the first term is the local Maxwellian which varies with time implicitly through the time dependence of the density and temperature, that is

$$F[v, n(t), T(t)] = n(t) \left(\frac{m}{2k_B T(t)} \right)^{3/2} \exp \left(-\frac{mv^2}{2k_B T(t)} \right). \tag{5.71}$$

Since the system is assumed to be spatially homogeneous and there is no bulk motion of the gas, the formalism employed here is a simpler version of the Chapman-Enskog method described in Sect. 5.4.1.

The time dependence of the distribution function is implicit through $n(t)$ and $T(t)$, that is

$$\frac{\partial f}{\partial t} = \frac{\partial f}{\partial n} \frac{dn}{dt} + \frac{\partial f}{\partial T} \frac{dT}{dt}. \tag{5.72}$$

With these substitutions into the Boltzmann equation, Eq. (5.67), the term linear in ϵ is the Chapman-Enskog integral equation

$$J[\phi(v)] = F(v) H(v), \tag{5.73}$$

where

$$H(v) = -A_0 \frac{\partial F}{\partial n} + \frac{2T A_1}{3n} \frac{\partial F}{\partial T} + F \int F_1 g \sigma_r(g) d\mathbf{v_1}, \tag{5.74}$$

evaluated with the local Maxwellian, and

$$\begin{aligned} A_0 &= \int\int F F_1 g \sigma_r(g) d\mathbf{v} d\mathbf{v}_1, \\ A_1 &= -\int\int F F_1 \left[x^2 - \frac{3}{2} \right] g \sigma_r(g) d\mathbf{v} d\mathbf{v}_1. \end{aligned} \tag{5.75}$$

A solution of the integral equation, Eq. (5.73), exists if the solutions of the homogeneous equation, namely $J[\psi_0] = 0$ and $J[\psi_1] = 0$, are orthogonal to the inhomogeneous term $F(v)H(v)$. The "summational invariants" for this problem, namely $\psi_0(v) = 1$ and $\psi_1(v) = v^2$, are orthogonal to the inhomogeneous portion of the Chapman-Enskog equation, Eq. (5.73), that is

$$\int F(v)H(v)d\mathbf{v} = 0,$$

and

$$\int F(v)H(v)v^2 d\mathbf{v} = 0.$$

These results are easily verified with the definitions of A_0 and A_1. These are referred to as the auxiliary conditions and were previously discussed in connection with the integral equations for heat conduction and viscosity, namely Eqs. (5.44) and (5.45).

Inspection of the terms in Eq. (5.73) reveals that all terms are of order ϵ. We consider the hard sphere elastic cross section, πd^2, and the line-of-centers reactive cross section, given by

$$\sigma_r(E) = \begin{cases} 0, & E \leq E^*, \\ \pi d_r^2(1 - \frac{E^*}{E}), & E > E^*. \end{cases} \tag{5.76}$$

The equilibrium rate coefficient is

$$k_{eq}(T) = A_0/n^2 = 4\pi d_r^2 \sqrt{\frac{k_B T}{\pi m}} \exp(-E^*/k_B T). \tag{5.77}$$

The expansion parameter can be identified as $\epsilon = (d_r/d)^2$ and thus we must have that $d_r \ll d$ for the Chapman-Enskog perturbative method of solution to be accurate. The inhomogeneous terms of the integral equations for transport processes in Sect. 5.4.1 also satisfy these "auxiliary conditions".

We expand the perturbation of the distribution function, $\phi(x)$, in Sonine-Laguerre polynomials

$$\phi(x) = \sum_{n=2}^{N} a_n S_\alpha^{(n)}(x^2), \tag{5.78}$$

with $\alpha = 1/2$ which is hereafter deleted. This expansion reduces the integral equation to a set of linear equations,

$$\sum_{n=2}^{N} J_{mn}^{(0)} a_n = \alpha_m, \tag{5.79}$$

where

$$\begin{aligned}\alpha_m &= \int F(v)H(v)S^{(m)}(x^2)d\mathbf{v},\\ &= -A_0\delta_{0m} - A_1\delta_{1m} + A_m, \quad m \geq 2,\end{aligned} \tag{5.80}$$

and

$$A_m = \int\int FF_1S_m(x^2)g\sigma_r(g)d\mathbf{v}d\mathbf{v}_1. \tag{5.81}$$

It has been shown (Shizgal and Karplus 1970) that these moments of the reactive collision frequency are given by

$$A_m = \frac{8}{2^m}\sqrt{\frac{\pi k_B T}{m}}\sum_{k=0}^{m} S_{mk}K_k, \tag{5.82}$$

where the S_{mk} coefficients are defined by Eq. (5.61) and

$$K_k = \frac{1}{\pi}\int_0^\infty e^{-\xi^2}\xi^{2k+3}\sigma_r(g)d\xi, \tag{5.83}$$

and $\xi = \sqrt{\mu g^2/2k_BT}$ is the reduced relative speed. For the line of centers reactive cross section, Eq. (5.76), the K_k integrals can be done iteratively with an integration by parts and thus the A_m integrals are known.

The main objective is to calculate with the distribution function, Eq. (5.70), the departure of the nonequilibrium rate coefficient, k_{neq}, Eq. (5.68), from the equilibrium rate coefficient, k_{eq}, that is

$$k_{neq} = k_{eq}(1-\eta), \tag{5.84}$$

where the desired quantity is η given by

$$\eta = -2\sum_{n=0}^{N} a_n\frac{A_m}{A_0}. \tag{5.85}$$

A MATLAB code is used to calculate the matrix elements, Eq. (5.65), and the α_m moments, Eq. (5.80). The code also solves the linear equations, Eq. (5.79), and calculates η with Eq. (5.85).

The rapid convergence of η versus the number of basis functions, N, is shown in Table 5.2. The convergence of η versus N is from below so that each estimate provides a lower bound indicative that a variational theorem is operative although we have not made explicit use of the variational theorem. The extremely small correction for $E^*/k_BT = 32$ is converged to 5 significant figures with 10 basis functions.

Table 5.2 Convergence of the nonequilibrium correction to the reaction rate coefficient for the line-of-centers model cross section

E^*/k_BT	8	16	32
N	$\eta \times 10^2$	$\eta \times 10^3$	$\eta \times 10^6$
1	3.2582	0.2021	0.0004
2	3.6496	0.5600	0.0046
3	3.6507	0.9019	0.0343
4	3.6569	1.0118	0.1581
5	3.6571	1.0167	0.4637
6	3.6571	1.0177	0.9056
7		1.0179	1.2633
8		1.0179	1.4072
9			1.4271
10			1.4271
Nonlinear variational[a]	3.6251	0.8924	0.7665

[a] Present and Morris (1969)

The variation of η with the reduced threshold energy E^*/k_BT is shown by the solid curve in Fig. 5.4(A). The unusual behavior with η decreasing for $E^*/k_BT < 5$ in spite of the increase in the reaction rate has been explained (Shizgal and Karplus 1970) on the basis of the speed dependence of the reactive collision frequency. The nonequilibrium effect vanishes for a reactive collision frequency that varies in such a manner analogous to the way changes in density and temperature change the distribution function. Thus, for a reactive cross section that varies as g or $1/g$, $\eta = 0$. This accounts for the minimum and maximum of η near the E^*/k_BT origin.

It is useful to compare with the nonlinear variational solution of the chemical kinetic Boltzmann equation introduced by Present and Morris (1969). They chose a solution (their Eq. (33)) which is made to satisfy the two auxiliary conditions and parameterized by the variational parameter s, that is

$$\phi(x^2) = C(s)\left[e^{sx^2} - \frac{sx^2 + 1 - \frac{5}{2}s}{\sqrt[5/2]{1-s}}\right]. \tag{5.86}$$

Substitution of this form of the solution into Eq. (5.73) and taking the scalar product with $\phi(x)$ gives an equation for $C(s)$. We then calculate the rate of reaction and divide by the equilibrium rate, Eq. (5.77). The correction to the rate of reaction parametrized by the variational parameter s and $q = E^*/k_BT$ is given by,

$$\eta(q,s) = \frac{2(1-2s)^2 e^{-q}}{s^4\sqrt{1-s}}\left[\sqrt{\frac{2-s}{2}}\exp\left(\frac{sq}{2-s}\right) - \frac{1 - \frac{3}{4}s + \frac{1}{2}sq}{\sqrt{1-s}}\right]. \tag{5.87}$$

The extremum value of $\eta(q,s)$ versus s for fixed q can be determined with a short MATLAB code.

The symbols in Fig. 5.4 show the results with the nonlinear variational approach (Present and Morris 1969) and appear indistinguishable from the spectral solution. However, the comparison of the numerical values with the variational approach and the Sonine polynomial expansion shown in Table 5.2 demonstrates that the variational approach gives poor results for the larger E^*/k_BT values.

The spectral convergence is also demonstrated with the decrease in the expansion coefficients versus n in Fig. 5.4(B) and the accuracy of the expansion for η in Fig. 5.4(C). The "exact" values for η are those calculated with the Sonine polynomial expansion with a sufficient number of terms to get convergence to 16 significant figures.

Explicit time dependent solutions of the Boltzmann equation were carried out to determine the range of validity of the Chapman-Enskog approach for the one component system treated here (Shizgal 1971) as well as for a binary system (Shizgal 1974). These studies suggest that the value of ϵ must be of the order of 10^{-3} to 10^{-4} for the Chapman-Enskog values to be accurate. Shizgal (1981a) used a

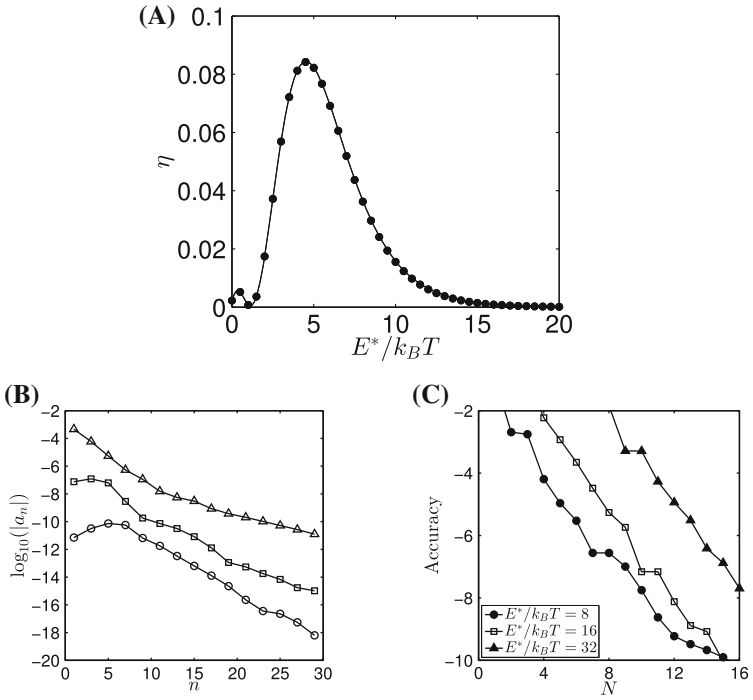

Fig. 5.4 (**A**) Variation of the nonequilibrium connection to the reaction rate, η, versus the reduced activation energy, E^*/k_BT, for the line-of-centers reactive cross section and hard sphere elastic cross section; the *solid symbols* are the results with the variational solution. (**B**) Convergence of the expansion coefficients of $\phi(x)$ versus n, with $E^*/k_BT = 10$ (*triangles*), 20 (*squares*) and 30 (*circles*). (**C**) Accuracy $= \log_{10}[1 - \eta/\eta_{exact}]$ where η_{exact} is determined to 16 significant figures with N sufficiently large

pseudospectral method based on Laguerre quadratures in reduced energy to solve the chemical kinetic Boltzmann equation, Eq. (5.67), but for a binary gas with unit mass ratio and the integral kernel operator, Eq. (5.110). This reactive system was also the basis for the study of the nonequilibrium effects associated with the escape of planetary atmospheres (Lindenfeld and Shizgal 1979b). The loss of atoms from an atmosphere is in the first instance given by the well-known Jeans escape flux (Fahr and Shizgal 1983) analogous to a chemical reaction where the reaction threshold energy is replaced by the escape energy from the planet.

5.4.5 *Pseudospectral Solution of the Boltzmann Equation for Shear Viscosity with the Maxwell Quadrature*

The Chapman-Enskog solution of the Boltzmann equation for the viscosity of a one component gas was summarized in Sect. 5.4.1. The integral equation for the function $B(x)$, Eq. (5.45), for the hard sphere cross section is the solution of the linear integral equation (Shizgal 2011; Siewert 2002)

$$\int_0^\infty e^{-x^2} x^2 k_J^{(2)}(x, y) B(x) dx - Z(y) B(y) = -y^2, \tag{5.88}$$

where the symmetric kernel, $k_J^{(2)}(x, y)$, is given by

$$k_J^{(2)}(x, y) = -\frac{2Z(0)}{x^4 y^4}\left[A(x, y) + C(x, y)\sqrt{\pi} e^{x^2} \mathrm{erf}(x)/2\right], \quad x < y, \tag{5.89}$$

with

$$A(x, y) = \frac{2}{35}x^7 - 3x^3 + 18x - y^2\left(\frac{2}{15}x^5 - 3x\right),$$

$$C(x, y) = -6x^4 + 15x^2 - 18 + y^2(2x^2 - 3),$$

as discussed by Siewert (2002). The kernel $k_J^{(2)}(x, y)$ is the $\ell = 2$ component of the expansion of the anisotropic kernel, Eq. (5.53). Equation (5.88) is equivalent to Eq. (5.45). The function $B(x)$ in this paper corresponds to $x^2 b(x)$ in the papers by Siewert (2002) and by Loyalka et al. (2007). The shear viscosity in reduced units is given in terms of $B(x)$, that is

$$\nu = \frac{16\sqrt{2}}{15} \int_0^\infty e^{-x^2} x^4 B(x) dx. \tag{5.90}$$

The details are provided elsewhere (Siewert 2002; Loyalka et al. 2007; Sharipov and Bertoldo 2009). Our interest here is with the numerical solution of the integral equation, Eq. (5.88) and the calculation of the viscosity, Eq. (5.90).

There have been several different methods used to get accurate solutions of Eq. (5.88). Siewert (2002) used a B-spline technique analogous to a recent work on time dependent solutions of the isotropic Boltzmann equation (Khurana and Thachuk 2012). Sharipov and Bertoldo (2009) have employed a two-dimensional mesh to discretize the Boltzmann integral equation, Eq. (5.45).

Loyalka et al. (2007) employed the expansion of the distribution function in the Sonine-Laguerre polynomials with up to 150 terms to reduce Eq. (5.45) to a set of linear algebraic equations. They used *Mathematica* to calculate the matrix representation of collision operator and invert the resulting set of linear equations algebraically for the function $B(x)$ in Eq. (5.90). This is the Galerkin solution of the integral equation, Eq. (5.88) or equivalently Eq. (5.45). The use of Mathematica avoids the round-off errors that would otherwise occur, and accurate converged solutions to the Boltzmann equation were obtained. Their work serves as an excellent benchmark for the solution of this integral equation and they report the viscosity to 34 significant figures, that is $\nu = 0.44902780628789243460904948953465 45$.

We have noted in Sect. 3.6.3 that the integral for the dimensionless viscosity converges very rapidly with respect to the number, N, of Gauss-Maxwell quadrature points and weights with $w(x) = x^2 e^{-x^2}$. Thus a solution of Eq. (5.88) based on the Gauss-Maxwell quadrature points should converge quickly. With this quadrature procedure, the solution of the integral equation, Eq. (5.88), is given by the inversion of the set of linear algebraic equations

$$\sum_{i=1}^{N} W_i e^{-z_i^2} z_i^2 k_J^{(2)}(z_i, z_j) B(z_i) - Z(z_j) B(z_j) = -z_j^2, \tag{5.91}$$

where $W_i = s w_i / w(x_i)$, $z_i = s x_i$. The scaling parameter s is chosen so that the quadrature points are in the interval $x \in [0, 6]$ for which $B(x)$ is known. The reduced shear viscosity is then given by

$$\nu = \frac{16\sqrt{2}}{15} \sum_{i=1}^{N} W_i e^{-z_i^2} z_i^4 B(z_i). \tag{5.92}$$

The solution to Eq. (5.91), $B(x)$, is shown in Fig. 5.5 and is a very slowly varying function of x. It is not surprising that the convergence of the solution is rapid. A graphically accurate solution is obtained with 16 quadrature points. The convergence is slower for large x but there is a small contribution to ν for $x > 6$ owing to the factor $x^4 e^{-x^2}$ in Eq. (5.90). The convergence of the solution of the Boltzmann equation obtained with the scaled Maxwell quadrature points is shown in Table 5.3 in comparison with the solution reported by Siewert (2002). The pseudospectral solution was spline fitted to the x values reported by Siewert (2002). The major contribution

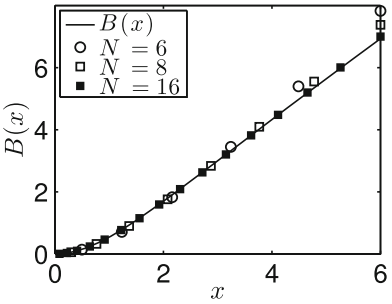

Fig. 5.5 The solution of the Boltzmann equation, Eq. (5.88), for the viscosity function, $B(x)$, versus the number of Maxwell quadrature points, N. The *solid curve* is the result by Loyalka et al. (2007) considered exact

Table 5.3 Solution of the Boltzmann equation for shear viscosity with N speed quadrature points; $(-n) \equiv \times 10^{-n}$

x	Siewert 2002	N = 20	N = 30	N = 40	N = 60
	$x^4 e^{-x^2} B(x)$				
0.3	0.40775 (−3)	0.40629 (−3)	0.40763 (−3)	0.40772 (−3)	0.40775 (−3)
0.4	0.21139 (−2)	0.21101 (−2)	0.21134 (−2)	0.21137 (−2)	0.21139 (−2)
0.5	0.72744 (−2)	0.72686 (−2)	0.72726 (−2)	0.72738 (−2)	0.72742 (−2)
1.0	0.20004	0.19983	0.20000	0.20003	0.20004
1.5	0.57830	0.57780	0.57820	0.57827	0.57829
2.0	0.49722	0.496901	0.49716	0.49720	0.49722
2.5	0.17667	0.17659	0.17665	0.17666	0.17667
3.0	0.30011 (−1)	0.30002 (−1)	0.30009 (−1)	0.30010 (−1)	0.30011 (−1)
3.5	0.26318 (−2)	0.26315 (−2)	0.26317 (−2)	0.26318 (−2)	0.26318 (−2)
4.0	0.12465 (−3)	0.12466 (−3)	0.12465 (−3)	0.12465 (−3)	0.12465 (−3)
ν	0.449027806	0.448816	0.448985	0.449014	0.449025

Reproduced in part from Shizgal (2011) with permission of the American Institute of Physics and from Siewert (2002) with permission from Elsevier

to the integral is approximately in the interval $x \in [0.4, 4.0]$. The scaling of the Gauss-Maxwell points with the parameter s is thus important so as to compute the solution in the range of x that contributes to the viscosity.

Siewert (2002) employed 301 "knots" with the Hermite cubic spline functions and a 4th order Gauss-Legendre quadrature to calculate the integral over subintervals. The final integral for the viscosity, Eq. (5.90), was computed with 100 Gauss-Legendre quadrature points. Sharipov and Bertoldo (2009) solved the Boltzmann equation as a two dimensional problem in two velocity coordinates and used 40 grid points in each velocity direction and 200 points with a Simpson's rule to evaluate ν to the same precision as in Table 2; that is $2\sqrt{\pi} \times 0.126668 = 0.449028$. The application of the speed quadrature points and weights to this problem is very straightforward and the convergence is rapid as seen in Table 5.3 and Fig. 5.5.

5.5 Spectral Theory for the Linearized Boltzmann Collision Operator

The Boltzmann equation, Eq. (5.30), is the basis for modelling transport phenomena in a one component gas. These transport processes include the classic rarefied gas dynamical problems such as the Kramers problem, Poseuille and Couette flow and other similar phenomena discussed elsewhere (Williams 1971; Cercignani 1988; Sharipov and Seleznev 1998; Siewert 2003). These and many other rarefied gas dynamical flows are described in detail in the book by Sone (2007). Spectral methods are employed in the solution of the Boltzmann equation for such systems (Wu et al. 2013; Ghiroldi and Gibelli 2014). These problems are beyond the scope of this book but in Sect. 5.7.2 we discuss the Milne problem for a binary gas that serves as an example of a rarefied gas dynamical problem. The numerical approximation of the linearized collision operator in the Boltzmann equation, J, is important in these applications.

Studies of the mathematical properties of J has a very long history (Alterman et al. 1962; Grad 1963; Foch and Ford 1970; Cercignani 1988) and is ongoing (Mouhot 2007; Dudynski 2013). Some of the mathematical works are directed towards constructive estimates of the first nonzero eigenvalue referred to as the "spectral gap" (Baranger and Mouhot 2005; Mouhot 2007). A comparison of the previously noted mathematical analyses and others (Alexandre 2009; Dudynski 2013) with the numerical estimates (Shizgal 1984; Gust and Reichl 2009) has not been made. The classical differential cross sections diverge at small scattering angle and the total cross section is infinite, except for the hard sphere cross section. For other than the hard sphere cross section, the mathematical treatments involve a cut-off of the divergent classical differential cross section (Grad 1949; Baranger and Mouhot 2005; Mouhot 2007; Alexandre 2009). However, the correct treatment of the elastic scattering is based on quantum theory for which the differential cross section at zero scattering angle is finite as is the total cross section.

The quantum mechanical cross sections can be calculated for physically realistic atomic potentials (Bernstein 1966; Child 1996; Canto and Hussein 2013) and cannot in general be factored as a product of a function of g and a function of θ. Mathematical treatments of the approach to equilibrium for the non-linear Boltzmann equation (see Sect. 5.8) rely on the spectral properties of the linearized operator (Grad 1958; Baranger and Mouhot 2005; Mouhot 2006; Alexandre 2009).

Realistic quantum cross sections have been used in the Boltzmann equation for relaxation processes (Kharchenko et al. 1998; Kharchenko and Dalgarno 2004; Sospedra-Alfonso and Shizgal 2013), in the study of gaseous transport coefficients Zhang et al. (2013), and in modelling electron (Lin et al. 1979a; Pitchford and Phelps 1982; Hagelaar and Pitchford 2005; Robson et al. 2005) and ion transport (Mason and McDaniel 1988; Viehland 1994; Danailov et al. 2008). These works are based on the linear collision operator for binary systems discussed in Sect. 5.6.

We approximate the eigenvalues of the collision operator, J, with a spectral approach in Sect. 5.5.1 and a pseudospectral method in Sect. 5.5.2. It is well known

that the spectrum of the collision operator consists of an infinite number of discrete eigenvalues and a continuum (Grad 1963; Kuščer and Williams 1967; Shizgal 1984; Gust and Reichl 2009). For the Maxwell molecule model with a constant collision frequency the spectrum is completely discrete as discussed in Sect. 3.6.4.

Our main interest in the sections that follow is the eigenvalue problem associated with the initial value problem, Eq. (5.46). There are an infinite number of discrete eigenvalues defined by

$$J\psi_n(x) = -\lambda_n\psi_n(x), \tag{5.93}$$

which satisfy $0 \leq \lambda_n \leq Z(0)$ and continuous eigenvalues, $\lambda > Z(0)$, given by

$$J\psi(x,\lambda) = -\lambda\psi(x,\lambda), \tag{5.94}$$

where $Z(0)$ is the elastic collision frequenxy, Eq. (5.51) at zero reduced speed or energy. This set of eigenstates (taken to be complete) can be used to represent a function, $\phi(x)$, by writing the expansion of the function in terms of the discrete and continuum eigenfunctions as given by,

$$\phi(x) = \sum_{n=0}^{\infty} c_n\psi_n(x) + \int_{Z(0)}^{\infty} C(\lambda)\psi(x,\lambda)d\lambda. \tag{5.95}$$

This property of the eigenvalue spectrum has been discussed elsewhere (Grad 1963; Cercignani 1988; Hoare 1971; Baranger and Mouhot 2005). In Chap. 6, Sect. 6.4.1, we compare this aspect of the spectrum of the Boltzmann equation with a similar behaviour for the Fokker-Planck equation for Coulomb collisions.

5.5.1 *Spectral Calculation of the Eigenvalue Spectrum of J*

In this section, we describe the calculation of the eigenfunctions and eigenvalues of J with a spectral method. The solution of the initial value problem, Eq. (5.46), is not presented here. However, in Sect. 5.6 we consider the solution of an analogous initial value problem for the equilibration of a binary mixture with energy exchange between the components.

We estimate the eigenvalues and eigenfunctions of J with the expansion of the eigenfunctions in the Sonine-Laguerre polynomials, $S_\alpha^{(k)}(x^2)$, with $\alpha = 1/2$, that is

$$\psi_n(x) = \sum_{k=0}^{N} a_k^{(n)} S^{(k)}(x^2). \tag{5.96}$$

where we have deleted the dependence of $S^{(k)}$ on α to simplify the notation. Since these basis functions are the eigenfunctions for the Maxwell molecule model, the usual expectation is that it would be a good choice for other interaction potentials (Phillips 1959; Tompson et al. 2010). However, there is no mathematical reasoning for this supposition.

The expansion coefficients $a_k^{(n)}$ are considered as linear variation parameters. The Rayleigh-Ritz variational approach was discussed in Chap. 1, Sect. 1.2.5. Variational methods are perhaps more familiar in the quantum context (Amore 2006; Balint-Kurti and Pulay 1995) than for kinetic theory problems. However, there has been considerable use of the variational theorem in kinetic theory (Phillips 1959; Cercignani 1969; Driessler 1981) based on maximum entropy principles (Snider 1964; Bobylev and Cercignani 1999).

We use the hard sphere differential cross section for which $\sigma(g, \Omega) = d^2/4$ and πd^2 is the total cross section. We use the expansion, Eq. (5.96), and thus the matrix representation given by Eq. (5.65). The first two eigenvalues are $\lambda_0 = \lambda_1 \equiv 0$ since particle number and energy are conserved, that is, $J_{nm}^{(0)} = 0$ for $(n, m) = 0$ and 1. The numerical diagonalization of the matrix $\mathbf{J}$ of dimension N defined by Eq. (5.65) yields successive approximations to the nonzero eigenvalues.

The convergence of the lower order eigenvalues, λ_2–λ_7, in units of $Z(0)$, is shown in Table 5.4 versus the number of basis functions, N. The convergence of each eigenvalue is from above consistent with a variational calculation. With 80 basis functions there are only 3 discrete nonzero eigenvalues ($\lambda_n < 1$). The other eigenvalues remain unconverged and lie in the continuum (Hoare and Kaplinsky 1970; Hoare 1971). Although this is a spectral method, the convergence of the eigenvalues is very slow with the Sonine-Laguerre basis set.

If we define the columns of the matrix $\mathbf{U}$ as the eigenvectors of the matrix $\mathbf{J}$, then $\mathbf{U}^{(-1)} \cdot \mathbf{J} \cdot \mathbf{U} = \mathbf{\Lambda}$, where $\Lambda_{nm} = \lambda_n \delta_{nm}$. The eigenfunctions can be written in terms of their expansion in the orthonormal Sonine-Laguerre basis functions, that is

Table 5.4 Convergence of the eigenvalues, λ_n, in units of $Z(0)$ of the linearized spherically symmetric ($\ell = 0$) Boltzmann equation with the Sonine-Laguerre basis functions

N	λ_2	λ_3	λ_4	λ_5	λ_6	λ_7
4	0.67660	1.06192	1.58295	2.30219		
6	0.67260	0.98776	1.35808	1.83700	2.41524	3.13509
8	0.67163	0.95494	1.24700	1.62541	2.06912	2.57270
10	0.67136	0.93797	1.18042	1.49760	1.86907	2.28307
20	0.67123	0.91513	1.05183	1.23130	1.45074	1.69800
30	0.67123	0.91226	1.01497	1.13918	1.29772	1.48081
40		0.91173	0.99982	1.09367	1.21770	1.36401
50		0.91161	0.99246	1.06723	1.16878	1.29073
60		0.91158	0.98848	1.05031	1.13600	1.24051
80			0.98477	1.03049	1.09529	1.17634

The eigenvalues, $\lambda_n < 1$, are in the discrete portion of the spectrum

$$\psi_n(x) = \sum_{k=2}^{N} U_{nk} \hat{S}^{(k)}(x^2). \tag{5.97}$$

where $\hat{S}^{(k)}(x^2) = S^{(k)}(x^2)/\sqrt{\Gamma(n+3/2)/n!}$. The orthogonality of the eigenfunctions is given by

$$\begin{aligned}\int_0^\infty w(x)\psi_n(x)\psi_m(x)dx &= \sum_{k=2}^{N}\sum_{\ell=2}^{N} U_{nk}U_{m\ell} \int_0^\infty w(x)\hat{S}^{(k)}(x^2)\hat{S}^{(\ell)}(x^2)dx, \\ &= \sum_{k=2}^{N} U_{nk}U_{mk} = \delta_{nk}, \end{aligned} \tag{5.98}$$

where Eq. (5.62) for the orthogonality of the Sonine-Laguerre polynomials has been used. The result, Eq. (5.98), is a statement of the orthogonality of the eigenvectors, $\mathbf{U}$, of the symmetric matrix $\mathbf{J}$. The eigenfunctions are all normalizable in L^2 with weight function $w(x) = x^2 e^{-x^2}$ whether they belong to the discrete spectrum or the continuum. However, we must address the meaning of the discretized eigenfunctions with $\lambda_n > 1$ as representing the continuum eigenfunctions in some approximate way (Reinhardt 1979).

5.5.2 *Pseudospectral Calculation of the Eigenvalue Spectrum of J*

We reconsider the eigenvalue problem of the previous section (for $\ell = 0$) defined by the equivalent integral equation, that is

$$\int_0^\infty e^{-x^2} x^2 k_J^{(0)}(x, y)\psi_n(x)dx - Z(y)\psi_n(y) = \lambda_n \psi_n(y), \tag{5.99}$$

where the symmetric kernel, $k_J^{(0)}(x, y)$, is given by

$$k_J^{(0)}(x, y) = Z(0) \begin{cases} \left[4e^{x^2}\mathrm{erf}(x) - \frac{4\sqrt{\pi}}{3}(x^2 + 3y^2)\right]/y\Big], & x < y \\ \left[4e^{y^2}\mathrm{erf}(y) - \frac{4\sqrt{\pi}}{3}(3x^2 + y^2)\right]/x\Big], & x > y \end{cases}$$

and discussed by other researchers (Desai and Nelkin 1966; Kuščer and Williams 1967; Yan 1969; Williams 1971; Siewert 2002). The kernel is the $\ell = 0$ component of the expansion Eq. (5.53).

The eigenfunctions are discretized on the grid defined by the Gauss-Maxwell quadrature with $p = 2$ that is with $w(x) = x^2 e^{-x^2}$. With this quadrature, the discretized form of the integral eigenvalue problem is

$$\sum_{j=1}^{N} w_j k_J^{(0)}(x_j, x_i)\psi_n(x_j) - Z(x_i)\psi_n(x_i) = \lambda_n \psi_n(x_i). \tag{5.100}$$

The matrix equation is symmetrized by setting $\hat{\psi}_n(x_i) = \sqrt{w_i}\psi_n(x_i)$ (Gust and Reichl 2010).

The computation of the matrix, $k_J^{(0)}(x_j, x_i)$, is much less prone to numerical round-off errors than the matrix representation with polynomial basis functions, Sect. 5.4.3. This pseudospectral method is more flexible as different quadratures associated with different basis functions can be used with very little additional effort, including a trapezoidal or Simpson rule. We can also scale the quadrature points and weights to improve convergence.

In order to impose detailed balance, that is to ensure that $\lambda_0 = 0$ to machine accuracy, we use the numerical value of the collision frequency, $Z(x_i)$, as determined by the integral over the kernel as discussed in Chap. 3

$$Z(x_i) = \sum_{k=1}^{N} w_k k_J^{(0)}(x_i, x_k). \tag{5.101}$$

The use of this approximate numerical result for $Z(x_i)$ in Eq. (5.99), removes the contribution from the cusp in the kernel and this method has been referred to as the singularity subtraction technique (Loyalka and Naz 2008), and was also discussed by Shizgal (1981a).

However, there is no constraint for λ_1 to be zero. Alternatively, one could define $Z(x_i)$ to ensure that energy conservation is obtained to machine accuracy, that is $\lambda_1 = 0$, but we would then find that $\lambda_0 \neq 0$. In this way, one of the two zero eigenvalues is of the order of 10^{-15} but not both. The other eigenvalue is much larger of the order of 10^{-5}. Recall that the spectral method gives trivially the two zero eigenvalues.

The convergence of the lower order eigenvalues is shown in Table 5.5 versus the number of Gauss-Maxwell quadrature points. The approach of λ_1 to zero is also shown. It is clear that the convergence of the eigenvalues is much faster with the Maxwell polynomials than with the Sonine-Laguerre polynomials except for λ_1 and λ_2. All the eigenvalues shown in the table are in the discrete portion of the spectrum and converged to five significant figures with 80 quadrature points.

There have been many qualitative discussions and diagrams of the approach of the eigenvalues to the continuum boundary (Cercignani 1988; Baranger and Mouhot 2005). An accurate representation is shown in Fig. 5.6. The upper graph depicts the value of each eigenvalue with a vertical line of unit length, the "spectral gap" being $\lambda_1 = 0.67121$. The density of eigenvalues increases very quickly near $\lambda_n = 1$;

Table 5.5 Convergence of the eigenvalues, in units of $Z(0)$, of the linearized spherically symmetric ($\ell = 0$) Boltzmann collision operator, with the Maxwell (p = 2) quadrature points and weights; quadrature points scaled so that $x_{max} = 6$

N	λ_1	λ_2	λ_3	λ_4	λ_5	λ_6	λ_7
10	−0.0182	0.63890	0.88444	0.95485	1.11878	1.48671	2.0014
20	−0.00121	0.66909	0.90988	0.98090	0.99541	1.0075	1.05629
30	−0.000243	0.67080	0.91123	0.98180	0.99673	0.99917	1.00288
40	−0.0000772	0.67120	0.91155	0.98199	0.99690	0.99949	0.99992
80	−0.0000316	0.67122	0.91157	0.98200	0.99691	0.99950	0.99993
BM[a]	0	0.671	0.912	0.982	0.997		
Mouhot[b]	0	0.0047					

[a] Bobylev and Mossberg (2008)
[b] The analytic bound reported by Mouhot (2007) with a constructive approach is $1/(96\sqrt{2e})$

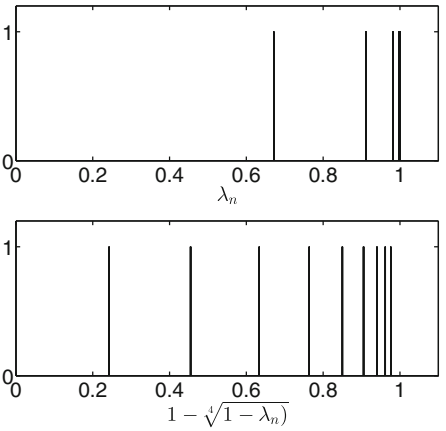

Fig. 5.6 (*Top graph*) The approach of the eigenvalues in units of $Z(0)$ of the linearized spherically symmetric ($\ell = 0$) collision operator, J, to the continuum boundary at $\lambda_n = 1$. (*Bottom graph*) Distorted diagram so as to decrease the density of eigenvalues near the continuum boundary

see Table 5.5. The lower graph is an artificial plot to spread out the eigenvalues near the continuum boundary. It is clear that the density of discrete eigenvalues near the boundary is very high. These discrete or "bound" eigenfunctions, $\psi_n(x)$, $n = 0$–5, are shown in Fig. 5.7 and exhibit $(n - 1)$ nodes. Of particular interest is the rapid variation of the higher eigenfunctions near the origin which explains the slow convergence with the Sonine-Laguerre polynomials. A large number of Sonine-Laguerre basis functions are required in order to accurately describe the behaviour of the eigenfunctions near the origin. The pseudospectral method is more accurate and flexible.

One can transform the integral equation to a differential equation, a procedure which is the opposite to finding a Green function for a differential equation so as to transform it to an integral equation. With this technique, originally developed by Wigner and Wilkins (1944) and subsequently by several other workers (Williams 1966; Kuščer and Corngold 1965; Kuščer and Williams 1967; Hoare 1971; Bobylev

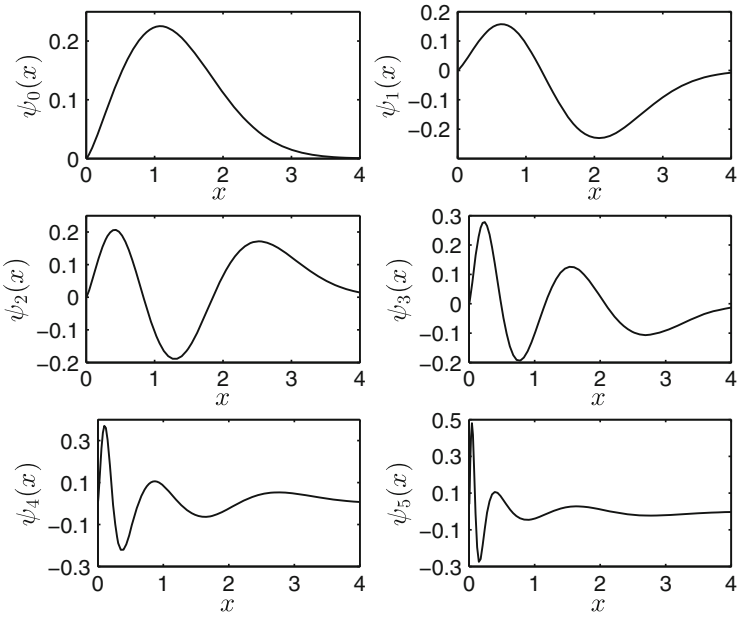

Fig. 5.7 The eigenfunctions, $\psi_n(x)$, of the linearized spherically symmetric ($\ell = 0$) Boltzmann collision operator determined with the Gauss-Maxwell quadratures with $w(x) = x^2 e^{-x^2}$

Table 5.6 Convergence of the eigenvalues of the linearized spherically symmetric ($\ell = 0$) Boltzmann collision operator with the multidomain method; λ_n in units of $Z(0)$

n	λ_n	$\frac{1-\lambda_n}{1-\lambda_{n+1}}$
2	0.67121	3.718
3	0.91156	4.913
4	0.98200	5.816
5	0.996904	6.149
6	0.9994966	6.231
7	0.9999192	6.247
8	0.9999871	6.247
9	0.99999793	6.247
10	0.999999667	6.212
	WKB	6.253

Reprinted from Shizgal (1984) with permission from National Research Council Research Press

and Mossberg 2008), the integral Boltzmann eigenvalue problem can be transformed to a Schrödinger equation. The Schrödinger equation is of an unusual form in that the potential is parameterized by the eigenvalue.

Bobylev and Mossberg (2008) solved the Schrödinger equation with a finite difference method and obtained the eigenvalues with a root searching algorithm.

Their results are shown in Table 5.5 together with the results by Mouhot (2007) with a constructive approach.

This Schrödinger equation in conjunction with a Wentzel-Kramers-Brillouin (WKB) analysis provides an understanding of the nature of the approach of the eigenvalues to the continuum boundary. A clear exposition was provided by Rahman and Sundaresan (1968) with the result that for the linearized collision operator, the eigenvalues obey the asymptotic result

$$\frac{1-\lambda_n}{1-\lambda_{n+1}} \approx \exp\left(\frac{4\pi}{\sqrt{47}}\right) \approx 6.2526. \tag{5.102}$$

In order to accurately verify the behavior of the eigenvalues in accordance with Eq. (5.102), a multidomain spectral method is used (Shizgal 1984). This involves subdividing the semi-infinite domain into many subintervals and the use of Gauss-Mehler quadrature points in each subdomain. Scaled Laguerre quadrature points are used in the last domain which extends to infinity. The division of the semi-infinite interval into subdomains varies from eigenfunction to eigenfunction, with a knowledge of the location of the nodes for each eigenfunction. The grid is thus optimized for each eigenfunction separately. This permits an accurate calculation of the discrete eigenvalues and the approach to the continuum boundary as shown in Table 5.6 in comparison with the WKB approximation. The asymptotic result, Eq. (5.102), appears to be attained by λ_7 or λ_8 but as is clear from the results in the table it is a numerical challenge to calculate accurate eigenvalues extremely close to 1.

5.6 Relaxation to Equilibrium in Binary Gas Mixtures

The approach to equilibrium of the distribution function of a minor constituent of mass m (sometimes referred to as a "test particle") dilutely dispersed in a background gas of mass M at equilibrium is a fundamental problem in kinetic theory (Kuščer and Williams 1967; Yan 1969) with important applications to hot atom relaxation (Park et al. 1989; Cline et al. 1990; Nan and Houston 1992; Matsumi et al. 1994; Nakayama et al. 2005; Zhang et al. 2007; Bovino et al. 2011).

The time dependent Boltzmann equation for a spatially uniform system in the absence of external forces is identical in form to Eq. (5.46) for the one-component gas, that is

$$\frac{\partial f(\mathbf{v},t)}{\partial t} = L[f(\mathbf{v},t)], \tag{5.103}$$

with the linear operator, L, defined by

$$L(f) = \int\int [F_1' f' - F_1 f] g\sigma(g,\theta) d\Omega d\mathbf{v}_1, \tag{5.104}$$

instead of Eq. (5.41) for the linearized collision operator.

The Boltzmann integral equation for this binary gas is of the same form as in Eq. (5.50) but with a different kernel that varies with the mass ratio, γ. In terms of the reduced velocities $\mathbf{x} = \mathbf{u}\sqrt{m/2k_BT}$ and $\mathbf{y} = \mathbf{v}\sqrt{m/2k_BT}$, and the cosine of the angle between the velocity vectors, $\overline{\mu}$, the kernel is given by

$$K_L(x, y, \overline{\mu}) = \frac{Z(0)(\gamma+1)^2}{2\pi\gamma^{3/2}} \frac{1}{\sqrt{x^2+y^2-2xy\overline{\mu}}} \times \exp\left[-x^2 + \frac{\gamma x^2 y^2(1-\overline{\mu}^2)}{x^2+y^2-2xy\overline{\mu}} - \frac{(\gamma-1)^2(x^2+y^2)}{4\gamma} - \frac{(\gamma^2-1)xy\overline{\mu}}{2\gamma}\right], \tag{5.105}$$

where $\gamma = M/m$ is the mass ratio of the two components Shizgal and Blackmore (1983). This result is derived with the definition, Eq. (5.103), and the kinematics of an elastic collision, Fig. 5.3, and Eqs. (5.47)–(5.49) (Chapman and Cowling 1970; Ferziger and Kaper 1972; Khurana and Thachuk 2013). In the sections that follow, we consider spectral and pseudospectral calculations of the eigenvalue spectrum of the integral operator, L, analogous to the results for J in the previous sections.

5.6.1 Spectral Calculation of the Eigenvalue Spectrum of the Linear Collision Operator, L, for a Binary Gas

We proceed as we did in Sect. 5.4.3 for the linearized Boltzmann collision operator. The matrix elements of L in the Sonine-Laguerre basis (for $\ell = 0$) are defined by

$$L_{nm}^{(0)} = \iiint F_1 F_2 S_1^{(n)} \left[S_1^{(m)'} - S_1^{(m)}\right] \sigma g d\Omega d\mathbf{v}_1 d\mathbf{v}_2, \tag{5.106}$$

evaluated as for the linearized case with the generating function for the basis functions, Eq. (5.63) and we have that

$$\langle G_s|L|G_t\rangle = 8\sqrt{\frac{2\pi k_B T_b}{\mu}} \frac{M_1 M_2 st}{(1-st)^2} \left(\frac{\sqrt{1-M_1(s+t)-[1-2M_1]st}}{1-[1-4M_1M_2]st}\right), = \sum_{n=0}^{\infty}\sum_{m=0}^{\infty} L_{nm}^{(0)} s^n t^m, \tag{5.107}$$

where $M_1 = m_1/(m_1+m_2)$, $M_2 = m_2/(m_1+m_2)$ and $\mu = m_1 m_2/(m_1+m_2)$. The matrix elements are evaluated as the coefficients of $s^n t^m$ in the power series expansion of $\langle G_s|L|G_t\rangle$ as in Sect. 5.4.3 for the linearized operator, J. A MAPLE code (Shizgal and Dridi 2010) developed for arbitrary differential cross section can

Table 5.7 Convergence of the eigenvalues, in units of $Z(0)$, of the linear ($\gamma = 1$) spherically symmetric ($\ell = 0$) Boltzmann collision operator with the Sonine-Laguerre basis functions

N	λ_1	λ_2	λ_3	λ_4	λ_5	λ_6
4	0.83191	1.23300	1.80103	2.55781		
6	0.82351	1.13057	1.53697	2.04776	2.64985	3.38573
8	0.82081	1.08006	1.40112	1.80739	2.27335	2.79345
10	0.81980	1.05092	1.31698	1.65904	2.05109	2.48123
20	0.81905	1.00022	1.14237	1.33917	1.57346	1.83352
30	0.81902	0.98819	1.08405	1.22258	1.39305	1.58660
40		0.98384	1.05604	1.16244	1.29671	1.45194
50		0.98192	1.04007	1.12607	1.23674	1.36656
60		0.98099	1.03005	1.10202	1.19613	1.30775

be used to extract the matrix elements based on Eq. (5.107) for the hard sphere cross section. Lindenfeld and Shizgal (1983) also provided a closed form expression for the matrix elements.

The numerical diagonalization of the matrix $\mathbf{L}$ of order N gives the eigenvalues and eigenfunctions. The derivation of the expression for $L_{nm}^{(0)}$ for the hard sphere cross section and arbitrary γ, which requires considerable algebra, is given by Eq. (28) and Appendix A in Lindenfeld and Shizgal (1983).

For $\gamma = 1$, the convergence of the eigenvalues versus the number of basis functions, N, is shown in Table 5.7. The convergence of the eigenvalues is from above consistent with a variational theorem. The smallest eigenvalue, $\lambda_0 = 0$, is consistent with particle conservation. With up to 60 basis functions, there are only two discrete eigenvalues, λ_1 and λ_2, whereas the others shown are in the continuum. Only λ_1 is converged to five significant figures with 30 basis functions. The convergence of the eigenvalues with the Sonine-Laguerre basis set is slow, similar to the results for J in Table 5.4.

5.6.2 *Pseudospectral Calculation of Eigenvalue Spectrum of the Linear Collision Operator, L, for a Binary Gas*

The kernel in the Boltzmann equation for a binary gas mixture is given by Eq. (5.105) and depends on $\overline{\mu}$ and the mass ratio, $\gamma = M/m$. We expand the kernel in Legendre polynomials in $\overline{\mu}$ as given by Eq. (5.53) for the linearized operator. The scalar kernels are denoted by $k_L^{(\ell)}(x, y)$ analogous to the $k_J^{(\ell)}(x, y)$ for the linearized collision operator, J. The eigenvalues and eigenfunctions of the collision operator for given ℓ are defined by the set of integral equations

$$\int_0^\infty k_L^{(\ell)}(x, y)\psi_{n,\ell}(x)dx - Z(y)\psi_{n,\ell}(y) = -\lambda_{n,\ell}\psi_{n,\ell}(y). \tag{5.108}$$

The collision frequency, $Z(x)$, in Eq. (5.108), is given by

$$Z(x) = \int_0^\infty k_L^{(0)}(x, y)dy,$$
$$= \frac{A}{2}\left[e^{-\gamma x^2} + \left[2\sqrt{\gamma}x + \frac{1}{\sqrt{\gamma}x}\right]\frac{\sqrt{\pi}}{2}\text{erf}(\sqrt{\gamma}x)\right], \tag{5.109}$$

where $A = n_b\pi d^2\sqrt{k_B T_b/2m}$ and $Z(0) = 2A$. The kernel $k_L^{(0)}(x, y)$ is the Wigner-Wilkins kernel (Hoare and Kaplinsky 1970) given by

$$k_L^{(0)}(x, y) = \frac{A}{2}Q^2\sqrt{\pi}\Big[\text{erf}[Qy + Rx] + e^{x^2-y^2}\text{erf}[Ry + Qx]$$
$$\pm\Big[\text{erf}[Qy - Rx] + e^{x^2-y^2}\text{erf}[Qy + Rx]\Big]\Big], \tag{5.110}$$

where we have used reduced speeds (x, y) and the $+$ in $\pm$ is for $y < x$ and the $-$ is for $y > x$. The hard sphere cross section is πd^2, $Q = \frac{1}{2}[\frac{1}{\sqrt{\gamma}} + \sqrt{\gamma}]$ and $R = \frac{1}{2}[\frac{1}{\sqrt{\gamma}} - \sqrt{\gamma}]$.

The pseudospectral solution of the eigenvalue problem based on a quadrature reduces Eq. (5.108) to the linear algebraic problem

$$\sum_{j=1}^{N} W_j x_j^2 k_L^{(0)}(x_j, x_i)\psi_{n,\ell}(x_j) - Z_i\psi_{n,\ell}(x_i) = -\lambda_{n,\ell}\psi_{n,\ell}(x_i). \tag{5.111}$$

For the most part, $\psi_n(x)$ and λ_n are for $\ell = 0$, unless otherwise noted. Since particle number is conserved, there is one zero eigenvalue, $\lambda_0 = 0$. The results for the Gauss-Maxwell quadrature is shown in Table 5.8. With 80 quadrature points, we find four discrete eigenvalues converged to 4 significant figures. The results reported by Bobylev and Mossberg (2008) are obtained from the solution of a Schrödinger equation with a potential parametrized by the eigenvalue sought. As a consequence, an iteration is required to converge to each eigenvalue as shown in Figs. 1 and 2 of their paper. The results in the table are also compared with the cubic B-spline solution by Khurana and Thachuk (2012) for which only two discrete eigenvalues are reported.

The study of the approach of the eigenvalues to the continuum boundary requires a very fine grid defined with the subdivision of the semi-infinite interval into 12 sub-intervals with 8 Fejér quadrature points in each interval except the last where a shifted Laguerre quadrature is used (Shizgal 1984). The interval boundaries are chosen to approximately coincide with the roots of the highest bound eigenfunction desired. We refer to this approach as the adaptive multidomain method.

Table 5.8 Convergence of the eigenvalues in units of $Z(0)$ of the linear ($\gamma = 1$) spherically symmetric ($\ell = 0$) Boltzmann collision operator for Gauss-Maxwell quadrature points ($p = 2$)

N	λ_1	λ_2	λ_3	λ_4	λ_5	λ_6
6	0.81359	0.97258	1.16137	1.55419	2.09752	0.00000
8	0.81616	0.97328	1.05678	1.29033	1.65256	2.11734
10	0.81736	0.97672	1.01756	1.15769	1.40627	1.74453
14	0.81831	0.97897	0.99904	1.04972	1.17109	1.36147
20	0.81874	0.97940	0.99772	1.00972	1.05415	1.13938
30	0.81893	0.97963	0.99829	1.00049	1.01072	1.03677
40	0.81898	0.97969	0.99834	0.99984	1.00274	1.01236
60	0.81901	0.97972	0.99838	0.99986	1.00025	1.00223
80	0.81902	0.97973	0.99838	0.99988	1.00001	1.00058
BM[a]	0.8190	0.9795	0.9985	0.999_5		
KT[b]	0.8190	0.9797				

[a] Eigenvalues determined from the solution of the Schrödinger equation (Bobylev and Mossberg 2008)

[b] Cubic B-spline solution of the integral eigenvalue problem with 60 intervals (Khurana and Thachuk 2012)

Table 5.9 Approach to the continuum boundary of the eigenvalues, in units of $Z(0)$, of the linear ($\gamma = 1$) spherically symmetric Boltzmann ($\ell = 0$) collision operator with the multidomain method

n	λ_n	$\frac{1-\lambda_n}{1-\lambda_{n+1}}$
1	0.8190221	
2	0.9797339	5.526
3	0.99838853	8.930
4	0.99988132	12.58
5	0.9999913460	13.58
6	0.99999936318	13.71
7	0.999999958353	13.59
8	0.9999999926736	15.29
	WKB	13.74

The lower order eigenvalues calculated in this way are shown in Table 5.9 in comparison with the WKB asymptotic behaviour (Rahman and Sundaresan 1968)

$$\frac{1-\lambda_{n,\ell}}{1-\lambda_{n+1,\ell}} \approx \exp\left[\frac{4\pi}{\sqrt{6(1+\frac{1}{\gamma})^2-(2\ell+1)^2}}\right], \tag{5.112}$$

which appears to occur by λ_6 or λ_7. It is clear that the calculation of these eigenvalues near to the continuum boundary is a challenging numerical exercise.

The eigenfunctions corresponding to these eigenvalues are shown in Fig. 5.8 and the rapid variation near to the origin is clear. There are several nodes very close to the origin and the others occur for much larger x. We contrast this behaviour

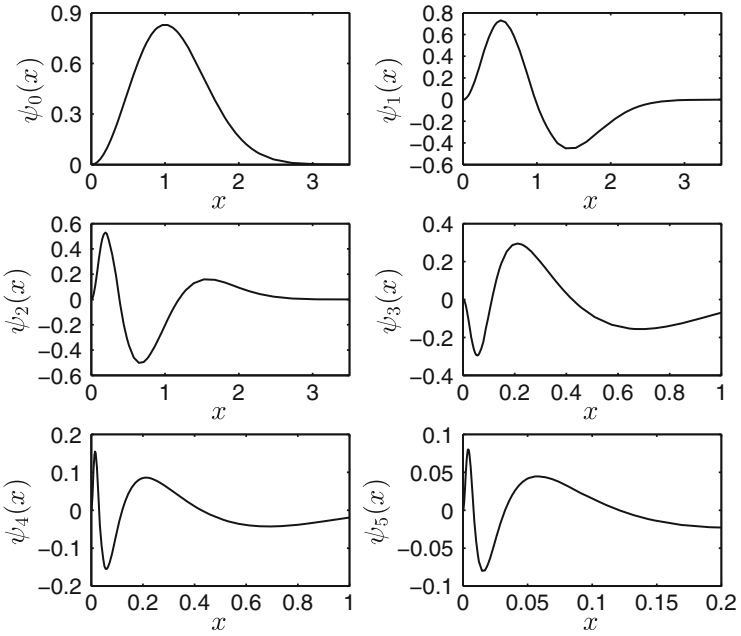

Fig. 5.8 The eigenfunctions, $\psi_n(x)$, of the linear Boltzmann collision operator ($\ell = 0, \gamma = 1$) determined with the adaptive multidomain quadrature

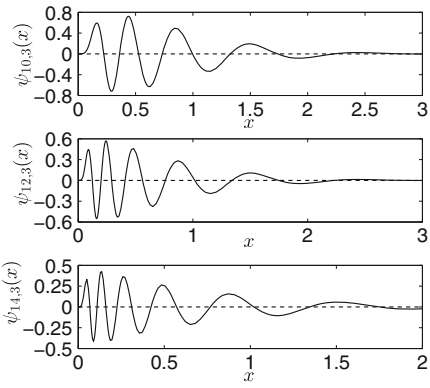

Fig. 5.9 Eigenfunctions of the linear ($\gamma = 1/8$) Boltzmann collision operator with the adaptive multidomain method for $\ell = 3$. The approach of the eigenvalues, $\lambda_{n,3}$, to the continuum boundary is shown in Table 5.10 in comparison with the asymptotic WKB result (Rahman and Sundaresan 1968)

with the eigenfunctions for $\ell = 3$ and $\gamma = 1/8$ in Fig. 5.9. Table 5.10 lists the corresponding eigenvalues and the WKB ratio and it is clear that these eigenvalues below the continuum boundary can be more easily evaluated. The oscillations of the eigenfunctions can be resolved over this larger domain than for the results in Fig. 5.8. With the multidomain approach, the variational theorem is more difficult to verify as the nodes and number of quadrature points between nodes is specific for a particular eigenfunction.

Table 5.10 Approach to the continuum boundary of the eigenvalues, in units of $Z(0)$, of the linear ($\gamma = 1/8$) Boltzmann collision operator with the adaptive multidomain method for $\ell = 3$

n	$\lambda_{n,3}$	$\frac{1-\lambda_{n,3}}{1-\lambda_{n+1,3}}$
1	0.42888	1.4444
2	0.60461	1.4978
3	0.73602	1.5675
4	0.83159	1.6405
5	0.89734	1.6912
6	0.93930	1.7197
7	0.96470	1.7459
8	0.97978	1.7691
9	0.98857	1.7873
10	0.99361	1.8004
11	0.99645	1.8092
12	0.99804	1.8150
13	0.99892	1.8186
14	0.99941	1.8203
	WKB	1.824

5.6.3 *Spectral Method of Solution of the Linear Boltzmann Equation with Quantum Cross Sections; Relaxation to Equilibrium and the Kullback-Leibler Entropy*

In this section, we consider the binary gas mixture defined in the previous section with the application to N-He and Xe-He mixtures for which accurate interatomic interaction potentials are known and the corresponding quantum differential cross sections can be calculated (Sospedra-Alfonso and Shizgal 2013). We write the spherically symmetric distribution function ($\ell = 0$) as $f(x,t) = F[1 + \phi(x,t)]$ and expand $\phi(x,t)$ in Sonine-Laguerre polynomials,

$$\phi(x,t) = \sum_{n=1}^{N} a_n(t) S^{(n)}(x^2), \tag{5.113}$$

and substitute $f(x,t)$ into Eq. (5.103) that defines the initial value problem. With the subsequent multiplication by $S^{(m)}(x^2)$ and integration over $\mathbf{v}$, the Boltzmann equation is reduced to the set of linear ordinary differential equations

$$\frac{d\hat{a}_m(t)}{dt} = \sum_{n=1}^{N} \hat{L}^{(0)}_{mn} \hat{a}_n(t), \tag{5.114}$$

where $\hat{a}_n = \sqrt{N_n} a_n$ such that $\hat{L}^{(0)}_{nm} = L^{(0)}_{nm}/\sqrt{N_n N_m}$ is symmetric, and $N_n = 2\Gamma(n + 3/2)/(n!\sqrt{\pi})$ is the normalization of the Sonine-Laguerre polynomials.

The matrix elements, $L_{nm}^{(0)}$ were previously evaluated, Eq. (5.107), for the hard sphere cross section using the generating function for the Sonine-Laguerre polynomials. This methodology can also be used for realistic cross sections (Shizgal and Dridi 2010) with the result that the matrix elements can be written in terms of the classic Omega integrals of transport theory (Hirschfelder et al. 1954; Chapman and Cowling 1970; Mason and McDaniel 1988) defined by

$$\Omega^{(\ell)}(k) = 2\pi \int_0^\infty \int_0^\pi e^{-z^2} z^{2k+3} (1 - \cos^\ell \theta) \sigma(E, \theta) \sin\theta d\theta dz, \tag{5.115}$$

where $z = \sqrt{E/k_B T_b}$ and

$$L_{nm}^{(0)} = \sum_{\ell=0}^{n} \sum_{k=1}^{n+m-\ell} C_{\ell,k} \Omega^{(\ell)}(k). \tag{5.116}$$

The coefficients, $C_{\ell,k}$ were determined with the generating function method and a MAPLE code is available (Shizgal and Dridi 2010). The differential cross sections vary rapidly with angle (see Fig. 3.19b) and a Simpson's rule integration can be used to accurately calculate the angular integral in $\Omega^{(\ell)}(k)$ and a Gauss-Laguerre quadrature for the reduced speed z. In this way, realistic cross sections can be used in a spectral based solution of the Boltzmann equation.

The time dependent solution is expressed in terms of the discrete eigenvalues, λ_n, and eigenvectors, U_{km}, of $\mathbf{L}$, that is

$$\sum_{k=1}^{N} L_{nk} U_{km} = -\lambda_n U_{nm}. \tag{5.117}$$

We show in Fig. 5.10 the results of a Sonine-Laguerre spectral calculation of the eigenvalue spectrum for the two gas mixtures, namely N in He and Xe in He with realistic quantum cross sections that define the collision operator (Sospedra-Alfonso and Shizgal 2013). The eigenvalues $\lambda_n < Z(0)$ are in the discrete spectrum while the eigenvalues $\lambda_n > Z(0)$ are in the continuum. The comparison with the equivalent hard sphere cross section shown in the figure demonstrates that the hard sphere cross section is a good approximation. For the Xe-He system with the small mass ratio, $\gamma = 0.030$, there are a large number of converged discrete eigenvalues whereas for the N-He system with a larger mass ratio, $\gamma = 0.29$, there are much fewer converged eigenvalues. The three discrete eigenvalues for N-He and the 9 discrete eigenvalues for Xe-He are converged to three significant figures with $N = 30$ and $N = 15$, respectively. This demonstrates the more rapid convergence of the Sonine-Laguerre basis functions for the Xe-He system which is closer to the Rayleigh limit than is N-He. In Chap. 6, we discuss the Fokker-Planck equations in the Rayleigh and Lorentz limits and the choice of basis functions.

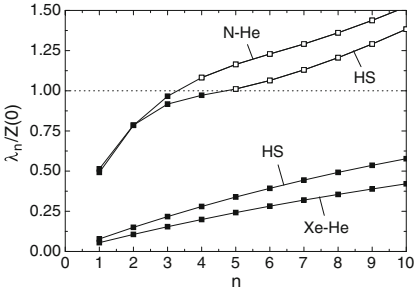

Fig. 5.10 Eigenvalue spectrum of the Boltzmann collision operator for binary mixtures with He as the background gas. The *filled squares* correspond to eigenvalues in the discrete spectrum and *open squares* are unconverged eigenvalues in the continuum. HS denotes the results with the hard sphere cross section, 18 Å^2 for N-He and 27 Å^2 for Xe-He. The other *curves* correspond to the results with a realistic cross section for each pair. Thirty Sonine-Laguerre polynomials were used. Reprinted from Sospedra-Alfonso and Shizgal (2013) with permission from the American Institute of Physics

The time dependent solution of the linear equations, Eq. (5.114), is

$$\hat{a}_n(t) = \sum_{k=1}^{N} c_k U_{nk} e^{-\lambda_k t}, \tag{5.118}$$

and the expansion of $\phi(x, 0)$ defines $\hat{a}_n(0)$. The expansion coefficients, c_k, in Eq. (5.118) are determined from the initial condition

$$c_k = \sum_{n=1}^{N} U_{kn} \hat{a}_n(0). \tag{5.119}$$

The eigenfunctions are given by the expansion in Sonine-Laguerre polynomials

$$\psi_n(x^2) = \sqrt{\frac{2}{\sqrt{\pi}}} \sum_{k=1}^{N} U_{kn} \frac{S^{(k)}(x^2)}{\sqrt{N_k}}, \tag{5.120}$$

and the time dependent distribution function is

$$f(x^2, t) = \frac{2}{\sqrt{\pi}} x^2 e^{-x^2} \left[1 + \sum_{n=1}^{N} c_n e^{-\lambda_n t} \psi_n(x^2) \right]. \tag{5.121}$$

It is readily shown with the orthogonality of the Sonine-Laguerre polynomials that the average energy of the energetic atoms is given exactly in terms of $a_1(t)$, that is

$$E(t) = \frac{3k_B T_b}{2} [1 - a_1(t)]. \tag{5.122}$$

However, the average energy in terms of $a_1(t)$ is coupled to the higher order expansion coefficients, $a_n(t)$ in Eq. (5.114), and the time dependence is multiexponential as given by Eq. (5.118). If the set of moment equations, Eq. (5.114), is truncated at $a_1(t)$, the resulting approximation to the energy relaxation is a pure exponential. Alternatively, we can approximate the distribution function with a local Maxwellian distribution function parametrized by the time dependent temperature (Mozumder 1981; Shizgal 1981b), that is

$$\frac{dT}{dt} = -K_{LM}[T_{eff}(t)]\Big[T(t) - T_b\Big], \tag{5.123}$$

where $T_{eff} = [MT(t) + mT_b]/(M + m)$ and

$$K_{LM}(T_{eff}) = \frac{16}{3\pi} M_1 M_2 \sqrt{\frac{T_{eff}}{T_b}} \int_0^\infty z^5 e^{-z^2} \sigma_{mt}(z^2 k_B T_{eff}) dz. \tag{5.124}$$

The momentum transfer cross section in Eq. (5.124) is defined by

$$\sigma_{mt}(E) = 2\pi \int_0^\pi (1 - \cos\theta)\sigma(E, \theta) \sin\theta d\theta. \tag{5.125}$$

We consider the approach to equilibrium with an initial test particle Gaussian energy distribution of the form

$$f(E, 0) = \frac{C}{\sqrt{k_B T_b}} \sqrt{E} \exp\left[- \alpha \sqrt{\frac{E}{k_B T_b}} - x_0)^2 \right], \tag{5.126}$$

where $T_b = 300\,\mathrm{K}$ and $N_b = 3.27 \times 10^{16}\,\mathrm{cm}^{-3}$ consistent with experimental conditions (Zhang et al. 2007). The parameters $\alpha = 5$ and $x_0 = 2$ are chosen, and C is a normalization. A major difficulty can be the expansion of the initial distribution with Eq. (5.113). The expansion of a Maxwellian at T_b in Sonine-Laguerre polynomials is equivalent to the representation of the Sonine-Laguerre polynomials with the generating function defined by Eq. (4.54) in Sect. 4.5.1. The Sonine-Laguerre expansion of many initial distribution functions, such as a Gaussian, that model energetic distributions with temperatures above the bath temperature will converge very slowly if at all.

The time dependence of the distribution functions is shown in Fig. 5.11(A) for N in He and in Fig. 5.11(B) for Xe in He for an initial energy of 0.12 eV. A sufficient number of basis functions are used so as to fit the initial distribution to three significant figures. Although there are only a few discrete eigenvalues in Eq. (5.121) that converge with an increase in N, there a large number of eigenvalues, $\lambda_n > Z(0)$ that are in the continuum. Nevertheless, the summation in Eq. (5.121) that replaces the

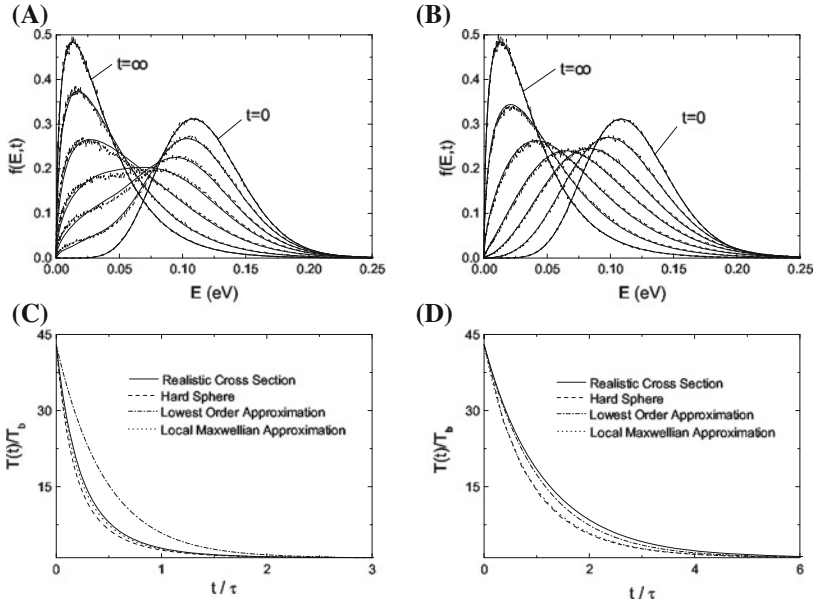

Fig. 5.11 (*Upper graphs*) Energy distribution function for (**A**) N-He and (**B**) Xe-He for $t/\tau = 0.07, 0.16, 0.29, 0.51$ and 0.29 where τ equals (**A**) 76 ns and (**B**) 56 ns; The initial distribution function is a Gaussian with $E(0) = 0.12$ eV; The *dashed curves* are the results with a Monte-Carlo simulation. (*Lower graphs*) Time evolution of the temperature ratio for (**C**) N-He and (**D**) X-He with an initial Gaussian with $E(0) = 1.67$ eV. The results are converged to three significant figures with 30 Sonine-Laguerre polynomials. Reprinted from Sospedra-Alfonso and Shizgal (2013) with permission from the American Institute of Physics

integral over the continuum eigenvalues, converges with an increase in N and thus the solution converges even though λ_k and c_k change with N. The dashed (noisy) curves in the figures are the results of Monte Carlo simulations (Sospedra-Alfonso and Shizgal 2013) that validate the results with the Sonine-Laguerre expansion.

The relaxation of the temperature is shown in Fig. 5.11(C), (D) for N-He and Xe-He mixtures, respectively, with $E(0) = 1.67$ eV. The curve identified as the lowest order approximation with the one moment, $a_1(t)$, is a pure exponential while the other results are multi-exponential curves. A major objective of the kinetic theory is the approach to equilibrium (Ziff et al. 1981; Mouhot 2006). We use the Kullback-Leibler entropy (Kullback and Leibler 1951; Mozumder 1981; Shizgal 2007) defined by

$$\Sigma_{SS}(t) = -4\pi \int v^2 f(v,t) \ln\left[\frac{f(v,t)}{F(v,T_b)}\right] dv, \tag{5.127}$$

and another similar functional that is a measure of the departure of the distribution function from the local Maxwellian F_{LM} and given by

$$\Sigma_{LM}(t) = -4\pi \int v^2 f(v,t) \ln \left[\frac{f(v,t)}{F_{LM}(v, T(t))} \right] dv. \tag{5.128}$$

The local Maxwellian varies with $T(t)$ and it is important to note that $\Sigma_{LM}(t)$ is not an entropy. These are two examples of measures for the departure of one function from another for which there are many choices especially in signal analysis (Cha 2007) analogous to the choice of least squares approximation used in Chap. 4 to analyze the convergence of different expansions.

The time dependence of both quantities is shown in Fig. 5.12 with $\Sigma_{SS}(t)$ as the dashed curves and $\Sigma_{LM}(t)$ as the solid curves for three different initial energies. $\Sigma_{SS}(t)$ is a monotonically increasing function of time consistent with an entropy whereas $\Sigma_{LM}(t)$ can exhibit extremum values as a function of time. The relaxation of the shape of the nonequilibrium distribution function can be determined experimentally with Doppler spectroscopy (Nakayama et al. 2005; Zhang et al. 2007). The translational energy relaxation can also be followed experimentally (Park et al. 1989).

The spectral method of solution of the Boltzmann equation with the Sonine-Laguerre polynomials provides sufficiently converged solutions so as to permit a useful comparison with experiment. The choice of the initial distribution is limited by its expansion in this basis set. Round-off errors can also occur in the calculation of the matrix elements if large basis sets are required.

A pseudospectral approach based on the Gauss-Maxwell or some other quadrature can also be employed with realistic quantum mechanical elastic scattering cross sections. The details of these applications is beyond the scope of this book and can be found elsewhere (Bovino et al. 2009, 2011; Sospedra-Alfonso and Shizgal 2012a), and references therein. The calculation of the spherically symmetric kernel for realistic cross sections requires an integration over E and θ of the differential cross section $\sigma(E, \theta)$ (see Fig. 3.19b). The cusp in the resulting kernel tend to be extremely narrow and the accurate integration over the cusp in the kernel requires a very fine grid (Kharchenko et al. 1998).

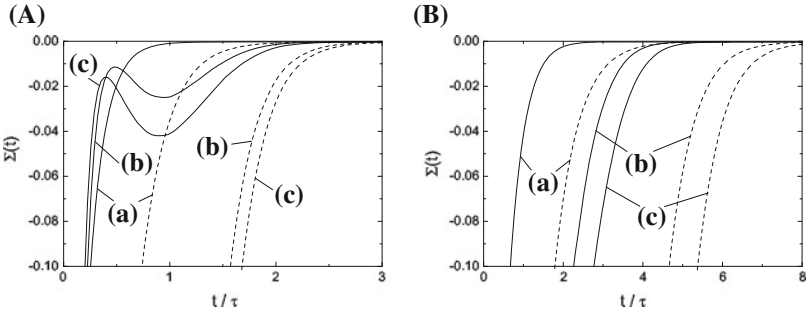

Fig. 5.12 Time evolution of the Kullback-Leibler relative entropies $\Sigma_{SS}(t)$ (*dashed curve*) and $\Sigma_{LM}(t)$ (*solid curve*) for (**A**) N-He ($\tau = 76$ ns) and (**B**) Xe-He ($\tau = 56$ ns). Initial average energies are (*a*) 0.12 eV, (*b*) 0.94 eV and (*c*) 1.67 eV with an initial Gaussian distribution. Reprinted from Sospedra-Alfonso and Shizgal (2013) with permission from the American Institute of Physics

In Chap. 6, we report the eigenvalue spectrum of the Fokker-Planck equation with the Coulomb cross section. We will show that the eigenvalue spectrum has an infinite number of discrete eigenvalues and a continuum. However, in contrast to the behaviour with the Boltzmann equation, the spectrum becomes completely continuous for a particular mass ratio (with the exclusion of $\lambda_0 = 0$). The continuum eigenfunctions are L^2 square integrable discrete eigenfunctions as discussed by Reinhardt (1979) for quantum mechanical problems. In the absence of a single nonzero discrete eigenvalue, that is the "spectral gap", the approach to equilibrium ceases to be a pure exponential (Corngold 1981).

5.7 Two Dimensional Anisotropic Distributions

In the previous sections, we provided a description for the relaxation to equilibrium of isotropic nonequilibrium distributions. In the sections that follow, we consider several physical systems for which the distribution function of the energetic species is anisotropic. Laser photofragmentation of molecules can produce energetic atoms with anisotropic nonequilibrium distributions (Cline et al. 1990; Nicholson et al. 1996). The relaxation of the anisotropy can be followed with Doppler spectroscopy. In Sect. 5.7.1, we consider a spectral solution of the Boltzmann equation with a model initial anisotropic distribution. The decay of the anisotropy can be uncoupled from the energy relaxation in the disparate mass ratio, $\gamma = M/m$, limits. This provides the rationale for the use of the Fokker-Planck equation in the Rayleigh limit, $\gamma \to 0$, and Lorentz limit, $\gamma \to \infty$, (Andersen and Shuler 1964) as discussed in Chap. 6.

In Sect. 5.7.2, we treat the Milne problem for a two component system previously considered in the context of the radiative transfer problem (the one-speed model) in Sect. 5.3. This Milne problem also serves as a model for the escape of planetary atmospheres (Fahr and Shizgal 1983). Both rarefied gas dynamical problems are in three dimensions, namely position, speed and the anisotropy variable, $\mu = \cos\theta$, where θ denotes the orientation of the particle velocity relative to a polar axis. A spectral method is used to solve the Boltzmann equation for the Milne problem whereas a combined spectral/pseudospectral method is used for the planetary escape problem (Shizgal and Blackmore 1986).

5.7.1 Pseudospectral/Spectral Solution of the Boltzmann Equation; Relaxation of Anisotropic Distributions in a Binary Gas

A nonthermal anisotropic distribution function of atoms can be produced in the laboratory by laser photolysis of a molecule producing an energetic atom. The nascent distributions then relax by collisions with background inert gas atoms

and the approach to equilibrium is followed with Doppler spectroscopy (Park et al. 1989; Taatjes et al. 1990). The relaxation of anisotropic nonthermal distributions of I^* produced by photofragamentation of C_3F_7I has been studied experimentally (Cline et al. 1990; Nicholson et al. 1996). It is possible to generate with linearly polarized light an initial distribution that is a product of an isotropic distribution and an anisotropy factor of the form

$$f(v, \mu, 0) = f(v, 0)[1 + \beta(0) P_2(\mu)], \tag{5.129}$$

where $\mu = \cos\theta$ and θ gives the orientation of the velocity vector, $\mathbf{v}$, relative to some polar axis. The parameter $\beta(t)$ is the anisotropy parameter which can also depend on the particle velocity. Matsumi et al. (1994) carried out similar studies of the anisotropy and velocity relaxation of energetic $O(^1D)$ atoms in different moderators.

In this section, we consider a pseudospectral solution of the linear Boltzmann equation with a hard sphere cross section and study the relaxation versus the mass ratio $\gamma = M/m$, with m the test particle mass and M the mass of the background species. We choose for convenience an initial anisotropic nonequilibrium distribution of the form

$$f(x, \mu, 0) = C \frac{(\mu + 1)^\beta}{x} \exp\left[- \alpha(E_0 - x^2)^2 \right], \tag{5.130}$$

where α, β and E_0 are constants to be specified and C is a normalization. The constant β is generally a small integer in keeping with the experimentally generated anisotropic distribution as a single Legendre polynomial, Eq. (5.129).

The Boltzmann equation for this spatially uniform system is given by Eq. (5.103) with the collision operator defined by Eg. (5.104) or equivalently the kernel in Eq. (5.105). The collision frequency is given by

$$Z(y) = 2\pi \int_0^\infty \int_{-1}^{1} K_L(x, y, \overline{\mu}) x^2 d\overline{\mu} dx, \tag{5.131}$$

which is equivalent to Eq. (5.109). The Wigner-Wilkins kernel, Eq. (5.110), is the spherical average of $K_L(x, y, \overline{\mu})$. We expand the kernel, Eq. (5.105), in Legendre polynomials, that is

$$K_L(x, y, \overline{\mu}) = \sum_{\ell=0}^{\infty} k_L^{(\ell)}(x, y) P_\ell(\overline{\mu}), \tag{5.132}$$

where the expansion coefficients are the kernels

$$k_L^{(\ell)}(x, y) = \frac{2\ell + 1}{2} \int_{-1}^{1} K_L(x, y, \overline{\mu}) P_\ell(\overline{\mu}). \tag{5.133}$$

Thus, the relaxation of the anisotropic distribution for the initial distribution given by Eq. (5.130), is described with the set of uncoupled integral equations for each ℓ, that is

$$\frac{\partial f_\ell(x,t)}{\partial t} = \int_0^\infty k_L^{(\ell)}(x,y) f_\ell(y,t) y^2 dy - Z(x) f_\ell(x,t), \tag{5.134}$$

where the initial distributions, $f_\ell(x,0)$, is determined from Eq. (5.130). The spherical components, $f_\ell(x,t)$, of the distribution function are defined as in Eq. (5.138). The kernels, $k_L^{(\ell)}(x,y)$ can be accurately evaluated with a Gauss-Legendre quadrature for the $\overline{\mu}$ integration in Eq. (5.133).

The set of integral equations, Eq. (5.134), can be solved with the Maxwell quadrature points, $\{x_i\}$, and big weights, $\{W_i = w_i/w(x_i)\}$, based on the weight function $w(x) = x^2 e^{-x^2}$ defined in Chap. 3, Sect. 3.3. The discretized version is thus

$$\frac{\partial f_\ell(x_i,t)}{\partial t} = \sum_{j=1}^{N-1} B_{ij} f_\ell(x_i,t), \tag{5.135}$$

where the matrix $\mathbf{B}$ is defined by

$$B_{ij} = W_j k_\ell(x_i,x_j) x_j^2 - Z(x_i)\delta_{ij}. \tag{5.136}$$

As before we express the solution to each integral equation in terms of the eigenvalues $\lambda^{(\ell)}$ and eigenfunctions $\mathbf{U}$, that is

$$\mathbf{B}\cdot\mathbf{U} = \mathbf{U}\cdot\lambda. \tag{5.137}$$

The ℓ dependence of the matrices in Eq. (5.137) is not shown explicitly. The initial values of $f_\ell(x,0)$ are determined from the initial condition, Eq. (5.130). The expansion of $f(x,\mu,t)$ is in Legendre polynomials in μ, that is

$$f(x,\mu,t) = \sqrt{\frac{2\ell+1}{2}} \sum_\ell^\infty f_\ell(x,t) P_\ell(\mu), \tag{5.138}$$

so that

$$f_\ell(x,t) = \sqrt{\frac{2\ell+1}{2}} \int_{-1}^{1} f(x,\mu,t) P_\ell(\mu) d\mu, \tag{5.139}$$

which is evaluated with Gauss-Legendre quadrature points $\{\mu_i\}$ and weights $\{v_i\}$, and written as the transform

$$f_\ell(x,t) = \sum_{i=1}^{N} T_{\ell i}^{(b)} f(x,\mu_i,t), \tag{5.140}$$

where the transformation matrix is

$$T_{\ell i}^{(b)} = \sqrt{\frac{2\ell+1}{2}} v_i P_\ell(\mu_i). \tag{5.141}$$

The inverse of this transformation is

$$f(x,\mu_i,t) = \sum_{\ell=0}^{N-1} T_{i\ell}^{(f)} f_\ell(x,t), \tag{5.142}$$

where

$$T_{i\ell}^{(f)} = \sqrt{\frac{2\ell+1}{2}} P_\ell(\mu_i), \tag{5.143}$$

and $\mathbf{T}^{(b)} \cdot \mathbf{T}^{(f)} = \mathbf{I}$.

The time dependent distribution is expressed in terms of the eigenvalues and eigenfunctions of $\mathbf{B}$, that is

$$f_\ell(y_i,t) = \sum_{j=0}^{N} U_{ij}^{(\ell)} C_j^{(\ell)} \exp(-\lambda_{j\ell} t), \tag{5.144}$$

with the $C_j^{(\ell)}$ evaluated with the initial distributions

$$C_j^{(\ell)} = \sum_{k=0}^{N-1} \left(U^{-1}\right)_{jk} f_\ell(x_k,0). \tag{5.145}$$

We choose $\beta = 2$ in the initial distribution and solve three integral equations, Eq. (5.134), with $\ell = 0, 1$ and 2. For each, 60 Gauss-Maxwell quadrature points were sufficient to give the convergent distributions shown in Figs. 5.13, 5.14 and 5.15. For each ℓ, the collision operator has a discrete and continuous eigenvalue spectrum. The continuous eigenfunctions are square integrable in the discrete L^2 space that is used (Reinhardt 1979). This is another illustration that the discretization of the continuum portion of the spectrum leads to numerically convergent solutions.

The relaxation of the anisotropic distribution is shown in Figs. 5.13, 5.14 and 5.15 for mass ratios $\gamma = 1/16, 1$ and 16, respectively, for the initial condition, Eq. (5.130) with $\beta = 2$, $E_0 = 900$ and $\alpha = 10^{-4}$. The results for the small mass ratio approaching the Rayleigh limit are shown in Fig. 5.13. The anisotropy of the distribution function is maintained while there is a relatively rapid energy exchange.

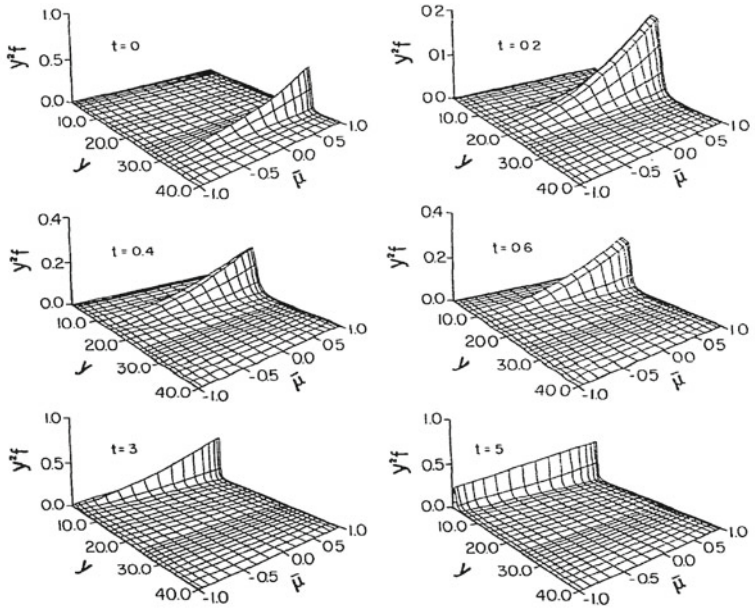

Fig. 5.13 Time evolution of the anisotropic distribution for mass ratio $M/m = 1/16$. The initial distribution is given by Eq. (5.130) with $\beta = 2$, $E_0 = 900$ and $\alpha = 10^{-4}$. The time t is in units of $\tau = [Nd^2\sqrt{2\pi k_B T/M}]^{-1}$. In the figure $\overline{\mu} \equiv \mu$. Reprinted from Shizgal and Blackmore (1983) with permission from Elsevier

There is an efficient transfer of energy on collision relative to the randomization of the particle direction. For the unit mass ratio case in Fig. 5.14, the anisotropy and the energy relaxation appear to occur on the same time scale. In addition, since the energy transfer for equal masses is very efficient; the energy relaxation is rapid as can be seen by the growth of the peak in the distribution in the thermal energy regime. This distribution function in this case is bimodal in speed with a peak at both high and low speeds.

The results in Fig. 5.15 for the larger mass ratio approaching the Lorentz limit, show an efficient change in direction of the light particle on collision. The anisotropy of the distribution disappears quickly and the energy relaxation occurs on a longer time scale. In the limit of very small mass ratios, which is applicable for the relaxation of electrons in atoms, the anisotropy decays many orders of magnitude faster than the energy relaxation. Thus, for electron transport in the Lorentz limit it is often sufficient to use the two-term approximation, that is with $\ell = 0$ and $\ell = 1$ (Pitchford et al. 1981; Pitchford and Phelps 1982; Shizgal and McMahon 1985; Hagelaar and Pitchford 2005); see Chap. 6, Sect. 6.3.

The relaxation of nonthermal distributions for the small and large mass ratio limits is well approximated by a Fokker-Planck equation (Andersen and Shuler 1964) as discussed in Chap. 6, Sect. 6.1.3. The results shown, computed with a

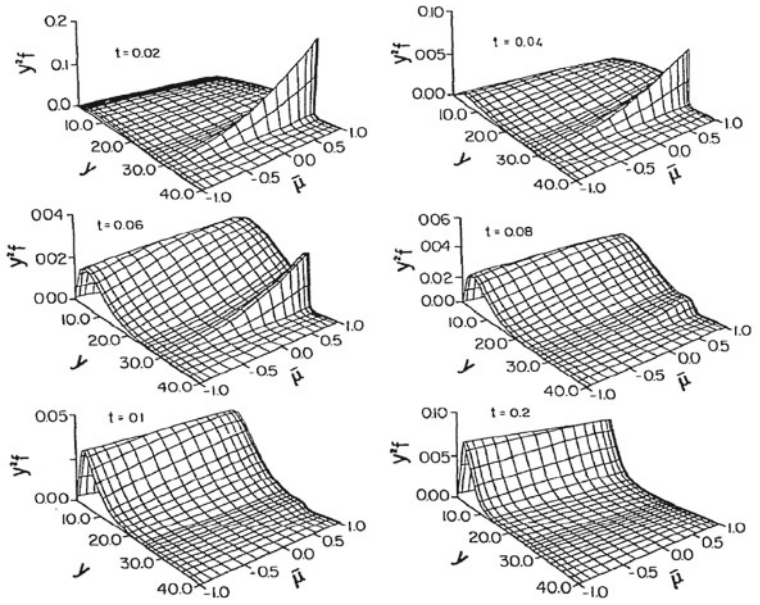

Fig. 5.14 Time evolution of the anisotropic distribution for mass ratio $M/m = 1$. The initial distribution is given by Eq. (5.130) with $\beta = 2$, $E_0 = 900$ and $\alpha = 10^{-4}$. The time t is in units of $\tau = [Nd^2\sqrt{2\pi k_B T/M}]^{-1}$. In the figure $\overline{\mu} \equiv \mu$. Reprinted from Shizgal and Blackmore (1983) with permission from Elsevier

spectral/pseudospectral method, provide useful graphically accurate depictions of the different behaviour in these limits.

5.7.2 *A Spectral Method of Solution of the Milne Problem*

The Milne problem, depicted in Fig. 5.16, refers to the diffusion of a minor constituent of mass m in a background species of mass M considered to be at equilibrium at temperature T_b (Lindenfeld and Shizgal 1983). The vertical line at $r = 0$ separates the medium that occupies the right half-space, $r > 0$, from the vacuum that is in the left half-space $r < 0$. A current density of magnitude **j** directed in the negative r-direction exists in the medium. The problem consists of determining the steady velocity distribution of the minor species within the half-space $r > 0$ and the angular distribution of emerging particles at the boundary subject to the condition that there are no particles incident from the left onto the medium. These boundary conditions are the same as those used for the radiative transfer problem in Sect. 5.3. For $\gamma \to \infty$, we have the Lorentz limit and the one-speed radiative transfer problem. This system is a typical rarefied gas dynamical half-space problem (Williams 1971; Cercignani 1988; Williams 2005).

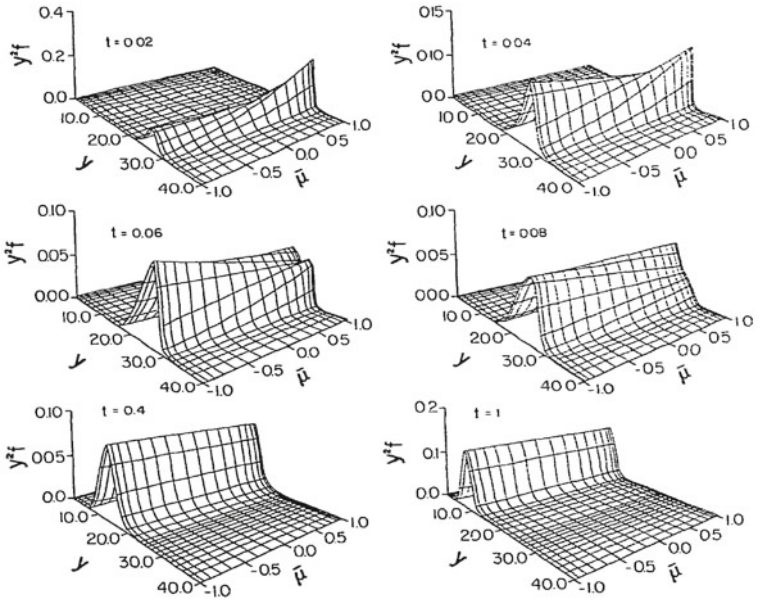

Fig. 5.15 Time evolution of the anisotropic distribution for mass ratio $M/m = 16$. The initial distribution is given by Eq. (5.130) with $\beta = 2$, $E_0 = 900$ and $\alpha = 10^{-4}$. The time t is in units of $\tau = [Nd^2\sqrt{2\pi k_B T/M}]^{-1}$. In the figure $\overline{\mu} \equiv \mu$. Reprinted from (Shizgal and Blackmore 1983) with permission from Elsevier

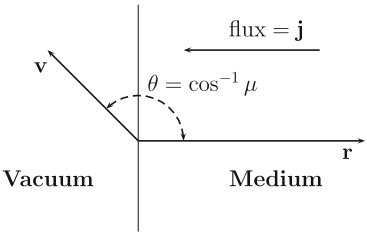

Fig. 5.16 The geometry of the Milne problem; The *vertical line* separates the vacuum from the medium. The orientation of the particle velocity, **v**, relative to the radial direction in space, **r**, is θ. There is a constant source of particles of flux **j** at infinity

Far from the boundary, in the positive r-direction, hydrodynamic equations are valid, which for the present model is the diffusion equation,

$$\overline{j} = -D\frac{dn^{(as)}(r)}{dr}. \tag{5.146}$$

This is the usual diffusion equation in the collision dominated regime that relates the flux $\overline{j}$ and the gradient of the asymptotic density profile, $n^{(as)}(r)$ and D is the diffusion coefficient. One finds that the extrapolation of the linear asymptotic dependence of the actual density profile intersects the r-axis at $r = -q$, where q is the extrapolation length and is a measure of the departure from hydrodynamic behaviour

near the boundary. The calculation of the density and temperature profiles and the extrapolation length are the main objectives.

For steady-state conditions, the Boltzmann equation for the velocity distribution function of test particles, $\overline{f}(r, v, \mu)$, is

$$v\mu \frac{\partial \overline{f}(r, v, \mu)}{\partial r} = n_b(r)\overline{L}[\overline{f}(r, v, \mu)], \tag{5.147}$$

where $\mu = \cos(\theta)$ and θ is the angle between $\mathbf{v}$ and the positive r-axis as shown in Fig. 5.16. In Eq. (5.147), $n_b(r)$ is the number density of the background medium and the linear Boltzmann collision operator for atom-atom collisions is defined by Eq. (5.104) except that the background density appears explicitly. We choose a hard sphere cross section, $\sigma_{el} = \pi d^2$, and rewrite the Boltzmann equation in dimensionless form.

With the transformation to dimensionless spatial variable,

$$z = \pi d^2 \int_0^r n_b(r')dr', \tag{5.148}$$

which is the "optical depth" of the medium, the Boltzmann equation can be written as

$$x\mu \frac{\partial f(z, x, \mu)}{\partial z} = n_b(r)L[f(z, x, \mu)], \tag{5.149}$$

where $L = \overline{L}/(\pi d^2 v_0)$, $f = \overline{f}[v_0/n_b(r)\pi d^2]^3$, $v_0 = \sqrt{2k_B T_b/m}$ and $x = v/v_0$ is the reduced speed.

We seek solutions of this equation subject to the boundary condition that no particles in the positive μ region return to the medium, that is

$$f(0, x, \mu) = 0, \qquad 0 < \mu < 1. \tag{5.150}$$

The general solution is written as the sum of a spatially transient part, f^{tr}, and an asymptotic part, f^{as}, that is

$$f = f^{tr} + f^{as}. \tag{5.151}$$

The transient solution dominates near the $z = 0$ boundary and it is anticipated that it decays out in a distance of the order of a few mean free paths. The asymptotic solution dominates at large distances where hydrodynamics is expected to be valid.

The transient solution is of the form,

$$f^{tr}(z, x, \mu) = \sum_{k=1}^{\infty} a_k e^{\lambda_k z} R_k(x, \mu), \tag{5.152}$$

where λ_k and $R_k(x,\mu)$ are the spatial eigenvalues and eigenfunctions, respectively, given by

$$L[R_k] = (z\mu)\lambda_k R_k. \tag{5.153}$$

We choose basis functions which are products of spherical harmonics and associated Laguerre polynomials, $L_n^{(\ell+1/2)}(x)$, that is

$$\phi_{nl}(x,\mu) = N_{n\ell} L_n^{(\ell+1/2)}(x) P_\ell(\mu), \tag{5.154}$$

where $N_{n\ell} = \sqrt{\frac{\sqrt{\pi}n!(2l+1)}{2\Gamma(n+\ell+\frac{2}{3})}}$ is the combined normalizations of the Sonine-Laguerre and Legendre polynomials. The eigenfunctions and eigenvalues are determined with the expansion of $R_k(x,\mu)$ in the basis functions $\phi_{n\ell}(x,\mu)$

$$R_k(x,\mu) = \frac{\exp(-x^2)}{\pi^{3/2}} \sum_{n=0}^{\infty}\sum_{\ell=0}^{\infty} b_{n\ell}^k \phi_{n\ell}(x,\mu). \tag{5.155}$$

The eigenvalue problem is then converted to the finite set of linear equations,

$$\sum_{n'=0}^{N}\sum_{\ell'=0}^{L}\left(L_{nn'}^{(\ell)}\delta_{\ell\ell'} - \lambda_k M_{n\ell,n'\ell'}\right) b_{n'\ell'}^k = 0. \tag{5.156}$$

The quantities $L_{n,n'}^{(\ell)}$ and $M_{n\ell,n'\ell'}$ are the matrix elements of the collision operator and of $x\mu$ in the drift term on the left hand side of Eq. (5.149), respectively. The matrix elements are defined by

$$\begin{aligned} L_{nn'}^{(\ell)} &= \langle\psi_{n\ell}|L^{(\ell)}|\psi_{n'\ell}\rangle, \\ M_{n\ell,n'\ell'} &= \langle\psi_{n\ell}|x\mu|\psi_{n'\ell'}\rangle. \end{aligned} \tag{5.157}$$

and $M_{n\ell,n'\ell'}$ is given by

$$M_{n\ell,n'\ell'} = \begin{cases} (l+1)\sqrt{(n+\ell+\frac{3}{2})/(2l+1)(2l+3)}, & n'=n,\ l'=l+1 \\ -(\ell+1)\sqrt{n/(2\ell+1)(2\ell+3)}, & n'=n-1,\ l'=\ell+1 \\ \ell\sqrt{(n+\ell+\frac{1}{2})/(4\ell^2-1)}, & n'=n,\ l'=\ell-1 \\ -\ell\sqrt{(n+1)/(4\ell^2-1)}, & n'=n+1,\ \ell'=\ell+1 \\ \\ 0, & \text{otherwise.} \end{cases}$$

and determined with the recurrence relations for the Legendre and associated Laguerre polynomials, namely,

$$\mu P_\ell = \frac{1}{2\ell+1}\Big[(\ell+1)P_\ell(\mu) + \ell P_{\ell-1}\Big],$$
$$x L_{n-1}^{(\ell+1/2)}(x) = n L_{n-1}^{(\ell+1/2)}(x) - n L_n^{(\ell+1/2)}(x) - (n+\ell-1/2) L_{n-1}^{(\ell-1/2)}. \quad (5.158)$$

Numerical diagonalization of the matrices in Eq. (5.156) with a QZ algorithm (Golub and Van Loan 1996), also known as the Schur decomposition, gives approximate eigenvalues and eigenfunctions to order $K = (N+1)(L+1)$. The transient solution is written as

$$f^{tr}(z, x, \mu) = \sum_{k=1}^{\frac{1}{2}K-1} a_k e^{\lambda_k z} R_k(x, \mu). \quad (5.159)$$

The spatial eigenvalues, λ_k, which includes the zero eigenvalue, occur in positive and negative pairs so that the sum over k in Eq. (5.152) includes only nonzero negative λ_k (Lindenfeld and Shizgal 1983; Alterman et al. 1962). This is similar to the radiative transfer problem in Sect. 5.3. If the positive eigenvalues are retained, the solution diverges. Any discretization of the Boltzmann equation without eliminating the positive spatial eigenvalues will lead to spurious results (Pierrard and Lemaire 1998).

The asymptotic solution is written in the form

$$f^{as}(z, x, \mu) = -(j/D) f^M(x)[q + z - \mu U(p)], \quad (5.160)$$

where the dimensionless flux and diffusion coefficient are given by $j = \overline{j}/v_0 [n_1(r)\pi d^2]^3$ and $D = \overline{D}/[v_0/n_1(r)\pi d^2]$, respectively. The function $U(x)$ satisfies the Chapman-Enskog equation for diffusion (Chapman and Cowling 1970), that is

$$L[\mu U(x)] = -x\mu, \quad (5.161)$$

and is solved with the expansion

$$\mu U(x) = \sum_{n'=0}^{\infty} d_{n'} \psi_{n'1}(x, \mu). \quad (5.162)$$

Consequently, the solution of Eq. (5.161) is given by

$$\sum_{n'=0}^{\infty} L^{(1)}_{n',n} d_{n'} = -\frac{1}{\sqrt{2}} \delta_{n,0} \quad (5.163)$$

and the diffusion coefficient is

$$D = \frac{d_0}{\sqrt{2}}. \quad (5.164)$$

The advantage of the associated Laguerre basis functions is that the diffusion coefficient is given in terms of the one expansion coefficient, d_0. However, the matrix equation, Eq. (5.163), must be inverted and the convergence of d_0 verified.

The general solution of the Boltzmann equation is written as the sum of the transient solution and the asymptotic solution, that is

$$f(z,x,\mu) = F(x)\left[\sum_{k=1}^{\frac{1}{2K}-1} a_k e^{\lambda_k z} \sum_{\ell=0}^{L}\sum_{n=0}^{N} b_{n\ell}^{k}\psi_{n\ell}(x,\mu) + \frac{1}{D}\left(q+z-\sum_{n=1}^{N} d_n\psi_{n\ell}(x,\mu)\right)\right]. \tag{5.165}$$

The coefficients $b_{n\ell}^{k}$ and λ_k are determined with the solution of the eigenvalue problem, Eq. (5.156). The d_k coefficients are calculated with the inversion of the Chapman-Enskog equation, Eq. (5.163). The general solution is then completely specified with the $(K/2-1)$ a_k coefficients and the extrapolation length with application of the boundary condition, Eq. (5.150).

However, it should be clear that the expansion Eq. (5.165) cannot satisfy exactly this boundary condition for all x and μ. There are several different methods to use to apply the boundary condition and no one method is a priori better than the others. This is a limitation of a spectral method based on polynomial basis functions. We do not provide the details of this aspect of the problem discussed elsewhere (Lindenfeld and Shizgal 1983; Garcia and Siewert 1996; Ghosh 2014) and references therein. The Marshak boundary condition (Davison 1957; Williams 1971) which sets moments of the distribution function to zero at the boundary provides convergent results with modest sized basis sets ($N = 9$ and $L = 11$).

One of the main objectives is the density profile of the test particle which is shown in Fig. 5.17. The solid lines are the results with the solution of the Boltzmann equation whereas the dashed lines represent the extrapolation of the asymptotic profiles for large x. The intercept on the negative z axis is $-q$.

The extrapolation length, q, versus mass ratio is shown in Table 5.11 with a limited basis set (N = 9, L = 11). The value of the extrapolation length in the one-speed case ($\gamma \to \infty$) is 0.7104 to four significant figures. A more precise value reported by Loyalka and Naz (2008) is 0.710446089599.

The Milne problem was also considered with the Coulomb cross section for collisions between charged particles (Barrett et al. 1992) for which the Boltzmann collision operator is replaced with the Fokker-Planck differential operator. This has been referred to as the Coulomb Milne problem (Lie-Svendsen and Rees 1996) and as a model for the outflow of light ions from the high latitude ionosphere and the solar wind (Echim et al. 2011). The Fokker-Planck equation is also the basis for the study of the plasma sheath problem. This is a Milne problem coupled to the Poisson equation which provides the electric field in the sheath near an electrode (Vasenkov and

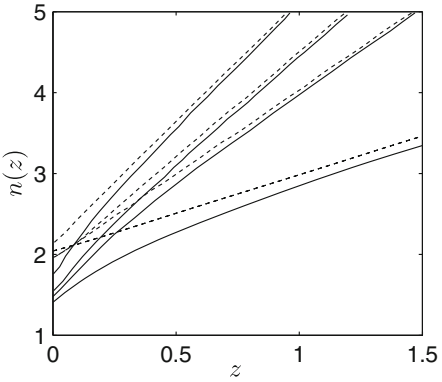

Fig. 5.17 The *solid lines* represent the density profile from the solution of the Boltzmann equation. The *dashed lines* are the asymptotic linear variation extrapolated back to the negative z axis with the intercept equal to $-q$. The mass ratios from *top* to *bottom* are $\gamma = \infty$ (the one-speed case), 10, 1 and 1/9, respectively. Reproduced from Lindenfeld and Shizgal (1983) with permission of the American Physical Society

Table 5.11 The variation of the extrapolation length versus mass ratio γ with the solution of the Boltzmann equation with $N = 9$ Sonine-Laguerre polynomials and $L = 11$ Legendre polynomials

$\gamma = M/m$	q
1	0.9370
1.5	0.8564
2.333	0.7984
4	0.7569
9	0.7278
19	0.7170
39	0.7123
99	0.7097
∞	0.7104

Reproduced in part from Lindenfeld and Shizgal (1983) with permission from the American Physical Society

Shizgal 2000, 2002) analogous to the recent treatment of the behaviour of electric arcs (Lowke and Tanaka 2006).

The Boltzmann equation, Eq. (5.149), may appear similar to the initial value problem whereby z plays the role of t, but there is an important distinction owing to the occurrence of μ on the left hand side. If one were to divide through by $z\mu$ and integrate directly in z there would be spurious results as noted by Pierrard and Lemaire (1998) in their modeling of the terrestrial polar wind.

5.7.3 A Mixed Spectral/Pseudospectral Solution of the Boltzmann Equation for the Escape of Light Atoms from a Planetary Atmosphere

The Milne problem presented in Sect. 5.7.2 also serves as a model for the escape of a minor species from a planetary atmosphere. For the terrestrial atmosphere, this refers to the escape of atomic hydrogen and helium from the high altitude rarefied region of the atmosphere referred to as the exosphere. The bottom of the exosphere is the exobase where the mean free path of the major species, namely atomic oxygen, is equal to the barometric scale height (Fahr and Shizgal 1983). If we assume that the distribution function of escaping species is a Maxwellian, the equilibrium escape flux from the exobase is the Jeans flux given by

$$F_J = 2\pi \int_{v_{esc}}^{\infty} \int_0^{\pi/2} F(v) v \cos\theta \sin\theta d\theta v^2 dv,$$
$$= \frac{n_c}{2}\sqrt{\frac{2kT_c}{m}}\left(1+\lambda_{esc}\right)e^{-\lambda_{esc}}, \tag{5.166}$$

where $\lambda_{esc} = mv_{esc}^2/2k_BT_c$ is the escape parameter, $v_{esc} = 11.2\,\text{km/s}$ is the escape speed and T_c is the temperature at the exobase often referred to as the critical level. The atmosphere above the exobase is assumed to be collisionless. The loss of energetic particles from the atmosphere perturbs the distribution function from Maxwellian such that the nonequilibrium escape flux, F, is less than the equilibrium Jeans escape flux, F_J, and $F/F_J < 1$. This is analogous to the nonequilibrium effects in reactive systems discussed in Sect. 5.4.4 except that in this application we are treating a spatially nonuniform system.

We consider a slab of atmosphere so that a plane parallel model is sufficient. We measure altitude in terms of the atmospheric "optical depth" that is

$$z = -\int_r^{r_{top}} \sigma_{tot} n_b(r') dr', \tag{5.167}$$

where $n_b(r)$ is the density of the heavier background gas bound to the planet. The Boltzmann equation for the distribution function of the minor escaping constituent, with neglect of the gravitational force in the drift term (Shizgal and Blackmore 1986), is Eq. (5.147) as in the Milne problem, that is,

$$x\mu\frac{\partial f}{\partial z} = \tilde{J}[f], \tag{5.168}$$

where $\mu = \cos\theta$ and $\tilde{J} = \sqrt{m/2k_BT_b}J/n_b(r)\pi d^2$. The physical situation is depicted in Fig. 5.18 where the exobase is the dashed line at $z = -1$, where the mean free

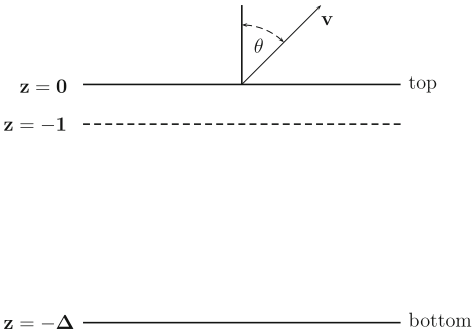

Fig. 5.18 Plane parallel model of an atmosphere with the critical level at $z = -1$ measured in terms of the atmospheric optical depth. The lower boundary at $z = -\Delta$ is in the collision dominated atmosphere whereas the escape of atoms is from the "top" of the atmosphere at $z = 0$

path is equal to the atmospheric scale height. At the lower boundary in the collision dominated region (the asymptotic condition in the Milne problem), the distribution is assumed to be a Maxwellian modified with a drift to account for the flux of particles from below. This is the Chapman-Enskog regime far from the top boundary. Therefore, at $z = -\Delta$, which is sufficiently deep within the collision dominated region, we impose the boundary condition with an anisotropy linear in μ, that is

$$f(x < x_{esc}, \mu, -\Delta) = F(x) + \mu U(x), \tag{5.169}$$

where $F(x)$ is the Maxwellian and $U(x)$ is to be determined.

This is supplemented with boundary conditions at the top taking into account the escape speed from the planet. Particles with less than the escape speed get reflected back down so that

$$f(x < x_{esc}, -\mu, 0) = f(x < x_{esc}, \mu, -\Delta), \quad \mu > 0, \tag{5.170}$$

and there are no incoming particles in excess of the escape speed, so that

$$f(x > x_{esc}, \mu, 0) = 0, \quad \mu < 0. \tag{5.171}$$

Shizgal and Blackmore (1986) used a mixed spectral/pseudospectral method of solution of the Boltzmann equation expressed in terms of the expansion of the anisotropy of the distribution function in Legendre polynomials

$$f(x, \mu, z) = \sum_{\ell=0}^{L} f_\ell(x, z) P_\ell(\mu) \tag{5.172}$$

which yields the set of coupled integral equations

$$\frac{\partial f_\ell(x,t)}{\partial t} + x\left(a_\ell \frac{\partial f_{\ell-1}(x,t)}{\partial z} + a_{\ell+1} \frac{\partial f_{\ell+1}(x,t)}{\partial z}\right) = \int_0^\infty k_L^{(\ell)}(x,y) f_\ell(y,t) dy - Z(x) f_\ell(x,t), \tag{5.173}$$

where $a_\ell = \ell/\sqrt{(2\ell-1)(2\ell+1)}$ and the recurrence relation for the Legendre polynomials has been used. We discretize Eq. (5.173) with the Gauss-Maxwell quadrature. However, in view of the boundary condition dependent on the reduced critical escape speed, $x_{esc} = \sqrt{\lambda_{esc}}$, we divide the semi-infinite speed interval into two subintervals, namely $[0, \sqrt{\lambda_{esc}}]$ and $[\sqrt{\lambda_{esc}}, \infty]$ so as to apply the boundary condition. Two sets of polynomials orthogonal with respect to $w(x) = x^2 e^{-x^2}$ separately on these intervals, together with the associated quadratures are calculated with the methods presented in Chap. 2. This procedure can be compared to the "double Gauss" method in radiative transfer (Sykes 1951; Stamnes et al. 1988) with the half-range Legendre polynomials.

Although we have retained the time dependence in Eq. (5.173), we are interested in the steady state problem. The Boltzmann equation is discretized with Gauss-Legendre quadrature points in z with the transformation of the interval $[-1, 1]$ to $[0, -\Delta]$ with quadrature points at the interval boundaries with the appropriate scaling. The two interval Maxwell quadratures in reduced speed, x, are used to discretize the kernels $k_L^{(\ell)}(x, y)$. The derivative with respect to z is evaluated with the physical space representation of the derivative operator with the transformed Legendre quadratures. As the dimension of the resulting linear matrix equation is large, the time dependence is retained and the steady solution determined with a time iteration. In this scheme the ith iterate is given by

$$\begin{aligned}\Delta f_i^{(\ell)}(x_n, z_m) = \Bigg[&\sum_{j=1}^{N} B_{nj}^{(\ell)} f_i^{(\ell)}(x_j, z_m) \\ &+ x_n \sum_{k=1}^{M} D_{mk} \left(a_\ell f_i^{(\ell-1)}(x_n, z_k) + a_{\ell+1} f_i^{(\ell+1)}(x_n, z_k) \right) \\ &- S[f_i^{(\ell)}(x_n, z_m) - g^{(\ell)}(x_n, z_m)] \Bigg] \Delta t, \end{aligned} \tag{5.174}$$

where $B_{nj}^{(\ell)}$ is the physical space representation of the kernels and D_{mk} is the Gauss-Legendre physical space matrix derivative operator in altitude, z.

An ansatz is made for the form of the initial distribution, given by

$$\begin{aligned} f^{(0)}(x, \mu, z) = F(x) \Bigg(&- \frac{z}{\Delta} \left[1 + \frac{3(1+\lambda)\exp(-\lambda)\mu}{2\sqrt{\pi}} \right] \\ &+ \left[1 + \frac{z}{\Delta} \right] [H(x_c) H(\mu) + h(-\mu)] \Bigg), \end{aligned} \tag{5.175}$$

where the Heaviside function is $H(x) = 1$ for $x > 0$ and $H(x) = 0$ for $x < 0$. Equation (5.175) satisfies the boundary condition at the top ($z = 0$) and the initial form of the anisotropy at the bottom ($z = -\Delta$). The Legendre polynomial expansion of Eq. (5.175) provides the initial Legendre coefficients, $f_0^{(\ell)}(x, z)$.

The term with S at the end of Eq. (5.174) is an added convergence term where at $t = 0$, $g^{(\ell)} = f_0^{(\ell)}$. At each time step, the boundary condition at the top ($z = 0$), Eq. (5.170), is imposed by transforming $f_i^{(\ell)}(x_n, 0)$ to $f_i(x_n, \mu, 0)$ and setting the distribution function for incoming particles ($\mu < 0$) to be equal to outgoing particles ($\mu > 0$) except for values of $x > \sqrt{\lambda_{esc}}$. Once the top boundary condition is imposed, the distribution function is transformed back to the Legendre polynomial basis. When the iterative scheme yields a converged solution $g^{(\ell)} = f_{i-1}^{(\ell)}$ and the last term in small square brackets in Eq. (5.174) will be zero.

This iterative procedure is very similar to the one used by (Lie-Svendsen and Rees 1996) concerning the escape of the minor ion, He^+, in a background of O^+ with the replacement of the integral Boltzmann collision operator with the differential Fokker-Planck operator for Coulomb collisions. The authors refer to this problem as the Coulomb Milne problem (Barrett et al. 1992). Thus the Milne problem serves as the basis for several different physical systems in space and plasma physics.

The principal objective is to determine the reduction of the actual flux, F, from the Jeans' flux, F_J. The ratio $F/F_J < 1$ owing to the depletion of particles with $v > v_{esc}$ in the tail of the Maxwellian. The ratio F/F_J is shown in Fig. 5.19 versus T_c, the temperature at the exobase. The results of the formalism described here are shown as the solid line with solid circles in comparison with two separate Monte Carlo simulations (Chamberlain and Campbell 1967; Brinkman 1970) and from the results reported by Pierrard (2003). The lower boundary condition in (Pierrard 2003) is not the asymptotic Chapman-Enskog distribution for this collisionally dominated regime. It is a Maxwellian with only upward moving ($\mu > 0$) particles. It is reasonable to expect that if the lower boundary is sufficiently deep in the atmosphere, that within a few mean free paths upwards from the lower boundary, the distribution function would attain the same form, Eq. (5.169), used by Shizgal and Blackmore (1986), that

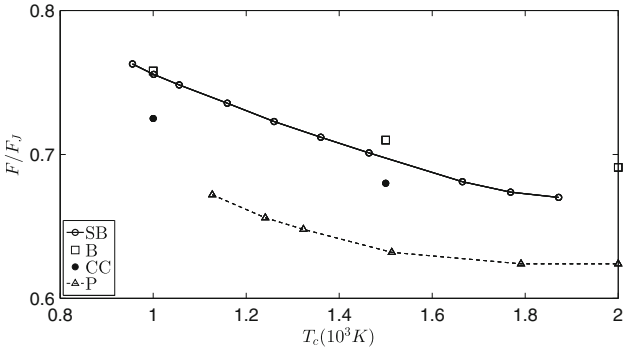

Fig. 5.19 The variation of the nonequilibrium escape flux, F, relative to the equilibrium Jeans flux, F_J versus the temperature at the exobase, T_c; the different results correspond to the work of *SB* (Shizgal and Blackmore 1986), *B* (Brinkman 1970), *CC* (Chamberlain and Campbell 1967) and *P* (Pierrard 2003). Reproduced from Shizgal and Blackmore (1986) and Pierrard (2003) with permission from Elsevier

is, a drifting Maxwellian. With increasing altitude, the distribution function will be further modified owing to the escape of particles at the top.

5.7.4 Electric Field Induced Ion Drift in Buffer Gases; Applications to Ionospheric and Space Physics

A classic problem in kinetic theory is the drift of ions of mass m dilutely dispersed in a background atomic or molecular gas of mass M and density $n_b(r)$ under the influence of an external spatially uniform and steady electrostatic field (Danailov et al. 2008; Viehland and Chang 2012). The distribution function is non-Maxwellian in speed, x, anisotropic in velocity and depends on the electrostatic field strength, E, and the background density, $n_b(r)$. The steady state Boltzmann equation for a gaseous ion in a background of a single atomic gas is

$$\mathbf{v} \cdot \nabla f + \frac{Z_{ion}\mathbf{E}}{m} \cdot \nabla_{\mathbf{v}} f = Lf, \tag{5.176}$$

where Z_{ion} is the ion charge, $\mathbf{E}$ is the electrostatic field directed along the polar axis and L is the linear collision operator given by Eq. (5.104). The anisotropy of the distribution function in velocity is expressed by the dependence on $\mu = \cos\theta$ where θ is the angle between $\mathbf{z}$ and $\mathbf{v}$. The Chapman-Enskog method discussed in Sect. 5.4.1 can be used for small electrostatic field strengths to calculate the diffusion coefficient D and the mobility K that appear in the expression for the ion flux

$$\mathbf{F}_{ion} = D\nabla n_b(r) + n_b(r)K\mathbf{E}. \tag{5.177}$$

The transport coefficients, D and K, are determined with the differential cross section $\sigma(g, \theta)$ for a particular ion-atom system. In this small E limit, the mobility is related to the diffusion coefficient by the Nernst-Townsend-Einstein relation $K = Z_{ion}D/k_BT$ (McDaniel and Mason 1973) and derived also on the basis of Brownian motion (Newburgh et al. 2006).

At higher electrostatic field strengths, the distribution function is more strongly perturbed from a Maxwellian in speed and anisotropy. We assume that the ions diffuse with a spatially uniform distribution and the Boltzmann equation for the distribution function, $f(\mathbf{v})$, is given by

$$\frac{Z_{ion}}{m}\mathbf{E} \cdot \nabla_v f = Lf. \tag{5.178}$$

The distribution function is expanded in the direct product of the Sonine-Laguerre functions in x^2 and Legendre polynomials in μ, that is

$$f(x, \mu) = F(x) \sum_{n=0}^{\infty} \sum_{\ell=0}^{\infty} f_{n,\ell} x^{\ell} S_n^{(\ell+1/2)}(x^2) P_\ell(\mu), \tag{5.179}$$

This procedure is very similar to the one used to treat the Milne problem in Sect. 5.7.2. With the substitution of Eq. (5.179) into (5.178), multiplication by the basis functions and integration over **v**, as we have done previously in other applications, we get the following set of linear equations for the expansion coefficients (see Sect. 6-1-1 in Mason and McDaniel (1988)),

$$\frac{Z_{ion}E}{Nm}\sqrt{\frac{m}{2k_BT}}\left[\ell(\ell+\frac{1}{2}+n)f_{n,\ell-1}-(\ell+1)f_{n-1,\ell+1}\right]=(\ell+\frac{1}{2})\sum_{k=0}L_{nk}^{(\ell)}f_{n,\ell}, \tag{5.180}$$

where the matrix elements of the linear collision operator, $L_{nk}^{(\ell)}$, are given by Eq. (6-1-19), and Table 5-4-2 in McDaniel and Mason (1973). The collision operator matrix elements are diagonal in ℓ and the terms in $\ell+1$ and $\ell-1$ from the drift term on the left hand side are coupled arising from the recurrence relations of the Legendre polynomials. The recurrence relation for the Sonine-Laguerre polynomials has also been used.

This is the spectral Galerkin solution of the Boltzmann equation with the Sonine-Laguerre basis functions orthogonal with the Maxwellian weight function. The mobility is given in terms of the single $f_{0,1}$ coefficient which is coupled to all the higher order coefficients. With increasing electric field strength, the anisotropy and non-Maxwellian features of the distribution function increase and the convergence for the mobility is slow and may even diverge.

To improve the convergence at higher electric field strengths, basis functions orthogonal with a weight function that closely approximates the form of the anticipated solution are preferable. In Chap. 4, we demonstrated the use of the scaling of the quadrature weights and points to improve the convergence of certain test functions with a scaling factor s which we identified with a "scaling" temperature, that is $s^2 = T_s/T$. In the ion-mobility literature (McDaniel and Mason 1973; Lin et al. 1979b; Viehland and Lin 1979; Mason and McDaniel 1988), this procedure is referred to as the two-temperature method with the reduced speed defined with T_s rather than with T. The matrix elements depend on T and T_s where T_s is varied to accelerate the convergence much in the same way as quadrature points are scaled.

However, with further increase in the electric field strength, the two-temperature method also fails to provide accurate results and a different set of basis functions is constructed, motivated again by choosing a weight function that better approximates the anisotropy of the anticipated distribution function. Thus, a drifting bi-Maxwellian weight function in terms of parallel, $v_{||}=v\mu$, and perpendicular, $v_\perp = v\sqrt{1-\mu^2}$, velocity components relative to the electric field direction are used, that is,

$$f(v_\parallel, v_\perp)=4\pi\sqrt{\frac{m}{2k_BT_\parallel}}\left(\frac{m}{2k_BT_\perp}\right)\exp\left(-\frac{mv_\perp^2}{2k_BT_\perp}\right)\exp\left(-\frac{m(v_\parallel-W)^2}{2k_BT_\parallel}\right). \tag{5.181}$$

with an unknown drift velocity W and unkown temperature parameters, $T_\perp$ and $T_\parallel$. The expansion in terms of reduced energies, $y_\perp = mv_\perp^2/2k_BT$ and $y_\parallel = m(v_\parallel - W)^2/2k_BT$, is

$$f(y_\parallel, y_\perp) = e^{-y_\parallel^2 - y_\perp^2} \sum_{n=0}^{\infty} \sum_{m=0}^{\infty} c_{nm} H_n(y_\parallel) S^{(m)}(y_\perp^2), \tag{5.182}$$

with $y_\parallel \in (-\infty, \infty)$ and $y_\perp \in [0, \infty]$. This approach is referred to as the three-temperature model as it depends on $T_\parallel$, $T_\perp$ and T. The basis functions used to model ion velocity distributions in the high-latitude ionosphere (St.-Maurice and Schunk 1976, 1979) are also the classical Laguerre polynomials $L_n^{(0)}(y_\perp)$ and Hermite polynomials, $H_n(y_\parallel)$.

The basis set used by researchers in gaseous ion transport is the product of three Hermite polynomials in the Cartesian velocity coordinates (Lin et al. 1979b; Mason and McDaniel 1988). The matrix elements of the collision operator can be calculated but with greatly increased complexity; see the Appendix in Lin et al. (1979b). The calculations are iterative in that an initial estimate of $T_\perp$, $T_\parallel$ and W must be made and subsequently updated from the moment solution. Thus the calculation has two convergence issues, namely (1) the convergence of the polynomial expansion and (2) the convergence of the iteration.

Viehland (1994) used a Gram-Charlier approach (Blinnikov and Moessner 1998) with a more flexible weight function with several unknown parameters that are updated with an iterative solution of the Boltzmann equation. The parameters in the weight function include as in the other methods W, $T_\parallel$, $T_\perp$ and T_s as well as the skewness and the kurtoses parallel and perpendicular to the electrostatic field. There are still other parameters related to energy and velocity correlations. The calculation of the matrix representation of the collision operator in this basis set defined by this weight function is more involved than for the two and three temperature models. The details of these calculations can be found in the Appendix of Lin et al. (1979b) with the matrix elements are expressed in terms of summations with 25 indices. With this approach, it is possible to compute gaseous ion transport coefficients directly from ab initio potential energy functions for atomic ions in atomic gases, with greater precision and accuracy than they can be measured.

It is clear that the choice of weight function and associated basis functions is crucial in the modelling of ion-mobilities as well as in other similar applications in ionospheric and space science. In the terrestrial ionosphere there is a geomagnetic field, $\mathbf{B}$, perpendicular to the ionospheric electric field $\mathbf{E}$. The use of different weight functions and polynomial basis functions in ionospheric physics was reviewed by St.-Maurice and Schunk (1979). The objective is to derive a small set of partial differential equations in the lower order moments. This approach is very similar to Grad's 13-moment method (Grad 1949; Struchtrup 2005). Models with an increasingly larger number of moments have been developed (Schunk 1977; Ma and St.-Maurice 2008).

The main thrust of the theoretical methods for the solution of the Boltzmann equation is to choose a weight function close to the anticipated solution. A non-classical weight function in $y_\perp$ is derived with the Bahatnager-Gross-Krook relaxation time approximation to the collision operator (Bhatnagar et al. 1954) that yields an analytic solution to the Boltzmann equation (St.-Maurice and Schunk 1974; Hubert 1983). This nonclassical weight function is then used to define a set of polynomials that provide a more rapid convergence than the expansions based on the Sonine-Laguerre polynomials (Shizgal and Hubert 1989). This basis set has also been used to provide lower order approximations of the nonequilibrium speed distributions observed in astrophysical winds (Leblanc and Hubert 1997). This subject is well beyond the scope of this book but we emphasize the strong overlap between these research fields.

5.8 The Nonlinear Isotropic Boltzmann Equation

In Sect. 5.5, we determined the eigenvalue spectrum of the collision operator for the linearized Boltzmann equation with expansions in the Sonine-Laguerre polynomials as well as with a multidomain spectral element method. The time scale of the approach to equilibrium for initial distributions close to the equilibrium Maxwellian distribution is determined by the eigenvalues of the linearized collision operator. In particular the lowest nonzero eigenvalue determines the final approach to equilibrium. In this section, we are concerned with the approach to equilibrium of a one component spatially uniform gas determined with the nonlinear Boltzmann equation given by

$$\frac{\partial f(\mathbf{v},t)}{\partial t} = \int\int \left[f_1(\mathbf{v}_1') f(\mathbf{v}') - f_1(\mathbf{v}_1) f(\mathbf{v}) \right] g\sigma(g,\Omega) d\mathbf{v}_1, \tag{5.183}$$

analogous to Eq. (5.30) without the gradients in space and velocity in the drift term on the left hand side. For this initial value problem, we assume that the distribution function is isotropic.

This problem has been considered by many researchers since the time of Ludwig Boltzmann and a complete review is a daunting task. We highlight here some of the major advances and also provide the results of recent numerical simulations.

The interest in the time evolution of the nonlinear Boltzmann equation increased dramatically with the discovery of an analytic solution for the Maxwell molecule model with the isotropic cross section, $\sigma(g,\Omega) = \kappa/g$. The result was originally reported in the MSc thesis by Krupp (1967) and later published independently by Krook and Wu (1976) and by Bobylev (1976, 1984). This explicit time dependent solution is given by

$$f_{BKW}(x,t) = \frac{2x^2 e^{-x^2/K(t)}}{\sqrt{\pi} K(t)} \left[\frac{5K(t)-3}{K(t)} + \frac{2(1-K(t))}{K^2(t)} x^2 \right],$$

where t is in units of $4\pi n\kappa$ and $K(t) = 1 - \frac{2}{5}e^{-t/6}$, analogous to a time dependent temperature. This model system serves as a benchmark to test different numerical methods for the solution of the nonlinear Boltzmann equation (Filbet et al. 2006; Filbet and Mouhot 2011; Wu et al. 2013; Ghiroldi and Gibelli 2014). The early work on the nonlinear Boltzmann equation was reviewed by Ernst (1981, 1984).

5.8.1 *Finite Difference Method of Solution of the Nonlinear Boltzmann Equation; Approach to Equilibrium*

We restrict our attention to isotropic distributions and the hard sphere collision cross section. Spectral methods with an expansion of the isotropic time dependent distribution function in the Sonine-Laguerre polynomials were employed long ago (Abe 1971; Weinert et al. 1980). Additional results were reported in a series of papers by Kügerl and Schürrer (1990) and by Ender et al. (2011).

The distribution function is expanded in the set of the Sonine-Laguerre polynomials $S^{(n)}(x^2)$, that is

$$f(x,t) = \frac{4}{\sqrt{\pi}} x^2 e^{-x^2} \sum_{n=2}^{\infty} c_n(t) S^{(n)}(x^2), \tag{5.184}$$

where $c_0(t) = 0$ and $c_1(t) = 0$ owing to particle and energy conservation, respectively. The expansion coefficients are given by

$$c_n(t) = \frac{\sqrt{\pi}}{2} \frac{n!}{\Gamma(n+3/2)} \int_0^{\infty} f(x,t) S^{(n)}(x^2) dx. \tag{5.185}$$

With the Sonine-Laguerre expansion, the nonlinear Boltzmann equation is reduced to an infinite set of coupled ordinary differential equations for time dependent $c_j(t)$ coefficients. The substitution of Eq. (5.184) into (5.183) yields the system of nonlinear ordinary differential equations

$$\frac{\mathrm{d}c_n(t)}{\mathrm{d}t} = \sum_{k=2}^{\infty} J_{nk} c_k(t) + \sum_{k=2}^{\infty} \sum_{\ell=2}^{\infty} N_{j,k\ell} c_k(t) c_\ell(t), \quad n \geq 2 \tag{5.186}$$

where the matrix elements of the linearized operator are denoted by $J_{nk} \equiv \langle n|J|k\rangle$ given by Eq. (5.65) and the nonlinear tensor, $N_{n,k\ell}$, is defined by

$$N_{n,k\ell} = \iiint F_1 F_2 S_1^{(n)} \left[S_1^{(k)\prime} S_2^{(\ell)\prime} - S_1^{(k)} S_2^{(\ell)} \right] \sigma g d\Omega d\mathbf{v}_1 \mathbf{v}_2, \tag{5.187}$$

and evaluated as described elsewhere (Shizgal and Karplus 1970; Abe 1971; Shizgal 1971; Kügerl and Schürrer 1990; Weinert et al. 1980). The Maxwellian weight

function in Eq. (5.187) is denoted by F. The spectral method based on the set of equations, Eq. (5.186) is analogous to the solution of the linearized Boltzmann equation in Sect. 5.4.3 with the added nonlinear terms.

The solution of the nonlinear Boltzmann equation is then obtained with the choice of an initial distribution, which provides the initial values of the expansion coefficients, $c_n(0)$, and the subsequent numerical integration of the set of equations, Eq. (5.186). This method of solution is limited to initial distributions close to the equilibrium Maxwellian owing to the difficulty of accurately calculating the nonlinear matrix elements $N_{n,k\ell}$ as well as the convergence of the initial distribution in the Sonine-Laguerre polynomials. The expansion in Sonine-Laguerre polynomials can suffer from spurious oscillations and give distributions that become negative in some regions. However, the method is attractive as the final approach to equilibrium will be determined by the linear terms in Eq. (5.186) and thus the spectral properties of J, discussed in Sect. 5.5.2. This spectral method of solution has been reported by other researchers (Abe 1971; Weinert et al. 1980; Kügerl and Schürrer 1990; Ender et al. 2011).

5.8.2 *Finite Difference Discretization of the Nonlinear Boltzmann Equation*

We solve the nonlinear Boltzmann equation with a stable finite difference method and determine the expansion coefficients, $c_n(t)$, with the numerical solution. For the hard sphere cross section, we define a dimensionless time t in units of $\tau = \sqrt{m/\pi k_B T_b}/(4nd^2)$ and the reduced speed $y = \sqrt{2k_B T/m}$. We rewrite the initial value problem defined by the nonlinear Boltzmann equation in the equivalent form (Kügerl and Schürrer 1990; Kabin and Shizgal 2003),

$$\frac{\partial f(y_1,t)}{\partial t} = \mathcal{F}_{in}(y_1,t) - \mathcal{F}_{out}(y_1,t), \tag{5.188}$$

where

$$\mathcal{F}_{out}(y_1,t) = f(y_1,t)\int_0^\infty S_{out}(y_1,y_2)f(y_2,t)dy_2, \tag{5.189}$$

and

$$\mathcal{F}_{in}(y_1,t) = \int_0^\infty\int_0^\infty S_{in}(y_1' \to y_1; y_2')f(y_1',t)f(y_2',t)dy_1'dy_2'. \tag{5.190}$$

For hard spheres, the scattering kernels can be written as follows (Kügerl and Schürrer 1990):

$$S_{out}(y_1, y_2) = \frac{1}{2}\begin{cases} y_1\left(1+\frac{y_2^2}{3y_1^2}\right) & \text{for } y_1 \geq y_2, \\ y_2\left(1+\frac{y_1^2}{3y_2^2}\right) & \text{for } y_1 \leq y_2, \end{cases}$$

$$S_{in}(y_1' \to y_1, y_2') = \frac{y_1}{y_1' y_2'} \min(y_1, y_2, y_1', y_2') H(y_2^2),$$

where $H(x)$ is the Heaviside step function and from energy conservation we have that $y_1^2 + y_2^2 = y_1'^2 + y_2'^2$. Particle number conservation gives the out-scattering kernel in terms of the in-scattering kernel by an integration, that is

$$S_{out}(y_1, y_2) = \int_0^\infty S_{in}(y_1 \to y_1', y_2) dy_1'.$$

We also have the detailed balance symmetry property

$$S_{in}(y_1' \to y_1, y_2') = S_{in}(y_2' \to y_1, y_1'). \tag{5.191}$$

We define the integral quantities

$$\begin{aligned} F_1(y_1, t) &= \int_0^{y_1} f(y, t) dy, \\ F_2(y_1, t) &= \int_{y_1}^\infty \frac{f(y, t)}{y} dy, \end{aligned} \tag{5.192}$$

so that $\mathcal{F}_{in}$ defined by the double integral (5.190) can be written as

$$\mathcal{F}_{in} = \sqrt{\frac{\pi}{2}}\left[2v_1 F_1(y_1, t) F_2(y_1, t) + y_1^2 F_2^2(y_1, t) + I(y_1, t)\right],$$

where the last term is the integral

$$I(y_1, t) = \iint_{S_0} \frac{y_1 y_2}{y_1' y_2'} f(y_1', t) f(y_2', t) dy_1' dy_2'. \tag{5.193}$$

The two dimensional integral is evaluated over the area S_0 defined by a circle $y_1'^2 + y_2'^2 = y_1^2$ and the straight lines $y_1' = y_1$ and $y_2' = y_1$. This is a significant

simplification of the original expression (5.190) because we have reduced most of the double integrals to the products of single integrals. With the substitution, $\xi_1 = y_1'^2/y_1^2$ and $\xi_2 = y_2'^2/y_1^2$, we get

$$I(y,t) = \frac{y_1^2}{4} \iint\limits_{S_1} \frac{\sqrt{\xi_1 + \xi_2 - 1}}{\xi_1 \xi_2} f(y_1', t) f(y_2', t) d\xi_1 d\xi_2. \tag{5.194}$$

where S_1 is a triangle with the vertices at (1, 0), (1, 1), and (0, 1). This integral can be efficiently evaluated with the cubature rule for a simplex (Stroud 1971).

5.8.3 Time Dependent Solutions

The reduced speed variable, y, is discretized uniformly according to $y_{i+1} = y_i + h$ on the finite interval $[0, y_{max}]$. The time variable is also discretized according to $t_{n+1} = t_n + \Delta t$. We integrate the nonlinear Boltzmann equation, Eq. (5.188), in t with an Euler integration algorithm so that the discretized version of the Boltzmann equation is

$$f^{(n+1)}(y_i) = f^{(n)}(y_i) + \Delta t[\mathcal{F}_{in}^{(n)}(y_i) - \mathcal{F}_{out}^{(n)}(y_i)]. \tag{5.195}$$

The term $\mathcal{F}_{out}^{n}(y_i)$ is determined from Eq. (5.189) with a Simpson rule integration over y_2 on the uniform grid. The double integral over ξ_1 and ξ_2 in Eq. (5.194) over the triangle S_1 is evaluated by dividing the triangle into several smaller triangles. The integral over each of these triangles is evaluated with a cubature for a triangle (Stroud 1971). With this technique, we have simplified the discretization of the in-scattering integral which presents the major challenge for the solution of the nonlinear Boltzmann equation.

Figure 5.20 shows the time evolution of the distribution function with the initial distributions (A) $f(y,0) = y^2 e^{-5y^2} + e^{4(y-3)^2}$ and (B) $f(y,0) = e^{-5\sqrt{|y-1|^2}} + e^{-5\sqrt{|y-3|^2}}$. The first has a large peak at $y = 3$ and a smaller peak at lower speeds. The second has two large peaks at $y = 1$ and 3, respectively. We choose $y_{max} = 8$ and 500 grid points in y. The time step Δt is taken sufficiently small so that the number density and temperature are conserved to 8 significant figures. The time dependent distributions shown in Fig. 5.20 do not drift and the shape evolves to a Maxwellian shown by the dashed curves.

We also consider an initial distribution function $f(x,0) = M(x)\left(\frac{5}{2} - 2x^2 + \frac{4}{5}x^4\right)$ used previously (Kügerl and Schürrer 1990), which corresponds to $c_0(0) = 1$, $c_1(0) = 0$ and $c_n(0) = \frac{4}{5}\delta_{n2}$, $n \geq 2$, in Eq. (5.185). The function $f(x,0)$ is a bimodal distribution with a slightly populated tail. In Fig. 5.21(A), we show the time dependent solution of the nonlinear Boltzmann equation with this initial condition. The dashed curve is the equilibrium Maxwellian. In Fig. 5.21(B), we show the

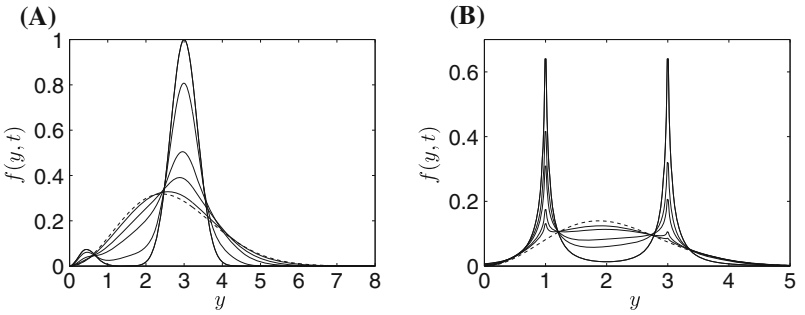

Fig. 5.20 Time evolution of the distribution function for the dimensionless time in units of τ from *top* to *bottom* equal to 0, 0.1, 0.4, 0.7 and 1.4; the *dashed curves* are the equilibrium distributions; (**A**) initial distribution $f(y,0) = y^2 e^{-5y^2} + e^{4(y-3)^2}$; (**B**) $f(y,0) = e^{-5\sqrt{|y-1|}} + e^{-5\sqrt{|y-3|}}$. Reproduced from Kabin and Shizgal (2003) with permission from the American Institute of Physics

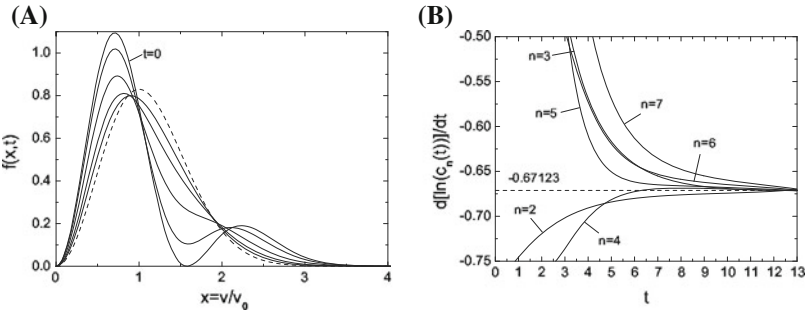

Fig. 5.21 (**A**) Time evolution of the distribution function for $f(x,0) = M(x)\left(\frac{5}{2} - 2x^2 + \frac{4}{5}x^4\right)$; The reduced times from *top* to *bottom* are 0.3, 1, 2 and 3. The *dashed curve* is the equilibrium Maxwellian; (**B**) The time dependence of the time derivative of $\ln c_n(t)$ showing that the approach to equilibrium for all coefficients is given by the "spectral gap", namely λ_2. Reproduced from Sospedra-Alfonso and Shizgal (2012b) with permission from the American Institute of Physics

time dependence of the time derivative of $\ln c_n(t)$ where the expansion coefficients are calculated with Eq. (5.185) and a Simpson rule integration over the distribution function $f^{(n)}(y_i)$ determined with the finite difference solution. It is clear from these results that the rate of approach to equilibrium is asymptotically the same for all coefficients and determined by the "spectral gap", namely $\lambda_2 = 0.67123$ of the linearized collision operator, J. We have used to advantage a finite difference algorithm to calculate the coefficients in a spectral representation of the distribution function without a direct solution of the nonlinear moment equations, Eq. (5.186). A primary objective has been the demonstration of the approach to equilibrium as given by the spectral gap.

The solution of the nonlinear Boltzmann equation for nonuniform systems presents considerable challenges for the accurate representation of distribution

functions that may vary rapidly in position and velocity. The direct simulation Monte Carlo (DSMC) method (Bird 1994) has been used for several decades to study such rarefied gas dynamical problems. The method has been used with success but is not useful for systems approaching the small Knudsen number collision dominated regime. Spectral methods, based on Fourier basis functions, for the nonlinear Boltzmann equation have been reported recently (Filbet et al. 2006; Heintz et al. 2008; Filbet and Mouhot 2011; Wu et al. 2013). The method requires that the velocity and spatial intervals are bounded. The Fourier transform in velocity

$$f^{(N)}(\mathbf{v}) = \sum_{k=-N}^{N} \hat{f}_k e^{\mathbf{k}\cdot\mathbf{v}}, \tag{5.196}$$

$$f_k(t) = \frac{1}{(2\pi)^3} \int f(\mathbf{v}) e^{-i\mathbf{k}\cdot\mathbf{v}} d\mathbf{v}, \tag{5.197}$$

is used to represent the distribution function much in the same way as other basis sets are used. Filbet and Russo (2003) reduced the nonlinear spatially homogeneous Boltzmann equation, Eq. (5.183), to Fourier form as given by

$$\frac{d\hat{f}_k}{dt} = \sum_{m=max(-N,k-N)}^{min(N,k+N)} \hat{f}_{k-m}\hat{f}_m \left[B(k-m,m) - B(m,m)\right] \tag{5.198}$$

where the "kernel modes", $B(n, m)$, are the Fourier transforms of the collision flux $B(g, \theta) = g\sigma(g, \theta)$ in the collision term. The structure of these moment equations is similar to Eq. (5.186) except that in the former, the linear term has been retained.

An excellent review of current numerical methods for the study of rarefied gas dynamical flows modelled with the nonlinear Boltzmann equation was presented by Narayan and Klöckner (2009) where the details of the derivation of Eq. (5.198) can be found. These authors have also provided a bibliography to the current numerical modeling efforts in this research area which is developing rapidly. Other direct methods of solution of the nonlinear homogeneous Boltzmann equation include the discontinous Galerkin method (Aleekseenko and Josyula 2014) and the pseudo-spectral method based on half-range Hermite polynomials (Ghiroldi and Gibelli 2014). A complete discussion of these recent applications with comparisons would require another chapter if not a separate volume.

References

Abe, K.: Sonine polynomial solution of the Boltzmann equation for relaxation of initially nonequilibrium distribution. Phys. Fluids **14**, 492–498 (1971)

Agarwal, R.K., Yun, K.-Y., Balakrishnan, R.: Beyond Navier-Stokes: Burnett equations for flows in the continuum-transition regime. Phys. Fluids **13**, 3061–3085 (2001)

Aleekseenko, A., Josyula, E.: Deterministic solution of the spatially homogeneous Boltzmann equation using discontinuous Galerkin discretizations in the velocity space. J. Comput. Phys. **272**, 170–188 (2014)

Alexandre, R.: A review of the Boltzmann equation with singular kernels. Kinet. Relat. Models **2**, 551–646 (2009)

Alterman, Z., Frankowski, K., Pekeris, C.L.: Eigenvalues and eigenfunctions of the linearized Boltzmann collision operator for a Maxwell gas and for a gas of rigid spheres. Astrophys. J. Suppl. **7**, 291–331 (1962)

Alves, G.M., Kremer, G.M., Marques Jr, W., Soares, A.J.: A kinetic model for chemical reactions without barriers: transport coefficients and eigenmodes. J. Stat. Mech. **2011**, P03014 (2011)

Amore, P.: A variational Sinc collocation method for strong-coupling problems. J. Phys. A: Math. Gen. **39**, L349–L355 (2006)

Andersen, H.C.: Derivation of hydrodynamic equations from the Boltzmann equation. In: Hochstim, A.E. (ed.) Kinetic Processes in Gasses and Plasmas, pp. 25–55. Elsevier, Holland (1969)

Andersen, K., Shuler, K.E.: On the relaxation of a hard sphere Rayleigh and Lorentz gas. J. Chem. Phys. **40**, 633–650 (1964)

Atenzi, S., Meyer-Ter-Vehn, J.: The Physics of Inertial Fusion. Clarendon Press, Oxford (2004)

Atkinson, K.E., Shampine, L.F.: Algorithm 876: solving Fredholm integral equations of the second kind in MATLAB. ACM Trans. Math. Softw. **34**, 21:1–21 (2008)

Balint-Kurti, G.G.: Time-dependent and time-independent wavepacket approaches to reactive scattering and photodissociation dynamics. Int. Rev. Phys. Chem. **27**, 507–539 (2008)

Balint-Kurti, G.G., Pulay, P.: A new grid-based method for the direct computation of excited molecular vibrational-states: test application to formaldehyde. J. Mol. Struct. (Theochem) **341**, 1–11 (1995)

Baranger, C., Mouhot, C.: Explicit spectral gap estimates for the linearized Boltzmann and Landau operators with hard potentials. Rev. Mat. Iberoam. **3**, 819–841 (2005)

Barrett, J., Demeio, L., Shizgal, B.: The Coulomb Milne problem. Phys. Rev. A **45**, 3687–3699 (1992)

Bernstein, R.B.: Quantum effects in elastic molecular scattering. Adv. Chem. Phys. **10**, 75–134 (1966)

Bhatnagar, P.L., Gross, E.P., Krook, M.: A model for collision processes in gases. I. Small amplitude processes in charged and neutral one-component systems. Phys. Rev. **94**, 511–525 (1954)

Binney, J., Tremaine, S.: Galactic Dynamics, 2nd edn. Princeton University Press, New Jersey (2008)

Bird, G.A.: Molecular Gas Dynamics and the Direct Simulation of Gas Flows. Clarendon, Oxford (1994)

Blinnikov, S., Moessner, R.: Expansions for nearly Gaussian distributions. Astron. Astrophys. Suppl. Ser. **130**, 193–205 (1998)

Bobylev, A.V.: A class of invariant solutions of the Boltzmann equation. Dokl. Akad. Nauk SSSR **231**, 571–574 (1976)

Bobylev, A.V.: Exact solutions of the nonlinear Boltzmann equation and the theory of relaxation of a Maxwellian gas. Theor. Math. Phys. **60**, 820–841 (1984)

Bobylev, A.V., Cercignani, C.: On the rate of entropy production for the Boltzmann equation. J. Stat. Phys. **94**, 603–618 (1999)

Bobylev, A.V., Mossberg, E.: On some properties of linear and linearized Boltzmann collision operators for hard spheres. Kinet. Relat. Models **4**, 521–555 (2008)

Bovino, S., Zhang, P., Kharchenko, V., Dalgarno, A.: Trapping hydrogen atoms from a Neon-gas matrix: a theoretical simulation. J. Chem. Phys. **131**, 054302 (2009)

Bovino, S., Zhang, P., Kharchenko, V., Dalgarno, A.: Relaxation of energetic $S(^1D)$ atoms in Xe gas: comparison of ab initio calculations with experimental data. J. Chem. Phys. **135**, 024304 (2011)

Boyd, J.P.: A spectrally accurate quadrature for resolving the logarithmic endpoint singularities of the Chandrasekhar H-function. JQRST **94**, 467–475 (2005)

Boyd, T.J.M., Sanderson, J.S.: The Physics of Plasmas. Cambridge University Press, Cambridge (2003)
Brinkman, R.T.: Departures from Jeans escape rate for H and He in the earth's atmosphere. Planet. Space Sci. **18**, 449–478 (1970)
Brun, R.: Introduction to Reactive Gas Dynamics. Oxford University Press, Oxford (2009)
Buhmann, R.D.: Radial Basis Functions. Cambridge University Press, Cambridge (2004)
Canto, L.F., Hussein, M.S.: Scattering Theory of Molecules. Atoms and Nuclei. Springer, New York (2013)
Case, K.M., Zweifel, P.F.: Linear Transport Theory. Addison-Wesley, Reading (1967)
Cercignani, C.: A variational principle for boundary value problems in kinetic theory. J. Stat. Phys. **1**, 297–311 (1969)
Cercignani, C.: The Boltzmann Equation and Its Applications. Springer, New York (1988)
Cha, S.-H.: Comprehensive survey on distance/similarity measures between probability density functions. Int. J Math. Models Methods Appl. Sci. **1**, 300–307 (2007)
Chamberlain, J.W., Campbell, F.J.: Rate of evaporation of a non-Maxwellian atmosphere. Astrophys. J. **149**, 687–705 (1967)
Chandrasekhar, S.: On the radiative equilibrium of a stellar atmosphere II. Astrophys. J. **100**, 76–86 (1944)
Chandrasekhar, S.: Radiative Transfer. Dover, New York (1960)
Chandrasekhar, S., Breen, F.H.: On the radiative equilibrium of a stellar atmosphere XIX. Astrophys. J. **105**, 143–144 (1947)
Chapman, S., Cowling, T.G.: The Mathematical Theory of Nonuniform Gases. Cambridge University Press, Cambridge (1970)
Child, M.S.: Molecular Collision Theory. Dover, New York (1996)
Cline, J.I., Taatjes, C.A., Leone, S.R.: Diode laser probing of $I(^2P_{1/2})$ Doppler profiles: time evolution of a fast anisotropic velocity distribution in a thermal bath. J. Chem. Phys. **93**, 6543–6553 (1990)
Corngold, N.: Kinetic equation for a weakly coupled test particle. II. Approach to equilibrium. Phys. Rev. A **24**, 656–666 (1981)
Danailov, D.M., Viehland, L.A., Johnson, R., Wright, T.G., Dickinson, A.S.: Transport of O^+ through Argon gas. J. Chem. Phys. **128**, 134302 (2008)
Davidović, D.M., Vukanić, J., Arsenović, D.: Two new analytic approximations of the Chandrasekhar's H function. Icarus **194**, 389–397 (2008)
Davison, B.: Neutron Transport. Oxford University Press, Oxford (1957)
de Groot, S.R., Mazur, P.: Non-equilibrium Thermodynamics. Dover, New York (1984)
Delves, L.M., Mohamed, J.L.: Computational Methods for Integral Equations. Cambridge University Press, Cambridge (1985)
Desai, R.C., Nelkin, M.: Atomic motions in a rigid sphere gas as a problem in neutron transport. Nucl. Sci. Eng. **24**, 142–152 (1966)
Dickinson, A.S., Certain, P.R.: Calculation of matrix elements for one-dimensional quantum-mechanical problems. J. Chem. Phys. **49**, 4209–4211 (1968)
Driessler, W.: On the spectrum of the Rayleigh piston. J. Stat. Phys. **24**, 595–606 (1981)
Driscoll, T.A.: Automatic spectral collocation for integral, integro-differential and integrally reformulated differential equations. J. Comput. Phys. **229**, 5980–5998 (2010)
Dudynski, M.: Spectral properties of the linearized Boltzmann operator in L^p for $1 \leq p \leq \infty$. J. Stat. Phys. **153**, 1084–1106 (2013)
Dziekan, P., Lemarchand, A., Nowakowski, B.: Master equation for a bistable chemical system with perturbed particle velocity distribution function. Phys. Rev. **E85**, 021128 (2012)
Echim, M.M., Lemaire, J., Lie-Svendsen, O.: A review on solar wind modeling: kinetic and fluid aspects. Surv. Geophys. **32**, 1–70 (2011)
Ender, A.Ya., Ender, I.A., Bakaleinikov, L.A., Flegontova, E.Yu.: Matrix elements and kernels of the collision integral in the Boltzmann equation. Tech. Phys. **56**, 452–463 (2011)

Ernst, M.H.: Nonlinear model Boltzmann equations and exact solutions. Phys. Rep. **78**, 1–171 (1981)
Ernst, M.H.: Exact solutions of the nonlinear Boltzmann equation. J. Stat. Phys. **34**, 1001–1017 (1984)
Eskola, L.: Geophysical Interpretation Using Integral Equations. Springer, Netherlands (2012)
Fahr, F.J., Shizgal, B.: Modern exospheric theories and their observational relevance. Rev. Geophys. Space Phys. **21**, 75–124 (1983)
Ferziger, J.H., Kaper, H.G.: Mathematical Theory of Transport Processes in Gases. North-Holland, Amsterdam (1972)
Filbet, F., Mouhot, C.: Analysis of spectral methods for the homogeneous Boltzmann equation. Trans. Am. Math. Soc. **363**, 1947–1980 (2011)
Filbet, F., Russo, G.: High order numerical methods for the space non-homogenous Boltzmann equation. J. Comput. Phys. **186**, 457–480 (2003)
Filbet, F., Mouhot, C., Pareschi, L.: Solving the Boltzmann equation in $N\log_2 N$. SIAM J. Sci. Comput. **28**, 1029–1053 (2006)
Fletcher, A.A.J.: Computational Techniques for Fluid Flow. Springer, New York (1991)
Foch, J.D., Ford, G.W.: The linear Boltzmann equation. In: de Boer, J., Uhlenbeck, G.E. (eds.) Studies in Statistical Mechanics, pp. 127–154. Elsevier, Holland (1970)
Ford, G.W.: Matrix elements of the linearized collision operator. Phys. Fluids **11**, 515–521 (1968)
Gad-el-Hak, M.: The fluid mechanics of microdevices—the Freeman scholar lecture. J. Fluids Eng. **121**, 5–33 (1999)
Ganapol, B.D.: Analytical Benchmarks for Nuclear Engineering Applications. Case Studies in Neutron Transport Theory. Nuclear Energy Agency OECD Publications, Paris (2008)
Garcia, R.D.M., Siewert, C.E.: A stable shifted-Legendre projection scheme generating P_N boundary conditions. Am. Nucl. Energy **23**, 321–332 (1996)
Garcia, R.D.M.: The application of non-classical orthogonal polynomials in particle transport theory. Prog. Nucl. Energy **35**, 249–273 (1999)
Ghiroldi, G.P., Gibelli, L.: A direct method for the Boltzmann equation based on a pseudo-spectral velocity space discretization. J. Comput. Phys. **258**, 568–584 (2014)
Ghosh, K.: Analytical benchmark for non-equilibrium radiation diffusion in finite size systems. Ann. Nucl. Energy **63**, 59–68 (2014)
Golub, G.H., Van Loan, C.F.: Matrix Computations. Johns Hopkins University Press, Baltimore (1996)
Grad, H.: Principles of the kinetic theory. In: Handbook of Physics, pp. 205–294. Springer, Berlin (1958)
Grad, H.: On the kinetic theory of rarefied gases. Commun. Pure Appl. Math. **2**, 331–407 (1949)
Grad, H.: Asymptotic theory of the Boltzmann equation. Phys. Fluids **6**, 147–181 (1963)
Gust, E.D., Reichl, L.E.: Molecular dynamics simulation of collision operator eigenvalues. Phys. Rev. E **79**, 031202 (2009)
Gust, E.D., Reichl, L.E.: Relaxation rates of the linearized Uehling-Uhlenbech equation for bosons. Phys. Rev. E **81**, 061202 (2010)
Hagelaar, G.J.M., Pitchford, L.C.: Solving the Boltzmann equation to obtain electron transport coefficients and rate coefficients for fluid models. Plasma Sources Sci. Technol. **14**, 722–733 (2005)
Harris, D.O., Engerholm, G.G., Gwinn, W.D.: Calculation of matrix elements for one-dimensional quantum-mechanical problems and the application to anharmonic oscillators. J. Chem. Phys. **43**, 1515–1517 (1965)
Hebert, A.: Applied Reactor Physics. Presse Internationales Polytechnique, Montréal (2009)
Heintz, A., Kowalczyk, P., Grzhibovskis, R.: Fast numerical method for the Boltzmann equation on non-uniform grids. J. Comput. Phys. **227**, 6681–6695 (2008)
Hiroi, T.: Recalculation of the isotropic H functions. Icarus **109**, 313–317 (1994)
Hirschfelder, J.O., Curtiss, C.F., Bird, B.: The Molecular Theory of Gases and Liquids. Wiley, New York (1954)

Hoare, M.R.: The linear gas. Adv. Chem. Phys. **20**, 135–214 (1971)
Hoare, M.R., Kaplinsky, C.H.: Linear hard sphere gas: variational eigenvalue spectrum of the energy kernel. J. Chem. Phys. **52**, 3336–3353 (1970)
Huang, K.: Statistical Mechanics. Wiley, New York (1967)
Hubert, D.: Auroral ion velocity distribution function: generalized polynomial solution of Boltzmann's equation. Planet. Space Sci. **31**, 119–127 (1983)
Jablonski, A.: Improved algorithm for calculating the Chandrasekhar function. Comput. Phys. Commun. **184**, 440–442 (2013)
Jerri, A.J.: Introduction to Integral Equations with Applications, 2nd edn. Wiley, New York (1999)
Jüngel, A.: Transport Equations for Semiconductors. Springer, New York (2009)
Kabin, K., Shizgal, B.D.: Exact evaluation of collision integrals for the nonlinear Boltzmann equation. AIP Conf. Proc. **663**, 35–42 (2003)
Kan, M.W.K., Yu, P.K.N., Leung, L.H.T.: A review on the use of grid-based Boltzmann equation solvers for dose calculation in external photon beam treatment planning. Biomed. Res. Int. **2013**, 692874 (2013)
Kapral, R., Ross, J.: Relaxation in a dilute binary gas mixture. J. Chem. Phys. **52**, 1238–1243 (1970)
Kawabata, K., Limaye, S.S.: Rational approximation formula for Chandrasekhar's H-function for isotropic scattering. Astrophys. Space Sci. **332**, 365–371 (2011)
Kawabata, K., Satoh, T., Ueno, S.: A direct numerical approach to the Chandrasekhar's H-function for arbitrary characteristic functions. Astrophys. Space Sci. **182**, 249–260 (1991)
Kharchenko, V., Dalgarno, A.: Thermalization of fast O(^{1}D) atoms in the stratosphere and mesosphere. J. Geophys. Res. **109**, D18311 (2004)
Kharchenko, V., Balakrishnan, N., Dalgarno, A.: Thermalization of fast nitrogen atoms in elastic and inelastic collisions with molecules of atmospheric gases. J. Atmos. Terr. Phys. **60**, 95–106 (1998)
Khazanov, G.V.: Kinetic Theory of the Inner Magnetospheric Plasma. Springer, New York (2011)
Khurana, S., Thachuk, M.: A numerical solution of the linear Boltzmann equation using cubic B-splines. J. Chem. Phys. **136**, 094103 (2012)
Khurana, S., Thachuk, M.: Kernels of the linear Boltzmann equation for spherical particles and rough hard sphere particles. J. Chem. Phys. **139**, 164122 (2013)
Kim, J.G., Boyd, I.D.: State-resolved master equation analysis of thermochemical nonequilibrium of nitrogen. Chem. Phys. **415**, 237–246 (2013)
Kourganoff, V.: Basic Methods in Transfer Problems. Oxford University Press, Oxford (1963)
Kremer, G.M.: An Introduction to the Boltzmann Equation and Transport Processes in Gases. Springer, New York (2010)
Krook, M., Wu, T.T.: Formation of Maxwellian tails. Phys. Rev. Lett. **36**, 1107–1109 (1976)
Krupp, R.S.: A nonequilibrium solution of the Fourier transformed Boltzmann equation. MSc thesis, MIT (1967)
Kügerl, G., Schürrer, F.: On the relaxation of binary hard-sphere gases. Phys. Fluids **2**, 609–618 (1990)
Kullback, S., Leibler, R.A.: On information and sufficiency. Ann. Math. Stat. **22**, 79–86 (1951)
Kundu, P., Cohen, I.M., Dowling, D.R.: Fluid Mechanics, 6th edn. Academic Press, Waltham (2012)
Kuščer, I., Corngold, N.: Discrete relaxation times in neutron transport. Phys. Rev. **139**, A981–A990 (1965)
Kuščer, I., Williams, M.M.R.: Relaxation constants of a uniform hard sphere gas. Phys. Fluids **10**, 1922–1927 (1967)
Kuščer, I., McCormick, N.J.: Some analytical results for radiative transfer in thick atmospheres. Trans. Theory Stat. Phys. **20**, 351–381 (1991)
Kustova, E.V., Giordano, D.: Cross-coupling effects in chemically non-equilibrium viscous compressible flows. Chem. Phys. **379**, 83–91 (2011)
Kythe, P.K., Puri, P.: Computational Methods for Linear Integral Equations. Birkhauser, Berlin (2002)

Leblanc, F., Hubert, D.: A generalized model for the proton expansion in astrophysical winds. I. The velocity distribution function representation. Astrophys. J. **483**, 464–474 (1997)
Lemaire, J.: Half a century of kinetic solar wind models. AIP Conf. Proc. **1216**, 8–13 (2010)
Lemaire, J., Scherer, M.: Model of the polar ion exosphere. Planet. Space Sci. **18**, 103–120 (1970)
Lemaire, J., Scherer, M.: Kinetic models of the solar and polar winds. Rev. Geophys. Space Phys. **11**, 427–468 (1973)
Liang, S.: Quantitative Remote Sensing of Land Surfaces. Wiley, New Jersey (2005)
Liboff, R.L.: Kinetic Theory: Classical, Quantum, and Relativistic Descriptions, 3rd edn. Springer, New York (2003)
Lie-Svendsen, O., Rees, M.H.: An improved kinetic model for the polar outflow of a minor ion. J. Geophys. Res. **101**, 2415–2433 (1996)
Light, J.C., Carrington Jr, T.: Discrete variable representations and their utilization. Adv. Chem. Phys. **114**, 263–310 (2000)
Lightman, A.P., Shapiro, S.L.: The dynamical evolution of globular clusters. Rev. Mod. Phys. **50**, 437–481 (1978)
Lin, S.R., Robson, R.E., Mason, E.A.: Moment theory of electron drift and diffusion in neutral gases in an electrostatic field. J. Chem. Phys. **71**, 3483–3498 (1979a)
Lin, S.Y., Viehland, L.A., Mason, E.A.: Three temperature theory of gaseous ion transport. Chem. Phys. **37**, 411–424 (1979b)
Lindenfeld, M.J., Shizgal, B.: Matrix elements of the Boltzmann collision operator for gas mixtures. Chem. Phys. **41**, 81–95 (1979a)
Lindenfeld, M.J., Shizgal, B.: Non-Maxwellian effects associated with the thermal escape of a planetary atmosphere. Planet. Space Sci. **27**, 739–751 (1979b)
Lindenfeld, M.J., Shizgal, B.: The Milne problem: a study of the mass dependence. Phys. Rev. **A27**, 1657–1670 (1983)
Liou, K.-N.: A numerical experiment on Chandrasekhar's discrete-ordinate method for radiative transfer: applications to cloudy and hazy atmospheres. J. Atmos. Sci. **30**, 1303–1326 (1973)
Liou, K.N.: An Introduction to Atmospheric Radiation. Elsevier, Amsterdam (2002)
Lowke, J.J., Tanaka, M.: LTE-diffusion approximation for arc calculations. J. Phys. D: Appl. Phys. **39**, 3634–3643 (2006)
Loyalka, S.K., Naz, S.: Milne's half-space problem: a numerical solution of the related integral equation. Ann. Nucl. Energy **35**, 1900–1902 (2008)
Loyalka, S.K., Tipton, E.L., Tompson, R.V.: Chapman-Enskog solutions to arbitrary order in Sonine polynomials I: simple, rigid-sphere gas. Phys. A **379**, 417–435 (2007)
Ma, J.Z.G., St.-Maurice, J.-P.: Ion distribution functions in cylindrically symmetric electric fields in the auroral ionosphere: the collision-free case in a uniformly charged configuration. J. Geophys. Res. **113**, A05312 (2008)
Mason, E.A., McDaniel, E.W.: Transport Properties of Ions in Gases. Wiley, New York (1988)
Matsumi, Y., Shamsuddin, S.M., Sato, Y., Kawasaki, M.: Velocity relaxation of hot $O(^1D)$ atoms by collisions with rare gases, N_2, and O_2. J. Chem. Phys. **101**, 9610–9618 (1994)
McCormick, N.J., Kuščer, I.: Singular eigenfunction expansions in neutron transport problems. Adv. Nucl. Sci. Technol. **7**, 181–282 (1973)
McCourt, F.R.W., Beenakker, J.J.M., Köhler, W.E.E., Kuščer, I.: Nonequilibrium Phenomena in Polyatomic Gases Volume 2: Cross Sections, Scattering, and Rarefied Gases. Oxford University Press, Oxford (1991)
McDaniel, E.W., Mason, E.A.: The Mobility and Diffusion of Ions in Gases. Wiley, New York (1973)
Milne, E.A.: Radiative equilibrium in the outer layers of a star; the temperature distribution and the law of darkening. Mon. Not. R. Astron. Soc. **81**, 361–375 (1921)
Monchick, L., Mason, E.A.: Free flight theory of gas mixtures. Phys. Fluids **10**, 1377–1390 (1967)
Mott-Smith, H.M.: A new approach in the kinetic theory of gases. MIT Linc. Lab. **V2**, 1–1 (1954)
Mouhot, C.: Rate of convergence to equilibrium for the spatially homogeneous Boltzmann equation for hard potentials. Commun. Math. Phys. **261**, 629–672 (2006)

Mouhot, C.: Quantitative linearized study of the Boltzmann collision operator and applications. Commun. Math. Sci. **1**, 73–86 (2007)
Mozumder, A.: Electron thermalization in gases. III epithermal electron scavenging in rare gases. J. Chem. Phys. **74**, 6911–6921 (1981)
Nakayama, T., Takahashi, K., Matsumi, Y.: Thermalization cross sections of suprathermal N(^{4}S) atoms in collisions with atmospheric molecules. Geophys. Res. Lett. **32**, L24803 (2005)
Nan, G., Houston, P.L.: Velocity relaxation of S(^{1}D) by rare gases measured by Doppler spectroscopy. J. Chem. Phys. **97**, 7865–7872 (1992)
Narayan, A., Klöckner, A.: deterministic numerical schemes for the Boltzmann equation, 1–51 (2009) ArXiv e-prints
Newburgh, R., Peidle, J., Rueckner, W.: Einstein, Perrin, and the reality of atoms: 1905 revisited. Am. J. Phys. **74**, 478–481 (2006)
Nicholson, J.W., Rudolph, W., Hager, G.: Using laser pulse dynamics to probe velocity distribution of excited iodine. J. Chem. Phys. **104**, 3537–3545 (1996)
Nielsen, S.E., Bak, T.A.: Hard sphere model for the dissociation of diatomic molecules. J. Chem. Phys. **41**, 665–674 (1964)
Oh, S.-K.: Modified Lennard-Jones potentials with a reduced temperature-correction parameter for calculating thermodynamic and transport properties: noble gases and their mixtures (He, Ne, Ar, Kr, and Xe). J. Thermodyn. **2013**, 828620 (2013)
Park, J., Shafer, N., Bersohn, R.: The time evolution of the velocity distribution of hydrogen atoms in a bath gas. J. Chem. Phys. **91**, 7861–7871 (1989)
Parker, E.N.: Dynamical theory of the solar wind. Space Sci. Rev. **4**, 666–708 (1965)
Parker, E.N.: Kinetic and hydrodynamic representations of coronal expansion and the solar wind. AIP Conf. Proc. **1216**, 3–7 (2010)
Pascal, S., Brun, R.: Transport properties of nonequilibrium gas mixtures. Phys. Rev. E **47**, 3251–3267 (1993)
Pekeris, C.L.: Solution of the Boltzmann-Hilbert integral equation. Proc. Natl. Acad. Sci. **41**, 661–669 (1955)
Pekeris, C.L., Alterman, Z.: Solution of the Boltzmann-Hilbert integral equation II; the coefficients of viscosity and heat transfer. Proc. Natl. Acad. Sci. **43**, 998–1007 (1957)
Peraiah, A.: Radiative transfer—Chandrasekhar—and after. Bull. Astron. Soc. India **24**, 397–536 (1996)
Phillips, N.J.: Collisional relaxation in gases. Proc. Phys. Soc. **73**, 800–806 (1959)
Pierrard, V.: Evaporation of hydrogen and helium atoms from the atmospheres of Earth and Mars. Planet. Space Sci. **51**, 319–327 (2003)
Pierrard, V., Lazar, V.: Kappa distributions; theory and applications in space plasmas. Sol. Phys. **267**, 153–174 (2010)
Pierrard, V., Lemaire, J.: A collisional model of the polar wind. J. Geophys. Res. **103**, 11701–11709 (1998)
Pitchford, L.C., ONeil, S.V., Rumble Jr, J.R.: Extended Boltzmann analysis of electron swarm experiments. Phys. Rev. A **23**, 294–304 (1981)
Pitchford, L.C., Phelps, A.V.: Comparative calculations of electron-swarm properties in N_2 at moderate E/N values. Phys. Rev. A **25**, 540–554 (1982)
Present, R.D., Morris, B.M.: Variational solution of the chemical kinetic Boltzmann equation. J. Chem. Phys. **50**, 151–160 (1969)
Prigogine, I., Xhrouet, E.: On the perturbation of Maxwell distribution function by chemical reactions in gases. Physica **15**, 913–932 (1949)
Rahman, M., Sundaresan, M.K.: Discrete relaxation modes for a hard sphere gas. Can. J. Phys. **46**, 2463–2469 (1968)
Reinhardt, W.P.: L^2 discretization of atomic and molecular electronic continua: moment, quadrature and J-matrix techniques. Comput. Phys. Commun. **17**, 1–21 (1979)
Robson, R.E., White, R.D., Petrović, Z.L.: Colloquium: physically based fluid modeling of collisionally dominated low-temperature plasmas. Rev. Mod. Phys. **77**, 1303–1320 (2005)

Ross, J., Mazur, P.: Some deductions from a formal statistical mechanical theory of chemical kinetics. J. Chem. Phys. **35**, 19–28 (1961)
Rybicki, G.B., Lightman, A.P.: Radiative Processes in Astrophysics. Wiley Interscience, New York (1979)
Rybicki, G.B.: Radiative transfer. J. Astrophys. Astron. **17**, 95–112 (1996)
Schunk, R.W.: Mathematical structure of transport equations for multispecies flows. Rev. Geophys. Space Phys. **15**, 429–445 (1977)
Sharipov, F., Seleznev, V.: Data on internal rarefied gas flows. J. Phys. Chem. Ref. Data **27**, 657–706 (1998)
Sharipov, F., Bertoldo, G.: Numerical solution of the linearized Boltzmann equation for an arbitrary intermolecular potential. J. Comput. Phys. **228**, 3345–3357 (2009)
Shizgal, B.: Nonequilibrium contributions to the rate of reaction. IV. Explicit time-dependent solutions. J. Chem. Phys. **55**, 76–83 (1971)
Shizgal, B.: Vibrational nonequilibrium effects in the (H_2-H_2) reactive system. J. Chem. Phys. **57**, 3915–3928 (1972)
Shizgal, B.: Time dependent solution of the chemical kinetic Boltzmann equation; two component isothermal system. Chem. Phys. **5**, 129–135 (1974)
Shizgal, B.: A Gaussian quadrature procedure for the use in the solution of the Boltzmann equation and related problems. J. Comput. Phys. **41**, 309–328 (1981a)
Shizgal, B.: Nonequilibrium time dependent theory of hot atom reactions. III. Comparison with the Estrup-Wolfgang theory. J. Chem. Phys. **741**, 1401–1408 (1981b)
Shizgal, B.: Discrete versus continuum relaxation modes of a hard sphere gas. Can. J. Phys. **62**, 97–103 (1984)
Shizgal, B., Blackmore, R.: Eigenvalues of the Boltzmann collision operator for binary gases and relaxation of anisotropic distributions. Chem. Phys. **77**, 417–427 (1983)
Shizgal, B., Blackmore, R.: A collisional kinetic theory of a plane parallel evaporating planetary atmosphere. Planet. Space Sci. **34**, 279–291 (1986)
Shizgal, B., Fitzpatrick, J.M.: Matrix elements of the linear Boltzmann collision operator for systems of two components at different temperatures. Chem. Phys. **6**, 54–65 (1974)
Shizgal, B., Fitzpatrick, J.M.: Possible failure of relaxation-time comparisons in the justification of local thermodynamic equilibrium. Phys. Rev. A **18**, 267–276 (1978)
Shizgal, B., Hubert, D.: The nonequilibrium nature of ion distribution functions in the high latitude auroral ionosphere. In: Muntz, E.P., Weaver, D.P., Campbell, D.H. (eds.) Proceedings of the 16th International Symposium on Rarefied Gas Dynamics, pp. 3–22. AIAA, Washington (1989)
Shizgal, B., Karplus, M.: Nonequilibrium contributions to the rate of reaction. I. Perturbation of the velocity distribution function. J. Chem. Phys. **52**, 4262–4278 (1970)
Shizgal, B., Karplus, M.: Nonequilibrium contributions to the rate of reaction. II. Isolated multicomponent systems. J. Chem. Phys. **54**, 4345–4356 (1971)
Shizgal, B., McMahon, D.R.A.: Electric field dependence of transient electron transport properties in rare gas moderators. Phys. Rev. A **32**, 3669–3680 (1985)
Shizgal, B.D., Lordet, F.: Vibrational nonequilibrium in a supersonic expansion with reaction: application to O_2-O. J. Chem. Phys. **104**, 3579–3597 (1996)
Shizgal, B.D.: Suprathermal particle distributions in space physics: Kappa distributions and entropy. Astrophys. Space Sci. **312**, 227–237 (2007)
Shizgal, B.D.: Pseudospectral methods of solution of the linear and linearized Boltzmann equations; transport and relaxation. AIP Conf. Proc. **1333**, 986–991 (2011)
Shizgal, B.D., Arkos, G.G.: Nonthermal escape of the atmospheres of Venus, Earth, and Mars. Rev. Geophys. **34**, 483–505 (1996)
Shizgal, B.D., Dridi, R.: Maple code for the calculation of the matrix elements of the Boltzmann collision operators for mixtures. Comput. Phys. Commun. **181**, 1633–1640 (2010)
Shore, S.N.: Blue sky and hot piles: the evolution of radiative transfer theory from atmospheres to nuclear reactors. Hist. Math. **29**, 463–489 (2002)

Siewert, C.E.: A concise and accurate solution to Chandrasekhar's basic problem in radiative transfer. JQRST **64**, 109–130 (2000)
Siewert, C.E.: On computing the Chapman-Enskog functions for viscosity and heat transfer and the Burnett functions. JQRST **74**, 789–796 (2002)
Siewert, C.E.: The linearized Boltzmann equation: concise and accurate solutions to basic flow problems. Z. angew. Math. Phys. **54**, 273–303 (2003)
Singh, G.S., Prasad, N., Kumar, B.: Transport properties of a binary gas mixture of molecules with internal energy. II. Thermal conductivity. J. Chem. Phys. **105**, 1537–1545 (1996)
Slevinsky, M., Safouhi, H.: Numerical treatment of a twisted tail using extrapolation methods. Numer. Algorithms **48**, 301–316 (2008)
Snider, R.F.: Quantum-mechanical modified Boltzmann equation for degenerate internal states. J. Chem. Phys. **32**, 1051–1060 (1960)
Snider, R.F.: Variational methods for solving the Boltzmann equation. J. Chem. Phys. **41**, 591–595 (1964)
Sone, Y.: Molecular Gas Dynamics: Theory, Techniques and Applications. Birkhauser, Boston (2007)
Sospedra-Alfonso, R., Shizgal, B.D.: Henyey-Greenstein model in the shape relaxation of dilute gas mixtures. Trans. Theory Stat. Phys. **41**, 368–388 (2012a)
Sospedra-Alfonso, R., Shizgal, B.D.: Hot atom populations in the terrestrial atmosphere. A comparison of the nonlinear and linearized Boltzmann equation. AIP Conf. Proc. **1501**, 91–98 (2012b)
Sospedra-Alfonso, R., Shizgal, B.D.: Energy and shape relaxation in binary atomic systems with realistic quantum cross sections. J. Chem. Phys. **139**, 044113 (2013)
Spitzer, L.J., Härm, R.: Evaporation of stars from open clusters. Astrophys. J. **127**, 544–550 (1958)
St.-Maurice, J.-P., Schunk, R.W.: Behaviour of ion velocity distributions for a simple collision model. Planet. Space Sci. **22**, 1–18 (1974)
St.-Maurice, J.-P., Schunk, R.W.: Use of generalized orthogonal polynomial solutions of Boltzmanns equation in certain aeronomy problems, Auroral ion velocity distributions. J. Geophys. Res. **81**, 2145–2154 (1976)
St.-Maurice, J.-P., Schunk, R.W.: Ion velocity distributions in the high-latitude ionosphere. Rev. Geophys. **17**, 99–134 (1979)
Stamnes, K., Tsay, S.-C., Wiscombe, W., Jayaweera, K.: Numerically stable algorithm for discrete-ordinate-method radiative transfer in multiple scattering and emitting layered media. Appl. Opt. **27**, 2502–2509 (1988)
Stroud, A.H.: Approximate Calculation of Multiple Integrals. Prentice Hall, Engelwood Cliffs (1971)
Struchtrup, H.: Macroscopic Transport Equations for Rarefied Gas Flows; Approximation Methods in Kinetic Theory. Springer, New York (2005)
Sykes, J.B.: Approximate integration of the equation of transfer. Mon. Not. R. Astron. Soc. **111**, 377–386 (1951)
Taatjes, C.A., Cline, J.I., Leone, S.R.: A general method for Doppler determination of cylindrically symmetric velocity distributions: an application of Fourier transform Doppler spectroscopy. J. Chem. Phys. **93**, 6554–6559 (1990)
Thomas, G.E., Stamnes, K.: Radiative Transfer in the Atmosphere and Ocean. Cambridge University Press, Cambridge (2002)
Tompson, R.V., Tipton, E.L., Loyalka, S.K.: Chapman-Enskog solutions to arbitrary order in Sonine polynomials V: summational expressions for the viscosity-related bracket integrals. Eur. J. Mech. B/Fluids **29**, 153–179 (2010)
Tricomi, F.G.: Integral Equations. Dover, New York (1985)
Vasenkov, A., Shizgal, B.D.: Nonhydrodynamic aspects of electron transport near a boundary: the Milne problem. Phys. Rev. E **63**, 016401 (2000)
Vasenkov, A., Shizgal, B.D.: Numerical study of a direct current plasma sheath based on kinetic theory. Phys. Plasmas **9**, 691–700 (2002)

Ven Den Eynde, G., Beauwens, R., Mund, E.: Calculating the discrete spectrum of the transport operator with arbitrary order anisotropic scattering. Trans. Theory Stat. Phys. **36**, 179–197 (2007)
Viehland, L.A.: Velocity distribution functions and transport coefficients of atomic ions in atomic gases by a Gram-Charlier approach. Chem. Phys. **179**, 71–92 (1994)
Viehland, L.A., Lin, S.L.: Application of the three temperature theory of ion transport. Chem. Phys. **43**, 135–144 (1979)
Viehland, L.A., Chang, Y.: Beyond the Monchick-Mason approximation: the mobility of Li ions in H_2. Mol. Phys. **110**, 259–266 (2012)
Volakis, J., Sertel, K.: Integral Equation Methods for Electromagnetics. Scitech, North Carolina (2012)
Wang-Chang, C.S., Uhlenbeck G.S.: Solution of the transport equation by S_N approximation. Technical Report CM-681, University of Michigan (1951)
Weinert, U., Lin, S.L., Mason, E.A.: Solutions of the nonlinear Boltzmann equation describing relaxation to equilibrium. Phys. Rev. A **22**, 2262–2269 (1980)
Wick, G.C.: Über ebene diffusionsprobleme. Z. Phys. **121**, 702–718 (1943)
Wigner, E.P., Wilkins Jr, J.E.: Effect of temperature of the moderator on the velocity distribution of neutrons with numerical calculations for H as moderator. Technical Report AECD-2275, US Atomic Energy Commission (1944)
Williams, M.M.R.: The Slowing Down and Thermalization of Neutrons. North-Holland, Amsterdam (1966)
Williams, M.M.R.: Mathematical Methods in Particle Transport Theory. Wiley-Interscience, New York (1971)
Williams, M.M.R.: The Boltzmann equation for fast atoms. J. Phys. A: Math. Gen. **9**, 771–783 (1976)
Williams, M.M.R.: The development of nuclear reactor theory in the Montreal laboratory of the National Research Council of Canada (Division of Atomic Energy) 1943–1946. Prog. Nucl. Energy **36**, 239–322 (2000)
Williams, M.M.R.: The Milne problem with Fresnel reflection. J. Phys. A: Math. Gen. **38**, 3841–3850 (2005)
Wu, L., White, C., Scanlon, T.J., Reese, J.M., Zhang, Y.: Deterministic numerical solutions of the Boltzmann equation using the fast spectral method. J. Comput. Phys. **250**, 27–52 (2013)
Yan, C.C.: Relaxation rate spectrum of the linearized Boltzmann equation for hard spheres. Phys. Fluids **12**, 2306–2312 (1969)
Yilmazer, A., Kocar, C.: Some benchmark results in spherical media radiative transfer problems. Trans. Theory Stat. Phys. **38**, 273–292 (2009)
Zhang, P., Kharchenko, V., Dalgarno, A.: Thermalization of suprathermal N(^{4}S) atoms in He and Ar gases. Mol. Phys. **105**, 1487–1496 (2007)
Zhang, X.-N., Li, H.-P., Murphy, A.B., Xia, W.-D.: A numerical model of non-equilibrium thermal plasmas. I. Transport properties. Phys. Plasmas **20**, 033508 (2013)
Ziff, R.M., Merajver, S.D., Stell, G.: Approach to equilibrium of a Boltzmann-equation solution. Phys. Rev. Lett. **47**, 1493–1496 (1981)